PAP-666



DISSERTATION

# MECHANICS OF RIPRAP IN OVERTOPPING FLOW

Submitted by

Rodney Jay Wittler

Civil Engineering Department

In partial fulfillment of the requirements

for the Degree of Doctor of Philosophy

Colorado State University

Fort Collins, Colorado

Fall 1994

COLORADO STATE UNIVERSITY

November 2, 1994

WE HEREBY RECOMMEND THAT THE DISSERTATION PREPARED UNDER OUR SUPERVISION BY RODNEY JAY WITTLER ENTITLED MECHANICS OF RIPRAP IN OVERTOPPING FLOW BE ACCEPTED AS FULFILLING IN PART REQUIREMENTS FOR THE DEGREE OF DOCTOR OF PHILOSOPHY.

Committee on Graduate Work

James C. Loftis, Head, Department of Chemical and Agricultural Engineering (Outside Member)

James F. Ruff

Morris M. Skinner

Steven R. Abt, Advisor

Head, Department of Civil Engineering

## ABSTRACT OF DISSERTATION

### THE MECHANICS OF RIPRAP IN OVERTOPPING FLOW

The purpose of riprap is to prevent erosion of underlying materials. A generalized riprap design equation results when equating the Manning, Strickler, and Shields (MSS) equations. Two experimental based factors, a correction factor and a stability coefficient, applied to the MSS equation, result in a highly calibrated generalized riprap design equation. An understanding of the mechanics is necessary for correct application of the equations and experimental based factors.

Three hypotheses give definition to the mechanics of riprap in overtopping flow. The first hypothesis regards the Shields parameter in low submergence flows, a flow regime common to riprap in overtopping conditions. Fractional analysis leads to the hypothesis that the Shields parameter is constant in the region of the Shields diagram where the Boundary Reynolds number is greater than $10^4$. The value and constancy of the Shields parameter in this region are important points of definition for the stability of a riprap mixture. The Shields parameter, by itself, is a poor expression for designing riprap because of the inherent assumptions that simplify the parameter. However, no other parameter identifies the primary factors that govern the mechanics of riprap in overtopping flow. With Shields parameter as a basis, it is possible to develop a more comprehensive and accurate riprap design equation.

The second hypothesis regards a characteristic size fraction. Reasoning, based on Shields parameter, leads to the hypothesis that a single size fraction cannot represent the entire riprap mixture. Indeed, flume data show that there is no single particle fraction size that is characteristic of the entire riprap mixture. Two riprap mixtures, a poorly graded and well-graded mixture, with

the same median rock size, exhibit differing degrees of stability. The poorly graded mixture withstands a greater unit discharge at failure than the well-graded mixture. Flume data from this investigation and Abt lead to an expression relating a uniformity coefficient to unit discharge. The coefficient of stability, $C_s$, compensates for variation in riprap mixture uniformity.

The combination of the Manning and Strickler equations, and the limiting point of critical shear stress defined by the Shields parameter, leads to a generalized riprap design equation. The derived equation differs from an empirical based equation, the Abt equation. The generalized equation and the Abt equation define the median rock size as a function of the slope and unit discharge. The third hypothesis states that the difference between the two equations is due to the overestimation of the hydraulic radius in aerated flow. Comparison of the two equations leads to an expression that compensates for the overestimation of the hydraulic radius. The expression for the aeration coefficient, $A_c$, apparently applies to other riprap design methods such as Stability Factors. There is a good agreement between $A_c$ and prototype scale data.

Rodney Jay Wittler
Civil Engineering Department
Colorado State University
Fort Collins, Colorado 80523
Fall 1994

## ACKNOWLEDGMENTS

*"And can the liberties of a nation be thought secure when we have removed their only firm basis-a conviction in the minds of the people that these liberties are the gift of God? That they are not to be violated but with His wrath? Indeed I tremble for my country when I reflect that God is just: that His justice cannot sleep forever."*§

*Thomas Jefferson*

*"The great tragedy of Science — the slaying of a beautiful hypothesis by an ugly fact."*

*T.H. Huxley*

The author acknowledges the following persons. Professor Steven R. Abt, Advisor, demonstrated great patience and other pedagogic skills while facilitating this course of study. He is a pioneer, a researcher whom I vainly attempt to emulate. Professor James F. Ruff, Professor Morris Skinner, and Professor James Loftis, members of the advisory committee, added thoughtful criticism and professional review during the preparation of the dissertation. Mr. Robert Brennan, a sage and simple man, consulted on these and many other studies. Professor Johannes Gessler put forth in his dissertation many of the premises that helped form this dissertation. Mr. Phil Burgi, Mr. Cliff Pugh, and Mr. Brent Mefford, faithfully and patiently fulfilled our contract of employment. Their patience was a prod to do likewise.

My wife Sandy patiently and lovingly supported and encouraged this work through many periods when others did not. Of course my mother and father made it possible. This work is in many ways the salary of parenthood. Dr. Jerry Richardson, Mr. Fred Doehring, and many other friends are all responsible for many of the valuable lessons learned outside the classroom.

Funds for this study came from many sources including the Colorado State Agricultural Experiment Station, the United States Nuclear Regulatory Commission, Professor Steven R. Abt, and the author. The author extends his deepest appreciation to all contributors.

§ Thomas Jefferson, "Notes on the States of Virginia." (Philadelphia; Matthew Carey, 1794), Query XVIII, page 237.

TABLE OF CONTENTS

# LIST OF FIGURES

# LIST OF TABLES

# LIST OF SYMBOLS

$Re_*$ ..... Boundary Reynolds number
$\overline{u}_y$ ..... Mean vertical profile velocity
$q_f^*$ ..... Predicted failure unit discharge
$\psi$ ..... Angle of Repose
$\nu$ ..... Kinematic viscosity
$\rho$ ..... Mass density of water
$\mu$ ..... Mean
$\tau$ ..... Shear stress
$\alpha$ ..... Slope angle
$\sigma$ ..... Standard deviation
$\gamma$ ..... Unit weight of water
$\rho_a$ ..... Aerated mass density of water
$\tau_{cr}$ ..... Critical shear stress
$\delta_l$ ..... Laminar sublayer
$\gamma_s$ ..... Unit weight of particle
$\lambda_{sub}$ ..... Relative submergence
$A$ ..... Area
$A_c$ ..... Aeration correction coefficient
$C$ ..... Chezy roughness coefficient
$C_d$ ..... Coefficient of Drag
$C_f$ ..... Correction coefficient
$C_s$ ..... Coefficient of Stability
$C_u$ ..... Coefficient of Uniformity
$d$ ..... Depth
$D$ ..... Particle diameter
$D_e$ ..... Equivalent spherical diameter
$E_I$ ..... Inertial energy
$E_L$ ..... Potential energy
$f$ ..... Darcy friction factor
$F_B$ ..... Buoyant force
$F_D$ ..... Drag force
$F_F$ ..... Friction force
$F_g$ ..... Gravitational force(s)
$F_i$ ..... Inertial force(s)
$F_L$ ..... Lift Force
$F_m$ ..... Mass forces (weight)
$F_N$ ..... Normal force
$F_R$ ..... Resultant force
$F_V$ ..... Viscous force
$g$ ..... Accelaration of gravity
$h_s$ ..... Average surface flow depth
$k$ ..... Characteristic particle dimension
$k_s$ ... Median particle diameter of Strickler
$l$ ..... Length of control volume
$L_d$ ..... Moment arm
$m$ ..... mass
$M_g$ ..... Gravitational moment(s)
$M_i$ ..... Inertial moment(s)
$n$ ..... Manning rouhgness coefficient
$n_p$ ..... Porosity
$p$ ..... Wetted perimeter
$q$ ..... unit discharge
$q_f$ ..... Failure unit discharge
$Q_I$ ..... Interstitial discharge
$Q_s$ ..... Surface discharge
$Q_T$ ..... Total discharge
R ..... Hydraulic Radius
$R$ ..... Roundness
$R^*$ ..... Corrected hydraulic radius
$R_a$ ..... Aerated hydraulic radius
$r$ ..... Edge radius
$r_e$ ..... Equivalent spherical radius
$S$ ..... Slope
SF ..... Satety Factor
$S_s$ ..... Specific gravity of particle
$T$ ..... Shields parameter
$T_a$ ..... Aerated Shields parameter
$T_c$ ..... Critical Shields parameter
$u$ ..... Local velocity
$u_*$ ..... Shear velocity
$V$ ..... Volume of a particle
$V_s$ ..... Average surface flow velocity
$w$ ..... Width
$x$ ..... Longitudinal coordinate
$y$ ..... Vertical coordinate
$z$ ..... Upper limit, Gaussian distribution
$z_o$ ..... Gaussian normalization variable

# CHAPTER 1

## INTRODUCTION

The term mechanics refers to forces that act on bodies. This dissertation considers the forces that act on rocks that make up a mixture of riprap. The rocks subject to the mechanical analysis are the rocks that form the uppermost layer of the riprap layer. This is the layer that is directly subject to the hydrodynamic forces of the flowing water. A riprap mixture is a collection of rocks of varying sizes, shapes, and relative position. The configuration under consideration is a planar embankment subject to water flow parallel to the slope of the embankment. The purpose for placing riprap on an embankment is to inhibit erosion of the underlying earthen material that constitutes the embankment.

The Shields parameter is an elegant descriptor of the relative stability of riprap in flowing water. The shear stress, $\tau$, a factor in the Shields parameter, is a random variable, that is, it varies according to the normal distribution. Therefore, the Shields parameter is also a normal parameter. Also, no two rocks in a mixture of riprap have the same size, shape, or relative position. These assumptions lead to the conclusion that there is no deterministic means for predicting the stability of any single rock in a mixture of riprap. The mechanics of riprap in flowing water is therefore a statistical exercise, dealing with averages, observed behavior of limited test populations, and theory. This dissertation attempts to describe the interaction of highly turbulent flow and the accompanying hydrodynamic forces and a riprap mixture.

The Shields parameter is the starting point in the discussion of the mechanics of riprap stability. Whether by fractional analysis, static analysis, moment analysis, or energy balance, the

Shields parameter appears to govern riprap mechanics. Similarly, the Boundary Reynolds number is a legitimate descriptor of the hydraulics of the boundary layer, the fluid layer in direct contact with the riprap layer. The relationship between the Boundary Reynolds number and the Shields parameter is the basis for understanding the incipient motion of a particular rock size of a riprap mixture. However, there are many definitions of the incipient motion. A definition of incipient motion is necessary to apply the Shields parameter to riprap in overtopping flow.

The purpose of installing riprap on an embankment subject to overtopping is to protect the embankment from erosion and catastrophic failure. Failure of the riprap hastens the erosion and failure of the embankment. What does it mean, though, for the riprap to fail? For riprap in overtopping flow, failure is the process of rock movement that leads to exposure of the underlying materials. This definition is circumspect in at least two ways. First, the definition allows for incidental movement. Second, it infers a process in the terms "leads to," that is, failure is a process, not a distinct threshold.

The Shields parameter, by definition, describes the incipient motion of a single rock. However, riprap comprises rocks of many sizes and shapes. The question arises, how does the designer apply the Shields parameter to a mixture of riprap? A solution is to describe the riprap mixture with a single size, such as the median diameter, and employ a factor that adjusts for various mixtures. First, however, it is necessary to hypothesize on the behavior of the Shields parameter in a particular flow regime. The particular regime of flow is riprap on steep slopes, subject to overtopping flow. Considering the formulation of the Shields parameter, comments by Shields [19], and experimental evidence, Shields parameter is constant in this flow regime. The premises for this hypothesis are established in Chapter 2.

The second hypothesis addresses the problem of various sizes of rock that constitute a riprap mixture. It is possible to develop a factor that, besides the median rock size, describes the

entire mixture. A simple factor for describing a mixture is a uniformity coefficient. A uniformity coefficient usually consists of a ratio of two or more size fractions of a mixture. A typical arrangement of the ratio results in a dimensionless value. The uniformity coefficient is one possible means of correlating hydraulic properties and riprap mixture properties. This correlation becomes a useful tool for the designer to assess the influence of uniformity upon the stability of a riprap mixture in overtopping flow.

The goal of this investigation is to derive a physically based, empirically calibrated expression for sizing a riprap mixture to withstand a prescribed flow in a set geometry. The geometry is a sloped plane, with flow parallel to the slope. The derivation begins with the Shields parameter. The Manning and Strickler equations, coupled with the Shields parameter, lead to an expression for the median rock size as a function of the unit discharge and slope.

The Manning, Strickler, and Shields equations have their own basis and governing conditions for its application. The Manning equation requires rough, uniform flow. Strickler [11] originates in the same way as the Nikuradse data analysis by Williamson [24]. Nikuradse and Strickler agree, and both follow the one-sixth power law of flow resistance. The Shields parameter has its own unique set of assumptions. These assumptions directly influence the interpretation and application of the Shields parameter. Therefore this investigation concentrates on the Shields parameter.

The riprap mixtures described in this investigation are typical, well graded, and poorly graded, dump placed, angular rock, mixtures. The hydraulic properties are the result of the material and geometry that were varied in a systematic fashion. Comparing the experimental data with predictions exposes some fallacies regarding the assumptions of hydraulic properties and factors. For instance, flow on steep slopes of high roughness induces air entrainment. It is logical to hypothesize that an air-water solution produces a slightly different hydrodynamic force field on

the riprap layer than a water-only solution. Yet hydraulic factors such as unit weight of water, and shear stress assume a water-only solution. The third hypothesis explains the effect of aerated water upon the stability of a riprap layer.

The first hypothesis is that the Shields parameter is descriptive of the mechanics of riprap in flowing water. If that assumption is true, then it is possible to pose the related hypothesis that the Shields parameter is constant in the regime of flows typical of riprap in overtopping flow. This hypothesis allows the coupling of the Shields parameter with the Manning and Strickler formulas. Chapter 2 presents the premises and draws conclusions that support the first hypothesis. Chapter 3 presents background of the investigation and resulting data.

Considering the data in Chapter 3, Chapter 4 poses the second hypothesis, that a single particle cannot describe a riprap mixture. Chapter 4 presents arguments and data supporting the hypothesis and presents a factor that describes an entire riprap mixture. This factor, the coefficient of stability, $C_s$, is applicable to the coupled Manning-Strickler and the Shields parameter formula as well as the Abt formula.

Chapter 5 combines the Manning and Strickler formulae with the Shields parameter. The resulting formula expresses the median particle size as a function of unit discharge and slope. Then, comparing the composite formula with the Abt formula, the chapter poses the third hypothesis of the investigation. The third hypothesis states that the difference between the analytical and empirical formulas is caused by previously undetermined effects of air in the solution. These effects are manifested in overestimated values of the hydraulic radius. Chapter 5 presents a factor, the aeration correction coefficient, $A_c$, that compensates for the overestimation.

The final chapter presents examples that demonstrate the factors $C_s$ and $A_c$, and supports the third hypothesis. One example utilizes the aeration compensation factor along with the well known Stability Factors [22] method. The aeration compensation factor corrects a potentially

serious deficiency in the method, that being the overestimation of median particle size on plane slopes greater than roughly two percent.

The culmination of this investigation will provide a physical and analytical basis for an empirical equation by Abt [1]. Further, the Abt equation will be generalized for variable riprap mixtures. Finally, this investigation will further the understanding of fluid behavior on steep slopes. The highly turbulent and aerated flow typical of flow over riprap on steep slopes experiences less shear than previously thought, due to aeration. The aeration compensation factor derived in this investigation reduces estimates of shear stress, thereby reducing the predicted median size of the riprap mixture.

# CHAPTER 2

## THE SHIELDS PARAMETER

The Shields parameter is a dimensionless form of shear stress that expresses the mechanics of riprap in flowing water. The parameter is an elegant descriptor of the primary factors and their relationships influencing the stability of riprap in overtopping flow conditions. However, because of many assumptions necessary to derive the common form of the Shields parameter, it is a poor tool for designing riprap. This chapter describes the Shields parameter and the Shields diagram, discusses the advantages and drawbacks to the parameter, and lays the basis for using the Shields parameter to derive a comprehensive riprap design equation.

### Background

Shields [19] published "Anwendung der Aehnlichkeitsmechanik und der turbulenz-forschung auf die geschiebebewegung: Mitteilung der Preussischen Versuchsanstalt fuer Wasserbau und Schiffbau" in 1936, in the German language. Most papers cite the translated title "Applications of similarity principles and turbulence research to bed-load movements." Quoting from the translation [20], Shields main proposition is:

> "The ratio of the active force of the water parallel to the bed, to the resistance of a grain on the bed is a universal function of the ratio of the grain size to the thickness of the laminar sublayer."

From Gessler [9] the following relationship puts Shields words into mathematical form.

$$T = \frac{\tau_{cr}}{(\gamma_s - \gamma)k} = f_1\left(\frac{k}{\delta_1}\right) = f_2\left(\frac{u_* k}{\nu}\right) \tag{1}$$

$T$ .....Shields Parameter
$\tau_{cr}$ .....Critical shear stress

$\gamma_s$ .....Specific weight of the grain
$\gamma$ .....Specific weight of the fluid
$\delta_1$.....Thickness of the laminar sublayer
$\nu$ .....Kinematic viscosity
$u_*$.....Shear velocity, $u_* = \sqrt{\tau/\rho}$
$\rho$ .....Density of fluid
$\tau$ .....Bottom shear stress
$k$ .....Grain size

Shields determined the functions $f_1$ and $f_2$ experimentally. Gessler [9] describes the difficulty of defining incipient motion.

> "During the course of the experiments the difficult question of the definition of incipient motion arose; due to various reasons the uniform size grains did not all begin to move at the same time. Shields defined the beginning of motion in the following way: he found in experiments with different bottom shear stresses, that were just above critical, small bedload transport rates per unit time. He extrapolated the function for bedload movement dependent on bottom shear stress obtained in this way in the direction of decreasing bottom shear stress to the point where the bedload transport is zero. He called the corresponding shear stress of this point the 'critical shear stress'."

Many early definitions of incipient motion were based upon the visual observations of the experimenters and thus were subject to human judgment. A number of researchers had worked on the definition and had failed to precisely define incipient motion. By defining "critical shear stress," Shields brought order to the pursuit of the answer to the incipient motion problem. Shields greatest contribution was the expression of shear in dimensionless form. However, that form has led to uninformed charges of spurious correlation that continue today.

Shields plotted the data in the functional form of equation 1 without fitting a curve to the data. Indeed, Shields had only one data point in what he called the third region of the diagram. This data point was not original with Shields, Gilbert [10] provided the point. The third region, according to Shields, is the region beyond Boundary Reynolds number of 1000.

Three years after Shields, Rouse [14] added a curve [29] to the Shields diagram. Rouse adopted Shields speculation that the parameter is constant in the third region and used the Gilbert

data point (0.060) as the constant value of the curve in this region. This value of the Shields parameter is still widely quoted.

Gessler [9] adjusted Shields data. By removing shear due to bed forms, Gessler concluded that the constant value of the Shields parameter is 0.047. Meyer-Peter & Müller [12] arrived at the same value in their bed-load formula. In addition to adjusting the Shields parameter, Gessler redefined the definition of incipient motion. Adding to Shields, Gessler contended that incipient motion is a random process. By this definition, the Rouse curve represents a mean probability of motion. Gessler proposed a Gaussian distribution for the probability of a particle remaining at rest, with a mean value of 0.047 and standard deviation, $\sigma$, of 0.57 in the shear stress term. Gessler attributed this value of $\sigma$ to Einstein [6]. However, Einstein reports the value to be 0.364. Einstein and Gessler both claim that $\sigma$ is a constant.

Shen [17] proposed a new value for the Shields parameter. In the region above Boundary Reynolds number of $10^3$, Shen proposes a value of 0.250. Shen attributed the transition to 0.250 from 0.060 as a correlation to the drag reduction occurring at particular Reynolds numbers, as reported by Schlicting [15].

The first hypothesis of this investigation is that the Shields parameter is indeed constant and has the value of 0.047 in the third region of the Shields diagram. The following sections present the arguments for the first hypothesis.

## The Shields Parameter

Examination of the mechanics of particles in flowing water by fractional analysis leads to four derivations of the Shields parameter.

### *Fractional Analysis: The Pi Theorem*

The Pi theorem is a process for methodically creating dimensionless parameters. The variables are the characteristic dimension of the particle, $k$, the mass density of the particle, $\rho_s$, the

acceleration of gravity, $g$, the mass density of the fluid, $\rho$, and the local fluid velocity, $u$. Matrix 1 shows the pertinent variables and their dimensions.

| *Variable* | *Mass* | *Length* | *Time* |
|---|---|---|---|
| $k$ | | 1 | |
| $g$ | | 1 | -2 |
| $\rho$ | 1 | 3 | |
| $\rho_s$ | 1 | 3 | |
| $u$ | | 1 | -1 |

*Matrix 1. Fractional analysis dimension matrix.*

The rank of the matrix is one indicating a single dimensionless variable group, symbolized by $T$. The uppercase "T" indicates a dimensionless relationship to the shear stress. The Greek letter $\tau$ is the common symbol for shear stress.

$$T = \mathrm{f}\left(\frac{\rho u^2}{\rho_s g k}\right) \Leftrightarrow \frac{\frac{m}{l^3}\frac{l^2}{t^2}}{\frac{m}{l^3}\frac{l}{t^2}l} \tag{2}$$

If $u$ is proportional to $u*$, then

$$T = \mathrm{f}\left(\frac{\tau}{\gamma k}\right) \tag{3}$$

a simple form of the Shields parameter.

## *Fractional Analysis: Similitude*

Similitude is a proportional comparison of forces, moments, or energy acting on a particle in a flow field. In all derivations of the Shields parameter assume that the particle in question occupies a position on the surface of a riprap mixture. The surface particles are directly subjected to the hydrodynamic forces, and as such are the first particles to pass the threshold of incipient motion. Force similitude is the simplest case, considering the magnitude and direction of forces. Moment similitude adds another dimension to force similitude by considering the moment arms of

the forces. Energy supersedes force magnitude and direction by considering potential and mechanical energy of a system.

### *Forces*

There are two primary forces acting on a particle in flowing water: The gravitational force associated with the particle, and the inertial force of the flowing water. The gravitational force, or weight, is a function of the mass density, and volume of the particle. The inertial force is a function of the form of the particle, the projected area perpendicular to the direction of flow, the flow velocity about the particle, and the mass density of the fluid. Figure 1 shows a typical particle and the primary forces acting on the particle.

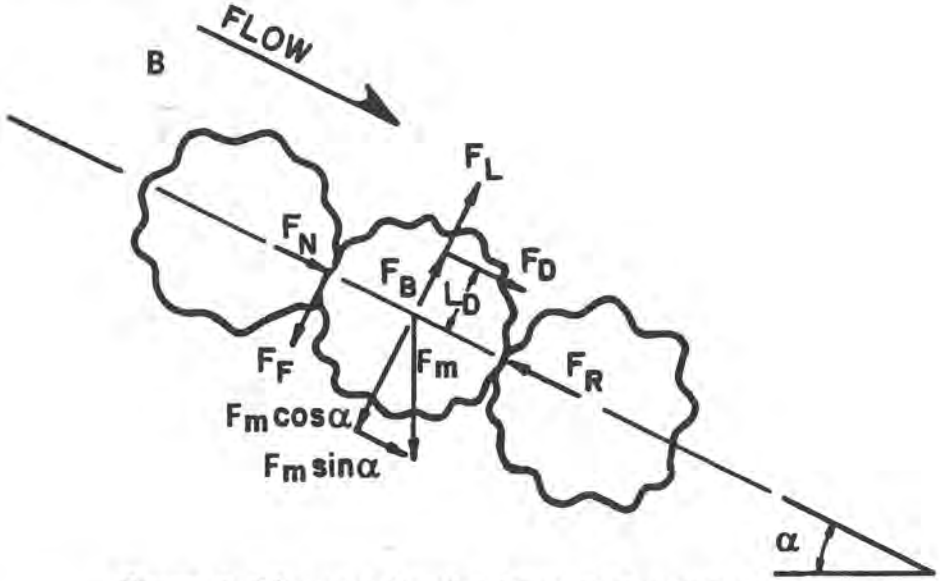


*Figure 1. Diagram showing forces and moment arms.*

The sum of the gravitational forces, $F_g$, in the slope-normal direction is the weight of the particle, $F_m$ plus the buoyant force, $F_b$.

$$\begin{aligned} F_g &= F_m + F_B \\ F_m &= mg\cos\alpha \\ F_B &= \rho V \end{aligned} \tag{4}$$

The gravitational force results from the following following proportionality's.

$$
\begin{aligned}
&V \propto k^3;\ m \propto \rho_s V = \rho_s k^3 \\
&F_m \propto \gamma_s k^3 \cos\alpha \\
&F_B \propto \gamma k^3 \\
&\therefore F_g \propto \gamma k^3 \left(S_s \cos\alpha - 1\right)
\end{aligned} \tag{5}
$$

The inertial forces, $F_i$, are equal to the drag force, $F_D$, where $C_d$ is the coefficient of drag and $A$ is the projected area of the particle on a slope-normal plane.

$$
\begin{aligned}
&F_i = C_d \frac{u^2}{2} A\rho \\
&A \propto k^2 \\
&\therefore F_i \propto \rho k^2 u^2
\end{aligned} \tag{6}
$$

The velocity, $u$, is the mean local velocity about the particle. If the shear velocity, $u_*$, is proportional to $u$, then the ratio of gravitatilnal forces and interstitial forces is a dimensionless group.

$$
\begin{aligned}
&\frac{F_g}{F_i} \propto \frac{\gamma k^3 \left(S_s \cos\alpha - 1\right)}{\rho k^2 u^2} \\
&u \propto u_* = \sqrt{\tau / \rho} \\
&\therefore \frac{F_g}{F_i} \propto \frac{\gamma k \left(S_s \cos\alpha - 1\right)}{\tau} = constant
\end{aligned} \tag{7}
$$

The ratio of gravitational and inertial forces is the inverse of the Shields parameter. In terms of force, the safety factor is a ratio of the stabilizing or resistive forces to the destabilizing forces. As shown in Equation 7, the Shields parameter is the inverse of a safety factor, if gravitational forces are stabilizing and fluid inertial forces are destabilizing.

### *Moments*

The similitude of moments acting on a particle is very similar to force similitude. The additional factor in the moment analysis is a moment arm, $L_d$. Figure 1 shows a conceptual location of the moment arm because the line of action of both gravitational and inertial forces is difficult to define. Although the direction of the gravitational force is well defined, its location relative to the pivot point depends upon the location of the centroid of the particle. Likewise,

neither the direction or location of the buoyancy, lift, and drag forces are unknown. However, the location of each force, with respect to the pivot point, is a factor of the particle diameter, $D$, and it is convenient to think of $k$ as a factor of the particle diameter. A theoretical value of $k$ will be developed and some of the practical considerations of the factor are discussed in following sections. In any case, the location or line of action of all forces acting on the particle must pass within some factor of the particle diameter.

The following equations are derived by taking moments about a contact point, assuming that there is no force at the upstream and downstream contact points at incipient motion. The gravitational force acts through a distance $l$, a factor of the characteristic dimension, $k$.

$$\begin{aligned} &M_g = F_g l \\ &l \propto k \\ &F_g \propto \gamma\left(S_s \cos\alpha - 1\right)k^3 \\ &\therefore M_g \propto \gamma\left(S_s \cos\alpha - 1\right)k^4 \end{aligned} \tag{8}$$

The inertial force acts through the distance $l$, again a factor of the characteristic dimension $k$.

$$\begin{aligned} &M_i = C_d \frac{u^2}{2} A\rho l \\ &l \propto k \\ &A \propto k^2 \\ &\therefore M_i \propto \rho k^3 u^2 \end{aligned} \tag{9}$$

The velocity term is the mean local velocity, $u$, about the particle. If the shear velocity, $u_*$, is proportional to $u$, then the ratio of $M_g$, and $M_i$, is a dimensionless group.

$$\begin{aligned} &\frac{M_g}{M_i} \propto \frac{\gamma\left(S_s \cos\alpha - 1\right)k^4}{\rho k^3 u^2} \\ &u \propto u_* = \sqrt{\tau/\rho} \\ &\therefore \frac{M_g}{M_i} \propto \frac{\gamma k\left(S_s \cos\alpha - 1\right)}{\tau} = constant \end{aligned} \tag{10}$$

The ratio of the moments results in the additional length dimension dividing to unity. The same proportionality, the Shields parameter, therefore exists whether considering ratios of forces or moments. With the uncertainty in the direction of forces and lines of action, it helps to explore other properties of flowing water, mechanical and potential energy.

### *Energy*

The energy, $E_L$, required to lift an unconstrained particle from a position of rest is equal to the potential energy of the particle, one particle diameter above it's initial position.

$$E_L = mgD \tag{11}$$

The mass of the particle is equal to the volume times the buoyant mass density of the particle. The volume of the particle is proportional to the particle diameter cubed.

$$\begin{aligned} &m = V(\gamma_s \cos\alpha - \gamma) \\ &V \propto D^3 \\ &E_L \propto D\gamma(S_s \cos\alpha - 1)D^3 = \gamma D^4(S_s \cos\alpha - 1) \end{aligned} \tag{12}$$

The inertial energy, $E_I$, is a function of mass and the local velocity squared.

$$\begin{aligned} &E_I \propto \tfrac{1}{2} m u^2 \\ &E_I \propto \rho D^3 u_*^2 \end{aligned} \tag{13}$$

Again, assume that the shear velocity is proportional to the local flow velocity. The ratio of the inertial energy to the potential energy is another dimensionless group.

$$\frac{E_I}{E_L} \propto \frac{\rho D^3 u_*^2}{\gamma(S_s \cos\alpha - 1)gD^4} = \frac{\tau}{\gamma D(S_s \cos\alpha - 1)} = constant \tag{14}$$

Again the dimensionless group is a form of the Shields parameter. In this case the Shields parameter contains the factor $D$, the diameter of the particle. This indicates that the factor $k$ is related to the diameter, $D$. It is the relationship between the characteristic dimension, $k$, and the diameter, $D$, that is undefined. The lack of definition hinders direct application of the Shields parameter to riprap design.

## *Summary*

Three methods of deriving the Shields parameter were presented. Gessler [8] presents an exhaustive treatise on the physical derivations of the Shields parameter. In the following sections the assumptions made in the derivations will help explain the limitations of the Shields parameter.

### Boundary Reynolds Number

The particle or Boundary Reynolds number is the ratio of two forces, the inertial, $F_i$, and viscous forces, $F_V$.

$$\begin{aligned} F_i &\propto \rho k^2 u^2 \\ F_V &\propto k u^2 \mu \frac{du}{dy} \end{aligned} \tag{15}$$

As with the Shields parameter, the assumption is that the shear velocity is proportional to the local velocity. Also, the shear stress, defined as the differential $\mu\frac{du}{dy}$ is proportional to $\mu\frac{u_*}{k}$. Following these two assumptions, the Boundary Reynolds number, $\mathrm{Re}_*$ is the ratio of the inertial and viscous forces in the boundary layer of the flow. Note that $\mathrm{Re}_*$ is a dimensionless parameter.

$$\begin{aligned} \frac{F_i}{F_V} &\propto \frac{\rho k^2 u^2}{k^2 \mu \frac{du}{dy}} = \frac{u^2}{\mu \frac{du}{dy}} \\ \therefore \frac{F_i}{F_V} &\propto \frac{u_* k}{\nu} = \mathrm{Re}_* \end{aligned} \tag{16}$$

Some argue that there is a spurious correlation between the Shields parameter and the Boundary Reynolds number, that is there is no functional relationship as stated in equation 1. The origin of the spurious correlation argument is the use of the same assumption regarding the local velocity. Substituting the shear velocity for the local velocity in both the derivation of the Shields parameter and the Boundary Reynolds number leads to both terms using the same variables. The derivations shown here refute the spurious correlation argument.

The purpose of this section is to show the physical basis of both the Shields parameter and the Boundary Reynolds number, their independence, and thus dispel assertions of spurious correlation. Shields presented the functional relationship between the Shields parameter and the Boundary Reynolds number in graphical form, the Shields diagram.

## The Shields Diagram

The Shields diagram, Figure 2, shows a functional relationship between what Shields described as a dimensionless shear stress on the ordinate axis, and the Boundary Reynolds number, on the abscissa. The basis of this data is Shields definition of incipient motion, that is, the dimensionless shear and corresponding Boundary Reynolds number at zero bedload. The data delineating the curve were obtained by Shields and several other workers from experiments with fully-developed turbulent flows and artificially flattened beds of noncohesive sediments.[29]

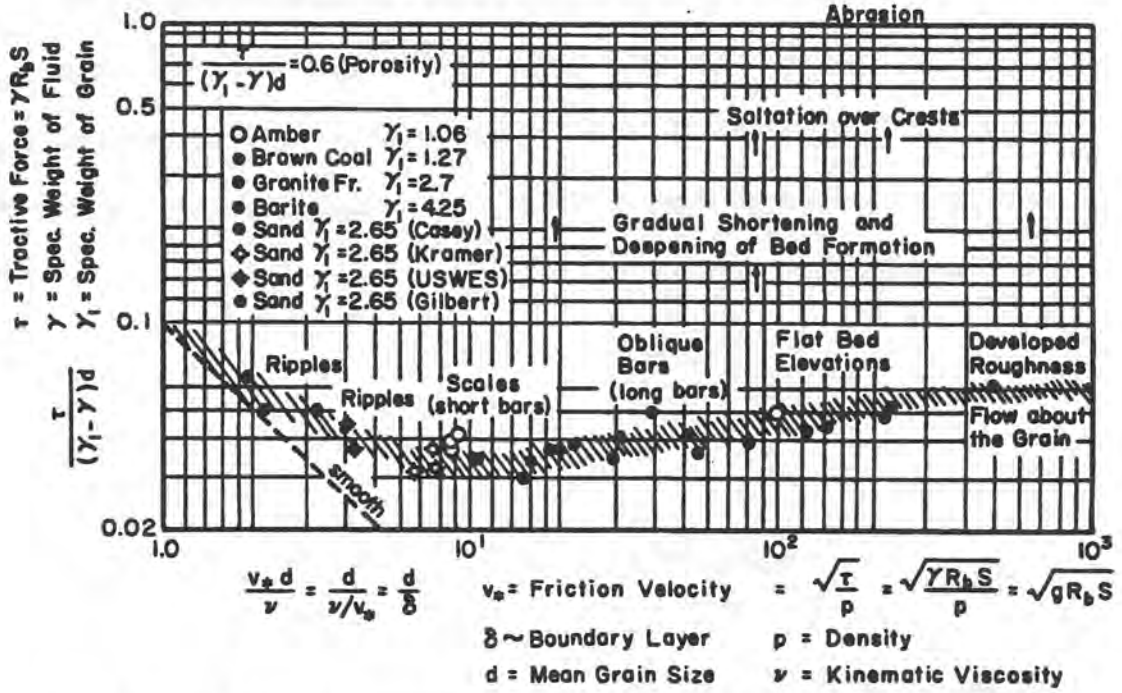


*Figure 2. The Shields diagram (from translated version of Shields paper by Ott).*

Rouse [14] later added the curve shown in Figure 3. The Rouse curve plots a constant Shields parameter, $T_c$, of 0.06 at $\mathrm{Re}_* > 10^4$.

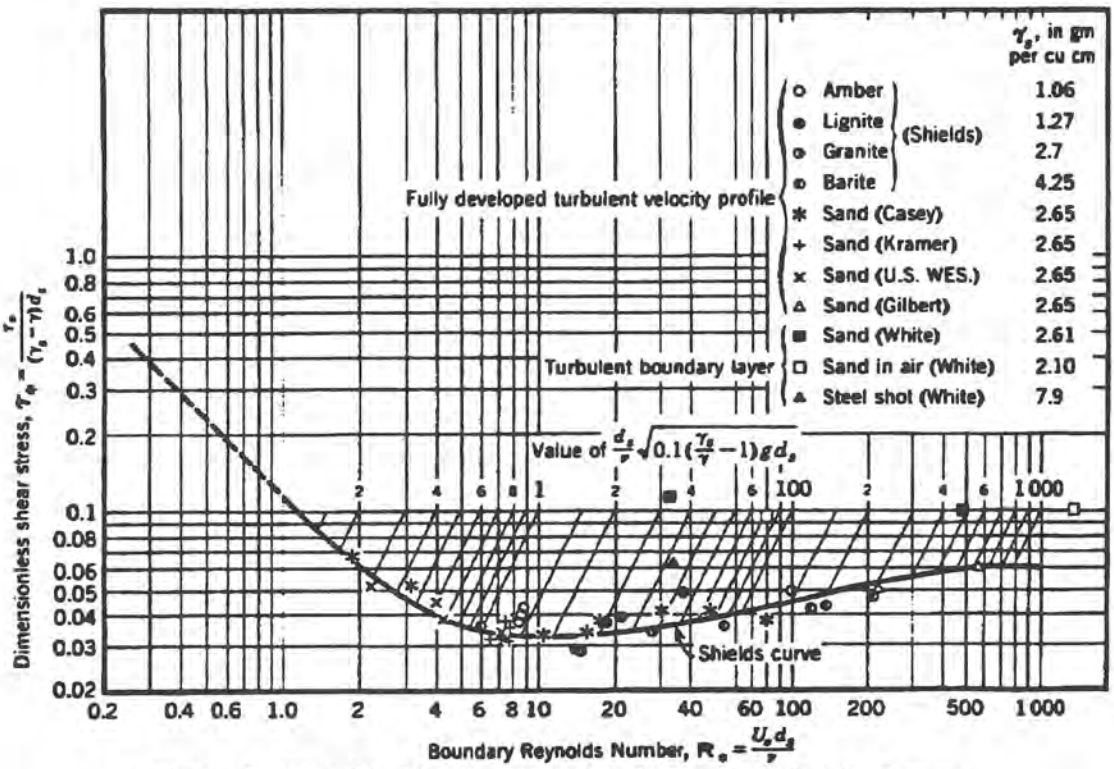


*Figure 3. The Shields diagram with the curve fitted by Rouse.*

Gessler [9] corrected Shields data and plotted Figure 4. Gessler asserted a Gaussian distribution of the probability of a particle of dimension $k$, staying at rest, indicated by the family of curves about the mean value, $\mu$, of 0.047 with a standard deviation , $\sigma$,. The probability function is a Gaussian distribution.

$$q = \frac{1}{\sqrt{2\pi}} \int_{-\infty}^{z_o} e^{\left(-z^2/2\right)} dz \tag{17}$$

where,

$$z_o = \frac{\frac{T_o \gamma (S_s - 1) D}{\tau} - 1}{\sigma} \tag{18}$$

The influence of $\sigma$ is clear from the expression for the upper limit of the integrand. If $\sigma$ is relatively small, indicating a narrow bandwidth of turbulent fluctuations, then $z_o$ is relatively large. Therefore, for a marginal increase in shear stress, there is only a marginal increase in the

probability of incipient motion. However, if $\sigma$ is relatively large, indicating a wide bandwidth of turbulent fluctuations, then $z_o$ is relatively small. Therefore, for a marginal increase in shear stress, there is a significant increase in the probability of incipient motion. The value of $\sigma$ may be related to the uniformity of the riprap mixture. For instance, a well graded material may produce a narrow band of turbulent fluctuations while a poorly graded mixture may produce a wide band of turbulent fluctuations. Future research should focus on the exact behavior of $\sigma$ as a function of mixture uniformity.

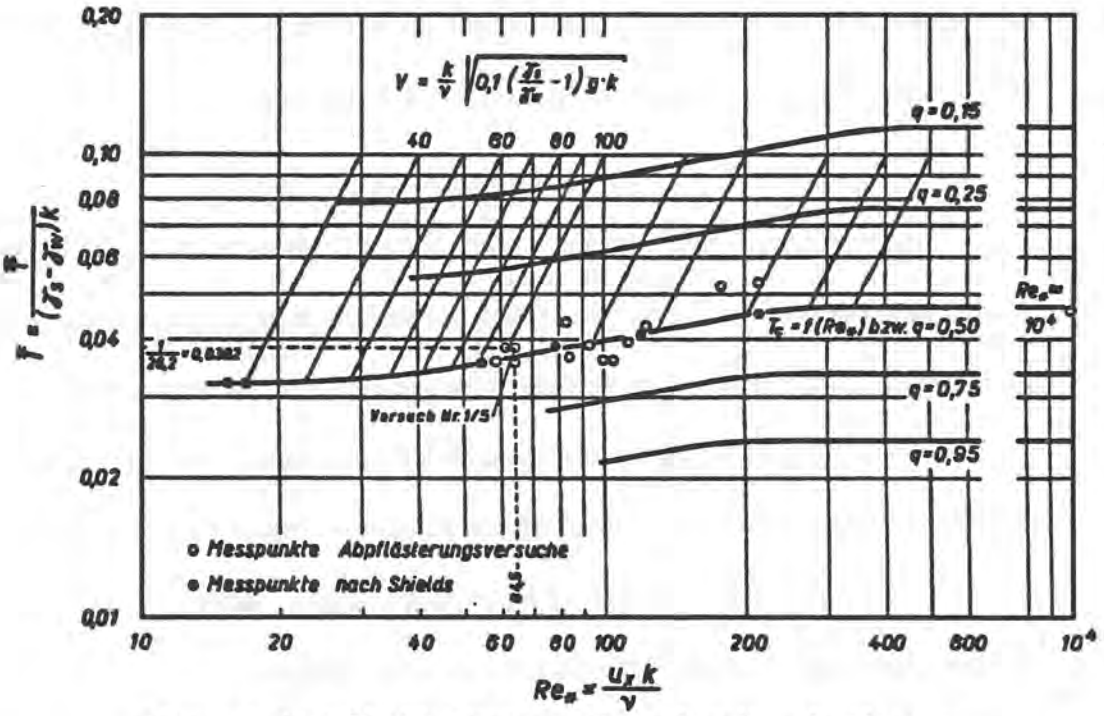

*Figure 4. The Shields diagram with modifications by Gessler.*

## Practical Aspects of the Shields Parameter

The following sections discuss some of the practical aspects of the Shields parameter. There is a section addressing the reliability of the estimate of the constant value of the Shields parameter, who made the estimates and how they have evolved. Other sections discuss the role of the angle of repose, the assumptions regarding the drag, lift, buoyancy, and weight of the particle, and the physical meaning of the variable $k$, contrasted with the accepted dimensional meaning.

### *The Gessler Correction to the Shields Parameter*

Gessler proposes that the constant value of the critical shear stress, $T_c$, is 0.047. Shields neglected to account for shear stress due to form drag from ripples and bed forms. Shields overestimated the value of the parameter by not accounting for the additional shear. Gessler removed the extra shear and adjusted the value of $T_c$ from 0.06 to 0.047. Gessler also redefined incipient motion when he recognized the dynamic nature of the forces resulting in incipient motion. Gessler [9] defines incipient motion as the state where a particle has a fifty percent probability of motion. Adopting this definition leads to a family of curves, normally distributed around the mean curve. Figure 4 shows the Shields diagram as corrected by Gessler.

### *Angle of Repose of Natural Material*

Notably absent from the common form of the Shields parameter is the angle of repose. Natural materials become unstable when posed, not stacked, at angles greater than or equal to the angle of repose. An example is sand poured into a pile until particles begin to slip down the face of the pile. The natural angle that the face forms with the horizontal is the angle of repose. As the material nears the angle of repose, the weight of the particles causes the particle to slide down the face of the pile. No external force is necessary to dislodge the particle. The Shields parameter does not allow for this condition and ignores a boundary condition.

A careful analysis [23] of the mechanics, considering moments about a downstream pivot point, leads to the following form of the Shields parameter.

$$\frac{\tau_{cr}}{\gamma(S_s\cos\alpha-1)k(\cos\alpha\tan\psi-\sin\alpha)}=constant \tag{19}$$

The factor $(\cos\alpha\tan\psi-\sin\alpha)$ indicates the behavior of the Shields parameter on various slopes, $\alpha$, and for various angle of repose, $\psi$. Since the ratio remains constant, as the slope approaches the angle of repose, the critical shear stress, $\tau_{cr}$, diminishes to zero. This condition indicates

incipient motion with no external forces. If the slope is greater than the angle of repose, then a shear in the upslope direction is necessary to maintain stability. If the slope is horizontal, then the factor becomes $\tan\psi$, a constant for a given material. Since most experiments with the Shields parameter are for very shallow slope applications, it is not surprising that consideration for these mechanics has not been widely published. However for riprap on steep slopes, these considerations are very important.

### *Drag, Lift, Buoyancy, and Weight*

Drag is the momentum deficit caused by flow about a particle. Drag is assumed to act over the area of a particle projected onto a plane perpendicular to the flow direction. This projection becomes very complex for irregular shaped materials. Porous materials also add to the complexity of the projection. Nevertheless, the projection is in the vertical plane.

Lift is the drop in pressure due to compressed stream lines acting on the area of the particle projected onto a plane parallel to the flow direction. Buoyancy and weight are each a factor of the volume of the particle. The remaining factor in buoyancy is the unit weight of the fluid. The remaining factor in the weight is the unit weight of the material.

Formulation of the Shields parameter requires the quotient of the weight, buoyant, lift, drag, and resultant forces. In the formulation, a volume divided by a projected area results in the variable $k$, with the dimension of length. Since both the volume and area of a particle are a function of the diameter of the particle, $k$ must also be a factor of the diameter.

Drag acts on a line parallel to the direction of flow. Lift acts in a direction perpendicular to the stream lines, or more simply the mean flow vector. Similarly, buoyancy acts perpendicular to the stream lines or the mean flow vector. Weight, however, acts parallel to gravity. On shallow slopes the difference in lines of action between buoyancy and weight is considered negligible and the two forces are assumed to act in the same direction. However, on steep slopes, the difference is

appreciable. This difference between buoyancy and weight shows up as the factor $S_s \cos\alpha$ in the formula for the Shields parameter.

### *The Characteristic Dimension k*

The characteristic dimension resulting from the quotient of forces that create the Shields parameter is symbolized by the factor $k$. The factor $k$ in the Shields parameter has the dimension of length. It is commonly assumed to be the diameter, $D$, of the particle. In reality, it is both the quotient of the volume and horizontal projection of the area of the particle and the quotient of the volume and the vertical projection of the area of the particle. If the particle in question is a sphere, then analytically, $k$ is equal to $2/3D$, or fractionally, $D_{67}$. In nature, very few particles are spherical. In a mixture of riprap, no two rocks share the same shape. Therefore, $k$ varies as the particles in a mixture of riprap.

### *Steep Slope: S or sin$\alpha$?*

Engineers often assume the bottom tractive force, or shear stress, $\tau$, to be equal to the product of the unit weight of water, $\gamma$, the hydraulic radius, $R$, and the slope, $S$.

$$\tau = \gamma RS \tag{20}$$

The basis of equation 20 rests upon the following assumptions: Normal depth of flow, wide channel such that the hydraulic radius is roughly equal to the depth, $d$, and a shallow slope such that $S$ is roughly equal to $\sin\alpha$. Both Henderson [11] and Chow [4] indicate that $S$ refers to $\sin\alpha$. The distinction is often ignored in practice. The tractive force is the resolved weight of a control volume of water shown in Figure 5. The volume has an area in contact with the wetted perimeter, $p$, with dimension $pl$, where $l$ is a unit distance in the stream wise direction, while $p$ is perpendicular to the flow. The thickness of the volume is the depth, the dimension perpendicular to the bed, $d$. The bed slopes at an angle $\alpha$. The flow is uniform so that the hydrostatic forces at the upstream and downstream ends of the control volume negate each other.

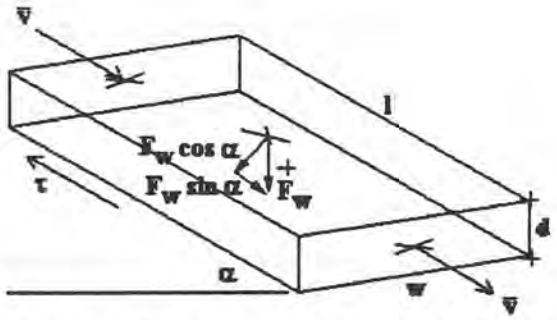


*Figure 5. Control volume for deriving an expression for shear stress.*

$$w = control\ volume\ width$$
$$A = wd \tag{21}$$
$$\tau = \frac{\gamma A l}{p l}\sin\alpha = \gamma R \sin\alpha$$

If $S$ is mistaken as $\sin\alpha$, the error is less than one percent until the slope exceeds roughly 15%. On embankments where slopes approach 33% the error is roughly five percent.

### *Relative Submergence*

Shields and others developed data in flows with large relative submergence. The definition of relative submergence, $\lambda_{sub}$, is the ratio of water depth to particle size.

$$\lambda_{sub} = \frac{d}{D} \tag{22}$$

$d$ .....Fluid depth
$D$ .....Grain size

Wittler and Abt [25] show that the stability factor method of Stevens [22] becomes increasingly conservative as slope increases. The question arises as to whether the stability factor method applies to flow that is steep, rough, and has relative submergence much less than tested by Shields. Shen [17] [16] proposes that the value of the Shields parameter is roughly five times greater at Boundary Reynolds numbers greater than $10^4$ than the accepted value of 0.047 at Boundary Reynolds number $170 < Re_* < 10^4$. The observations of Wittler, Abt, and Shen raises a question regarding the Shields parameter. If the Shields parameter is the basis of the stability factors riprap design method, and Shen has observations of increase values of the Shields parameter based upon

fields measurement, is the Shields parameter constant in the flow regime where $Re_* > 10^4$? This question is also the basis of the first hypothesis of this investigation. An answer to the question is presented in the following section on the behavior of the Shields parameter at $Re_* > 10^4$.

The assumption that the local velocity, $u$, is proportional to the shear velocity, $u_*$, bears further investigation. Gessler [8] states

> *"...some of the discussion about effect of relative depth on incipient motion probably reflects the fact that introducing mean velocity instead of shear velocity necessarily leads to such an apparent effect."*

Shear velocity, $u_*$, and mean velocity, $u$, are related by the log-velocity law.

$$\frac{\bar{u}_y}{u_*} = 5.75 \log_{10}\left(30.2 \frac{yx}{D}\right) \tag{23}$$

The logarithmic term contains a relative submergence term, $y/D$. The effects of relative submergence are not clear. However, in an intuitive sense, the differing regimes of flow of Shields and steep, air-entrained, low submergence flow, suggests that some effect may exist. Shields tested millimeter sized material in flow with a slope less than one-hundredth of one percent and greater than a meter in depth. Shen and Abt tested flow with slopes three orders of magnitude greater, material size two and one-half orders of magnitude greater, and relative submergence three orders of magnitude greater than Shields. Even though the basis of the Shields parameter is a ratio of forces, the assumptions that allow simple quantification of those forces may not apply to these vastly different regimes of flow.

## Behavior of the Shields Parameter at Boundary Reynolds Number >$10^4$

How does the Shields parameter behave in flow regimes not considered by Shields, yet common to riprap in overtopping flow?. The question is important since the Shields parameter is an integral part of riprap design. The Shields parameter describes the mechanics of incipient motion, or in riprap terminology, failure. Investigators such as Shen [16][17] assert that the

Shields parameter is not constant for Boundary Reynolds number greater than $10^4$. Characteristics of this flow regime are low relative submergence ($d/D_{50} < 5$) and bulked or aerated water. The hypothesis of a constant Shields parameter in this flow regime will be proved.

## *Rationale for a Constant Shields Parameter*

The following sections address reasoning supporting the hypothesis that the Shields parameter is constant in the third region of the Shields diagram where $Re_* > 10^4$. The basis for analyzing the Shields parameter in the large Boundary Reynolds number region are the assumptions made in the derivation of the Shields parameter and making hypothetical modifications to the force, moment, or energy ratios.

There are three regions in the Shields diagram. The characteristic of the first region is the non-constant value of the Shields parameter that corresponds to the laminar boundary layer regime where the Boundary Reynolds number is less than roughly 200. The second region is characterized by a Boundary Reynolds number greater than 200. In this region, the value of the Shields parameter is constant. Shen proposes that in the third region, where the Boundary Reynolds number is greater than $10^4$, the constant value increases from 0.06 (corrected to 0.047 by Gessler) to 0.25, and then remains constant. Application of riprap design procedures such as Stability Factors [22] in a steep, low submergence flow regime, requires knowledge of the behavior of the Shields parameter. Both Shen [16][17] and Abt [1] report values of the Shields parameter much greater than 0.047 in the region where $Re_* > 10^4$.

### *Shen*

Shen and Wang [16][17] propose that the Shields parameter achieves a constant value of 0.25 at $Re_* > 10^4$. They base this proposition on data collected in China in flood channels. Figure 6 shows the proposed behavior of the Shields parameter. The mean relative submergence of

the tests by Shen and Wang is 7.9 and the average energy slope is 0.047, or 4.7 percent. Shen and Wang explain the increase in the Shields parameter as a drag reduction that Schlicting [15] reports occurring at Reynolds number of $10^5$ to $10^6$. Shen used the median stone size, $D_{50}$, for $k$ (or d in Figure 6) in the calculations of the Shields parameter (K* in Figure 6). Shen did not document the flow depth and slope measurement techniques.

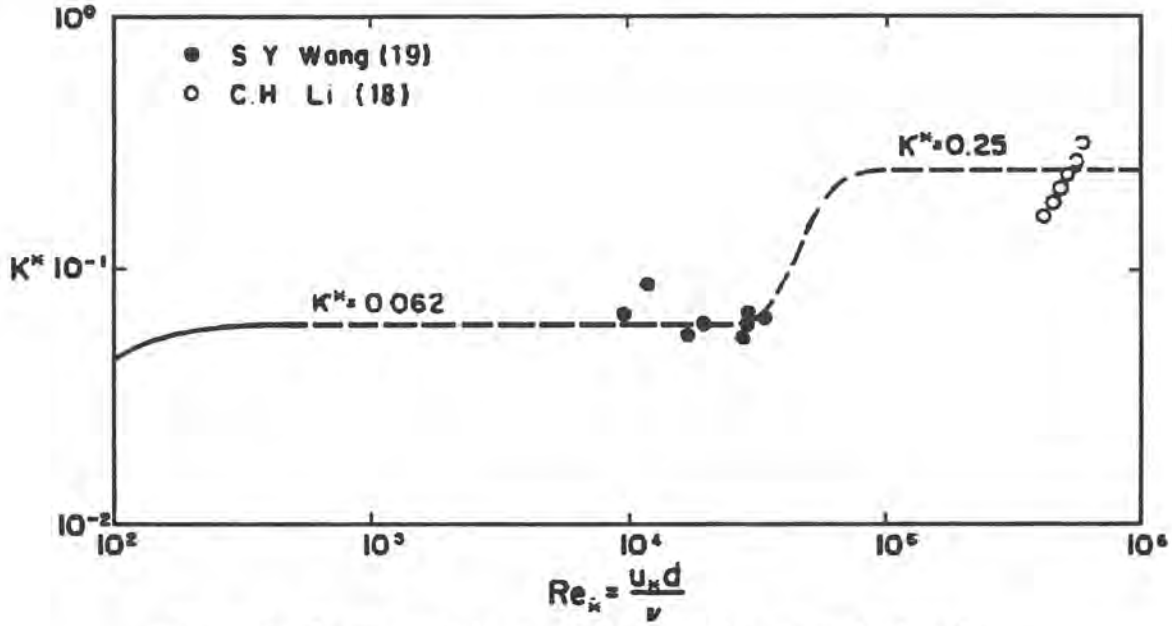


*Figure 6. Proposed behavior of the Shields parameter by Shen.*

***Abt***

The results of Abt et. al. [1] are similar to those of Shen. Abt reported maximum Shields parameter values of 0.12. Abt used the median stone size, $D_{50}$, for $k$ in calculations of the Shields parameter. Median rock sizes of 1, 2, 3, 4, and 6 inches were tested on bed slopes of 1%, 2%, 5%, 10%, 15%, and 20%. Relative submergence ranges from 0.48 to 2.01. Abt reported highly aerated flow, periods of instability followed by periods of stability. Each embankment was tested to ultimate failure of the riprap blanket. The flow depth was the piezometric head measured at the filter-riprap interface corrected to the virtual riprap surface.

## *Aeration-Bulking*

Aeration or bulking is the process of ingesting air into flowing water. Air is ingested by a mechanism related to the momentum and viscosity of the air-water interface. The practical effect of aeration is an inflated depth of flow and a deflated fluid density. Equation 7 facilitates a hypothetical demonstration of the effects of aeration upon the Shields parameter.

$$\frac{F_g}{F_i} \propto \frac{\gamma k^3 (S_s \cos\alpha - 1)}{\rho k^2 u^2}$$
$$u \propto u_* = \sqrt{\tau/\rho} \qquad (7)$$
$$\therefore \frac{F_g}{F_i} \propto \frac{\gamma k (S_s \cos\alpha - 1)}{\tau} = constant$$

The gravitational force has four components: gravitational acceleration, $g$, particle mass density, $\rho_s$, fluid mass density, $\rho$, and characteristic dimension, $k$. Gravitational acceleration is not influenced by aeration nor is the particle size and particle mass density. Therefore, in the numerator of the force ratio, aeration influences only the mass density of the fluid.

The inertial force has three components: fluid mass density, $\rho$, particle size, $k$, and the local velocity, $u$. The characteristic dimension is not influenced by aeration. It is unclear whether aeration increases or decreases the local velocity. Therefore aeration influences only fluid mass density in the inertial force.

A simplified form of equation 7 shows how aeration might influence the Shields parameter, $T$. The subscript 'a' indicates an aerated condition.

$$T_a \propto \frac{\rho_a}{(\rho_s - \rho_a)}$$
$$\rho_a = aerated\ fluid\ mass\ density \qquad (7a)$$
$$T_a = aerated\ Shields\ parameter$$

Assuming that the air water mixture is 50% air and 50% water.

$$\frac{T}{T_a} = \frac{\dfrac{(\rho_s - \rho)}{\rho}}{\dfrac{\rho_s - \rho_a}{\rho_a}} \tag{24}$$

If the particle has a specific gravity of 2.65, then

$$\frac{T}{T_a} = \frac{\dfrac{(2.65-1)}{1}}{\dfrac{2.65-5}{5}}$$

$$\frac{T}{T_a} = 0.384 \tag{25}$$

$$\therefore T_a = 2.6T$$

Equation 25 shows that 50% aeration causes the calculated value of the Shields parameter to be 2.6 times greater than actual.

One effect that aeration has on the Shields parameter is the determination of measured factors in laboratory or field measurements. The form that Shields proposed demonstrates the errors that can creep into field or laboratory measurements.

$$T = \frac{\tau}{(\gamma_s - \gamma)k} = \frac{\gamma RS}{(\gamma_s - \gamma)k} \tag{26}$$

Assuming a 50%-50% air-water mixture, it is possible to examine the aeration effects upon measurements of the Shields parameter.

In aerated flow the fluid unit weight, $\gamma$, is overestimated. It is common to assume that $\gamma$ has a value of 62.4 lb/ft$^3$ when in actuality a 50% air-water solution weighs 31.2 lb/ft$^3$, an error factor of two. Bulking the water increases the volume without significantly increasing the weight. Consequently in a column of bulked water the hydraulic radius is similarly overestimated by a factor of two. Meanwhile, the buoyant weight of the particle is underestimated by a factor of 1.3 as shown in equation 27.

$$\frac{(\gamma_s - \gamma)}{(\gamma_s - 0.5\gamma)} = \frac{(2.65-1)}{(2.65-0.5)} = 1.30 \tag{27}$$

Therefore, the overall potential error results in overestimating the Shields parameter by a factor of 5.21 as demonstrated in the following calculation.

$$T = \frac{\tau}{(\gamma_s - \gamma)k}$$

$$\tau = \gamma RS$$

$$\frac{T}{T_a} = \frac{\dfrac{\gamma RS}{(\gamma_s - \gamma)k}}{\dfrac{\gamma_a R_a S}{(\gamma_s - \gamma_a)k}} \tag{28}$$

$$\therefore \frac{T}{T_a} = \frac{\dfrac{62.4(2R)S}{62.4(2.65-1)k}}{\dfrac{31.2RS}{62.4(2.65-0.5)k}} = 5.21$$

Recall that Shen [16][17] reported a five-fold increase in the apparent value of the Shields parameter over the corrected value of 0.047, while Abt [1] reported a two and one-half-fold increase using piezometric depth. The piezometric depth indicates the hydrostatic depth of flow, regardless of bulking, as shown in the development of the hydraulic radius in the section on steep slopes. If Shen used the bulked depth and non-bulked unit weight of water, then he could have simply miscalculated the values, creating an illusory effect. Abt on the other hand used the non-bulked weight but used piezometric depth, not bulked depth. This reduces the illusory effect by a factor of two. While miscalculating the Shields parameter, Abt came closer by a factor of two than Shen, to the true value of Shields parameter, 0.047. Clearly, aeration is not a rationale for asserting that the Shields parameter increases for any value of Boundary Reynolds number.

### *Coefficient of Drag*

The Shields parameter is the inverse of the ratio of the gravitational and inertial forces. Therefore, the Shields parameter is the ratio of the inertial and gravitational forces.

$$\frac{F_i}{F_g} \propto \frac{\rho k^2 u^2}{\gamma k^3 (S_s \cos\alpha - 1)}$$

$$u \propto u_* = \sqrt{\tau/\rho} \tag{7}$$

$$\therefore T = \frac{F_i}{F_g} \propto \frac{\tau}{\gamma k (S_s \cos\alpha - 1)} = constant$$

The numerator of the Shields parameter is an expression of the inertial force, that before any assumptions, is the product of the square of velocity, area, fluid density, and the coefficient of drag, $C_d$. Shen based the increase in the Shields parameter upon a corresponding decrease in $C_d$, as previously noted by Schlicting [15]. If $C_d$ decreases, then the numerator of the Shields parameter decreases, and therefore, the Shields parameter decreases.

$$F_i = C_d \frac{u^2}{2} A\rho \tag{6a}$$

Therefore, drag reduction is not a rationale for asserting that the Shields parameter increases in the region of the Shields diagram where the Boundary Reynolds number is greater than $10^4$.

## Conclusions

The purpose of this chapter is to investigate the behavior of the Shields parameter at Boundary Reynolds number greater than $10^4$. The hypothesis is that the Shields parameter is constant in this flow regime. Investigation of the background and derivation of the Shields parameter indicates that the Shields parameter should not increase, and indeed it is more likely that the Shields parameter decreases or remains constant when $Re_* > 10^4$. The apparent and reported increase in the Shields parameter is the incorrect assumptions regarding the measurement of flow properties and default values of unit weight of water in the calculation of the Shields parameter.

# CHAPTER 3

## FACILITIES, MATERIALS, AND PROCEDURES

This investigation utilizes data from three studies. The first two studies are by Abt [1]. This chapter describes the experiments performed for this, the third study.

### Facilities

The site of the experiments was the Engineering Research Center, Colorado State University, Fort Collins, Colorado, USA. The experimental flume was 3.0 ft (0.91 m) wide, 2.0 ft (0.61 m) deep, and 32.0 ft (9.75 m) long. The flume was simply supported and pivoted at the downstream support. A hydraulic lift allows the entire flume to tilt about the downstream support permitting a wide range of slopes, up to twenty percent. Figure 7 shows a schematic of the flume.

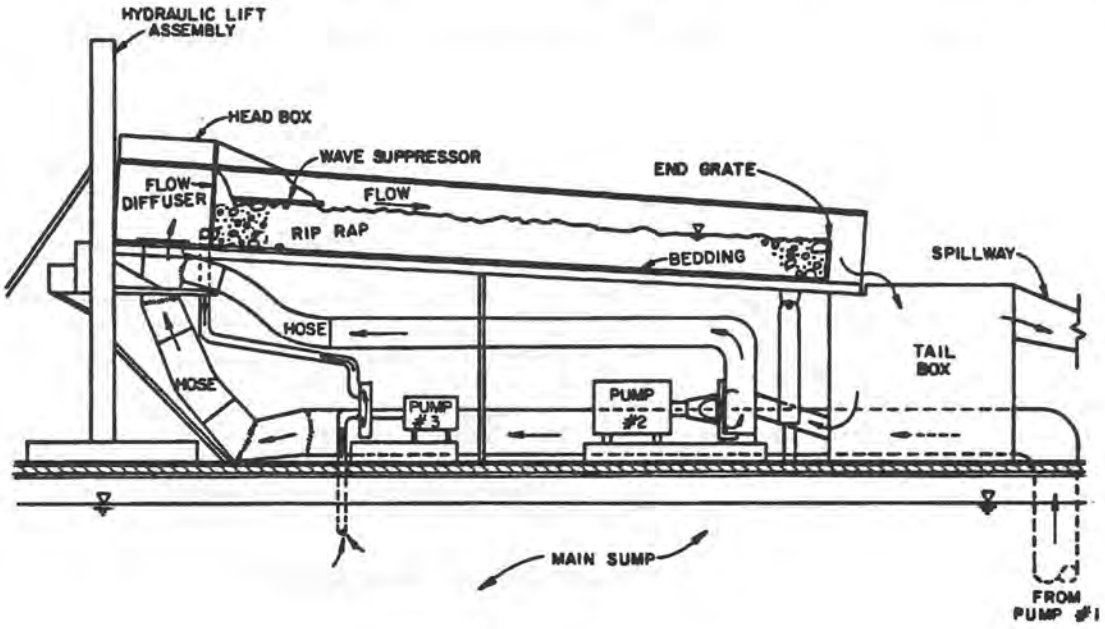


*Figure 7. Schematic of flume.*

Three pumps and pipeline networks supplied water to the flume, as shown in Figure 7. Pump #3 supplied small discharges for establishing and measuring interstitial flows. A Venturi meter measured discharge from this pump. The primary water supply was provided by a 14 inch, three-speed centrifugal pump, pump #1. An Annubar flow element measured discharge from this pump. The primary supply was augmented by an eight inch, two-speed centrifugal pump, pump #2. An eight inch by five inch orifice measured the discharge from this pump. The maximum combined discharge was roughly 10.0 $ft^3/s$ (0.283 $m^3/s$).

The flume was equipped with a walkway along the entire length of the flume. Instruments such as point gages and velocity probes were mounted upon a carriage that was supported by the walls of the flume. The Plexiglas flume walls allowed visual inspection of the substrates of the material placed in the flume. Figure 8 shows the coordinate system. Piezometers were installed on 5.0 ft (1.52 m) centers along the flume center line, beginning 6.7 ft (2.04 m) downstream from the flow diffuser as shown in Figure 9. The piezometers were placed between the bedding and riprap layers. This type of placement, similar to that of Abt [1], yields hydrostatic levels from the piezometer. Included in Figure 9 are details of the piezometer installations and two cross sections of the flume.

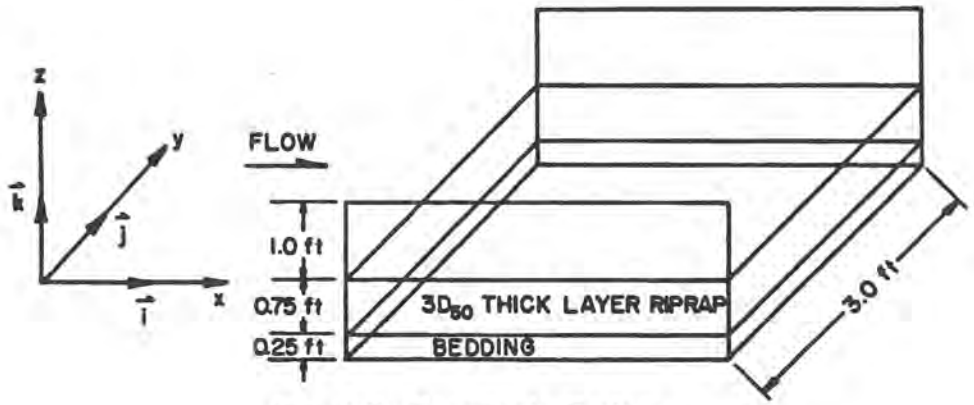


*Figure 8. Coordinate System*

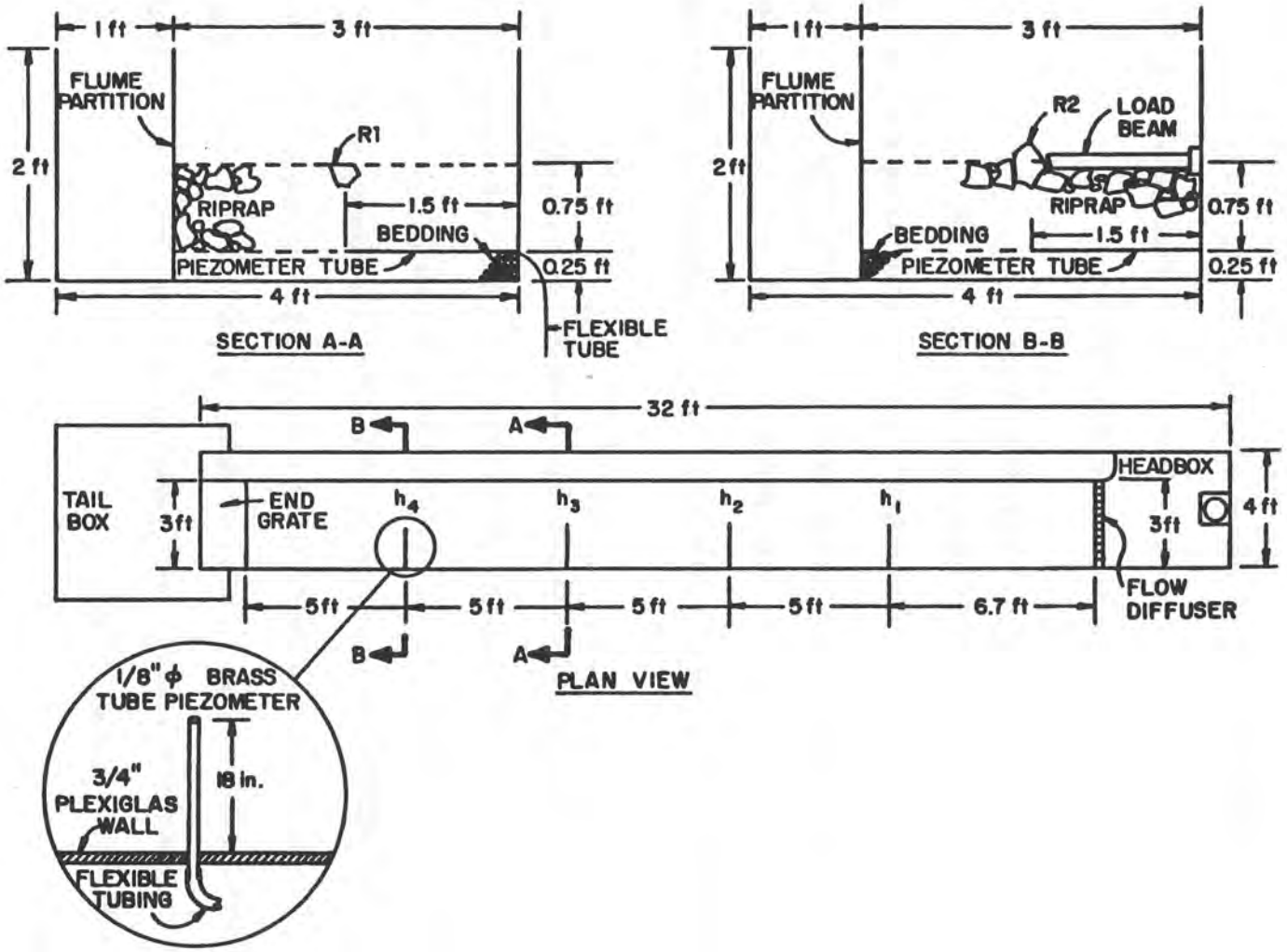


*Figure 9. Plan and details of flume.*

### *Piezometers*

Four piezometers were installed on five foot centers along the centerline of the flume. Figure 9 shows the details of the piezometer installation. Piezometers measure the hydrostatic levels along the centerline of the flume. The piezometers were designated h1, h2, h3 and h4, from upstream to downstream. The water levels were monitored on a manometer board as shown in Figure 11. The piezometer h4 was placed directly below the specimen rock R2

### *Velocity Measurement*

Free surface, non-interstitial velocity was measured with a Marsh-McBirney®, magnetic current meter. The sensing probe was mounted on a graduated rod and the velocity was measured at a depth sixty percent of the local depth below the water surface. The rod had a three-inch diameter foot pad that rested on the riprap surface. In the highly turbulent flows, velocities often were estimated to be the mean of the high and low fluctuations indicated by the current meter.

### *Instrumentation*

One rock was selected and mounted on a specialized load-beam instrument. The purpose of the rock was to sense the total lift and drag on a typical rock. The lift and drag sensing rock specimen was designated "R2". The mass of R2 is 0.0551 slugs (804 g). The weight of R2 is 1.7725 LB (7.885 N). The specific gravity of R2 is 2.65. The mounting rod of the load beam, Figure 10, was inserted into a single 0.25 inch (6.35 mm) bore of Specimen R2. The load beam was located in the flume as shown in Figure 9, detail B-B. The load beam had strain gages on two faces of its square cross section in order to detect load in the longitudinal, or stream wise direction, and in the direction normal to the slope.

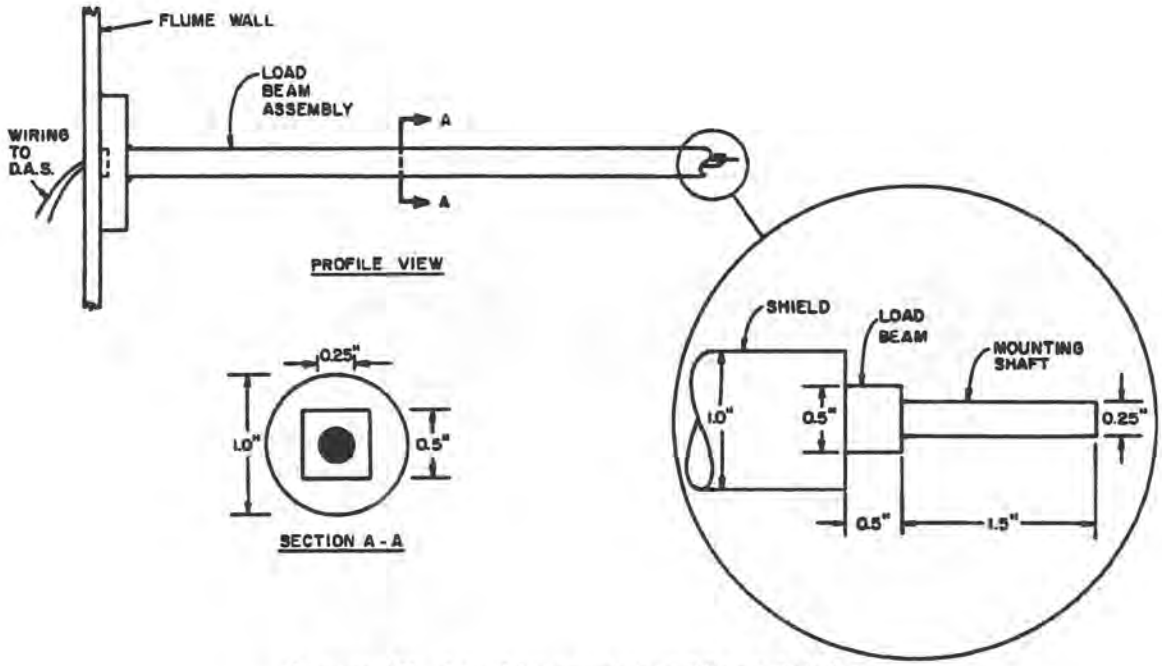


*Figure 10. Load beam assembly and details.*

### *Data Acquisition System*

A Keithly®, Series 500 Data Acquisition System (DAS) digitized the load beam signal. The analog to digital (A/D) converter is a 14 bit converter with 1 part in 16,383 resolution. The DAS communicated the two channels, x and z components, of the digitized strain gage signals to an AT-compatible Personal Computer (PC). Figure 12 is a schematic of the data collection system.

## Materials

This section describes three mixtures of riprap in addition to those tested and described by Abt [1].

### *Selection Criteria*

The riprap was selected primarily on the basis of size, angularity, quality, and roughness. Sample rocks were selected from available materials for detailed analysis. The candidate rocks had all passed a four inch sieve and were retained on a two inch sieve. Exact size of the candidate rocks was based upon the equivalent spherical diameter of a sphere having the same surface area

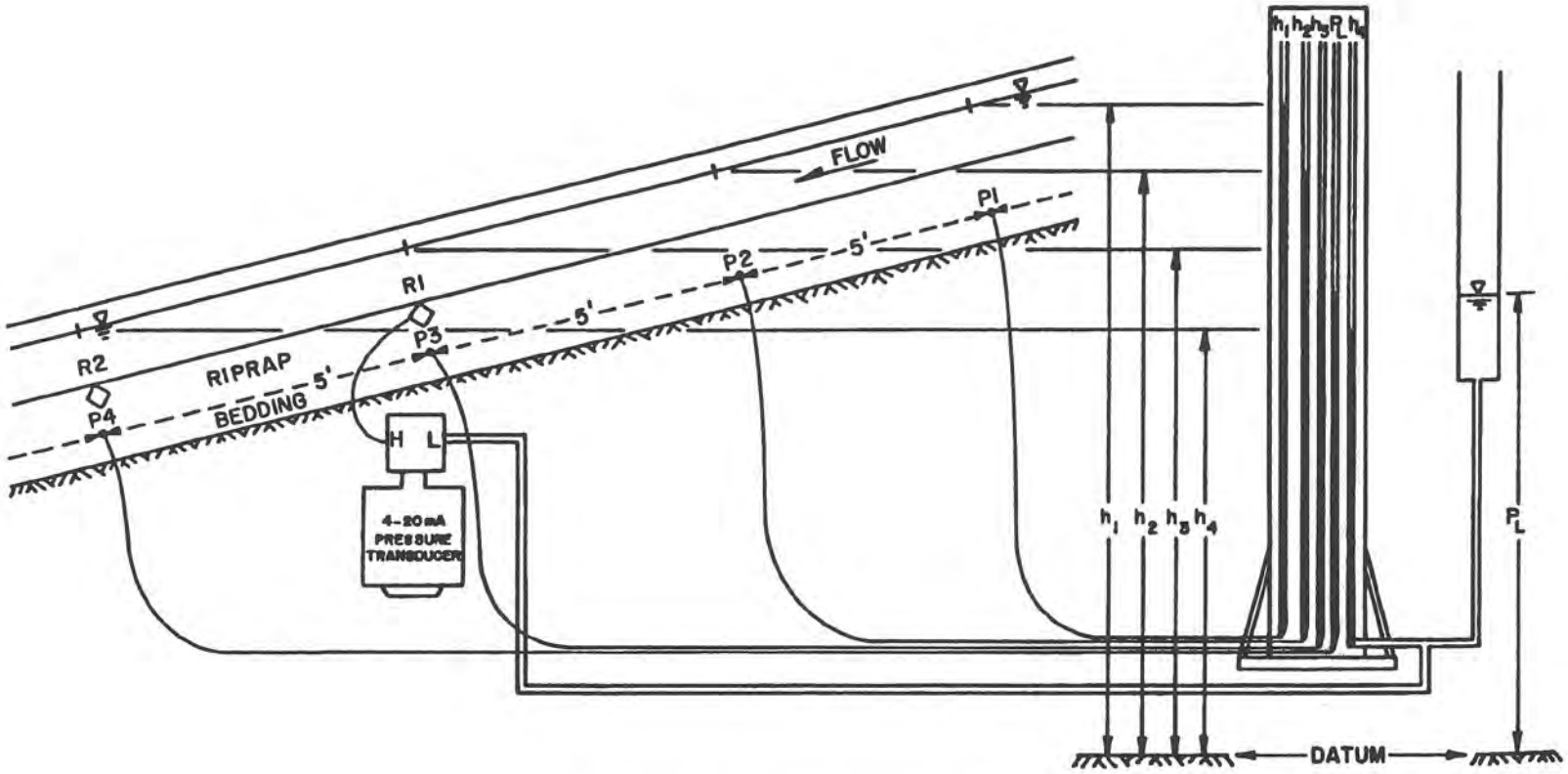


*Figure 11. Manometer schematic.*

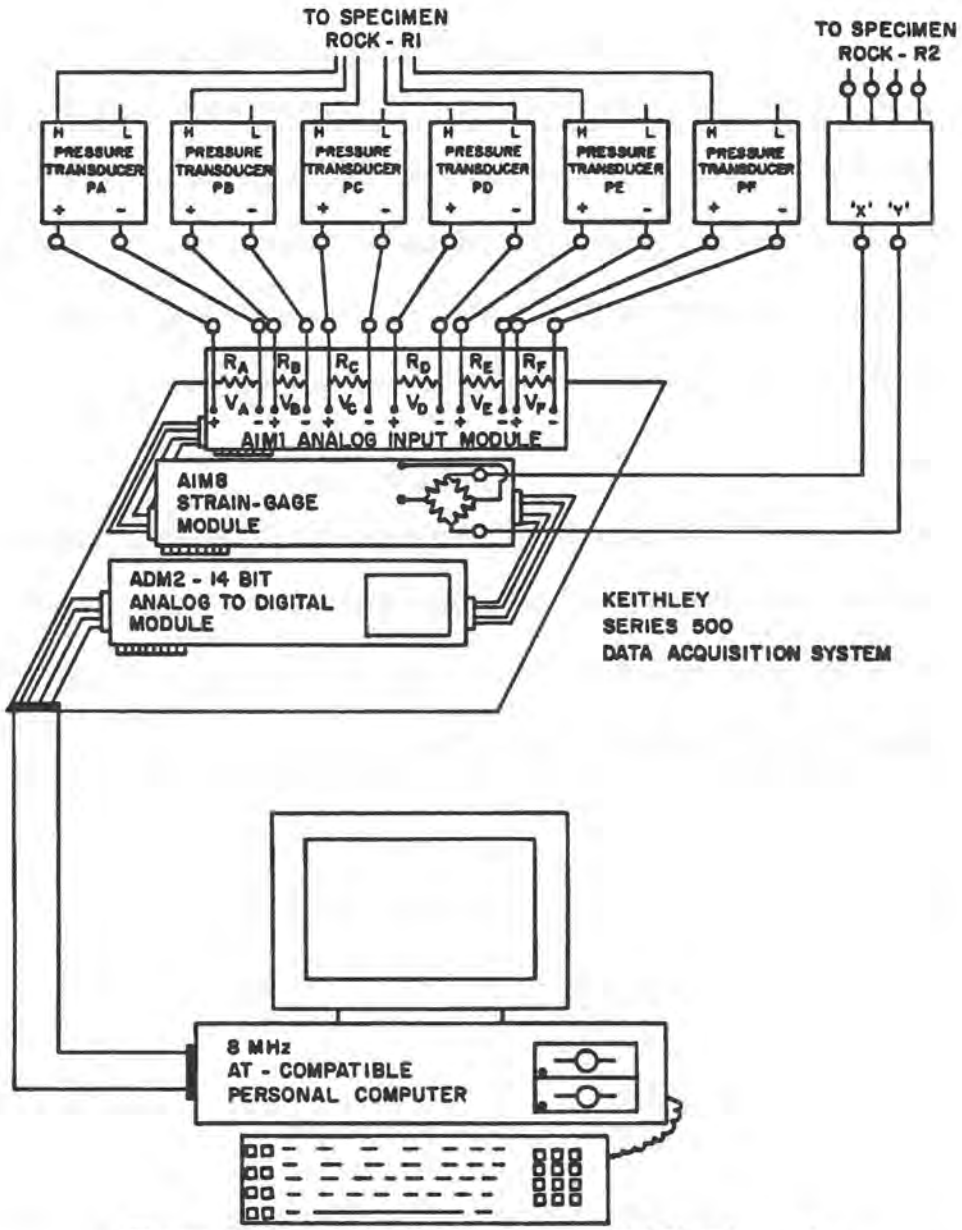


*Figure 12. Data Acquisition System (DAS) schematic.*

as that of the subject rock. A spherical diameter that was within five percent of the $D_{50}$ of the riprap mixture was desired. Roundness is the ratio of the average radii of the edges of the rock to the radius of the smallest circle inscribing the rock. The candidate rocks had the greatest value of roundness, that is they were the most angular. Quality was judged on the absence of faults and fresh faces, consistency of the granular pattern, and overall appearance and integrity of the rock. The three mixtures each had a median grain size of roughly three inches.

## Geologic Description of Riprap

The riprap used in these experiments was derived from a quarry near Golden, Colorado, USA. Sample rocks were selected from a pile of sieved riprap passing a four inch (10.16 cm) screen and retained on a two inch (5.08 cm) screen. Several candidate specimens were preselected and removed to the laboratory for final selection. The samples were classified as pre-Cambrian or Cambrian Granite. The rocks were typical fine-grained, slightly schistose granitic rocks.

## Roundness

A specimen rock was selected for determination of roundness. Roundness is the ratio of the curvature of the edges of the rock and the diameter of the smallest sphere that inscribes the stone. The surface area of the specimen rock is 34.3191 square inches (221.41 $cm^2$). The equivalent spherical diameter is calculated from

$$A_s = 4\pi r_e^3 \tag{29}$$

where $A_s$ is the surface area of a sphere of radius $r_e$. Thus

$$D_e = 2r_e = 2\sqrt{\frac{A_s}{4\pi}} \tag{30}$$

$$D_e = 3.305\,\text{in}$$
$$D_e = 8.395\,\text{cm}$$

and $D_e$ is the equivalent spherical diameter. The average radius of the edges of the specimen was estimated to be 0.125 inches (3.175 mm) or less. An estimate of the roundness of specimen may be made by the expression for roundness,

$$R = \frac{r}{r_e} \tag{31}$$

where $R$ is the roundness and $r$ is the radius of the edges. The estimate of $R$ for the specimen is approximately 26.5. A sphere would have an $R$ of 1.0 while a cube would have an $R$ of infinity.

## Riprap Gradations

The three gradations of riprap and one gradation of bedding tested in this study are described in this section. The gradations are described by the coefficient of uniformity, $C_u$, and other geotechnical properties. Bedding was sized according to the following criteria:

$$\frac{D_{15}(riprap)}{D_{85}(bedding)} < 5 \tag{32}$$

$$5 < \frac{D_{15}(riprap)}{D_{15}(bedding)} < 40 \tag{33}$$

$$\frac{D_{50}(riprap)}{D_{50}(bedding)} < 50 \tag{34}$$

after Sherard et al. [18] where $D_{15}$, $D_{85}$, and $D_{50}$, refer to the size fraction that 15, 85 or 50 percent is smaller by weight, respectively.

In order to determine the effect of mixture upon the stability of riprap, and to define a premise of the second hypothesis, that a single size cannot describe an entire mixture, a wide range of gradations were investigated. The three selected mixtures were designed to supplement data from Abt [1], and represent typical quarry derived, nonsieved mixtures. The three values of $C_u$ are 1.56, 2.92 and 5.33. As $C_u$ increases, the mixture becomes more well-graded. The $D_{50}$ of the three mixtures was nearly identical, at 3.30 inches (8.38 cm), 3.25 inches (8.25 cm) and 3.20 inches (8.13 cm). Specifying a single value of $D_{50}$ effectively removed one variable from the analysis and facilitates a demonstration of the effect of mixture, rather than size, upon the stability of the mixture.

In addition to size fractions, other geotechnical properties include the angle of repose, $\psi$, the porosity, $n_p$, the unit weight, $\gamma_s$, and the specific gravity, $S_r$. Table 1 presents these properties for the three riprap mixtures. Figure 13 shows the gradations that are tabulated in Table 2.

Table 1. Material properties.

| Property | Gradation #1 | Gradation #2 | Gradation #3 |
|---|---|---|---|
| $C_u$ | 2.92 | 1.56 | 5.33 |
| $\psi$ | 34.9 | 35.3 | 32.52 |
| $n_p$ | 0.413 | 0.443 | 0.399 |
| $\gamma_s$ (lb/ft$^3$) | 100.00 | 94.79 | 106.22 |
| $S_s$ | 2.60 | 2.52 | 2.70 |

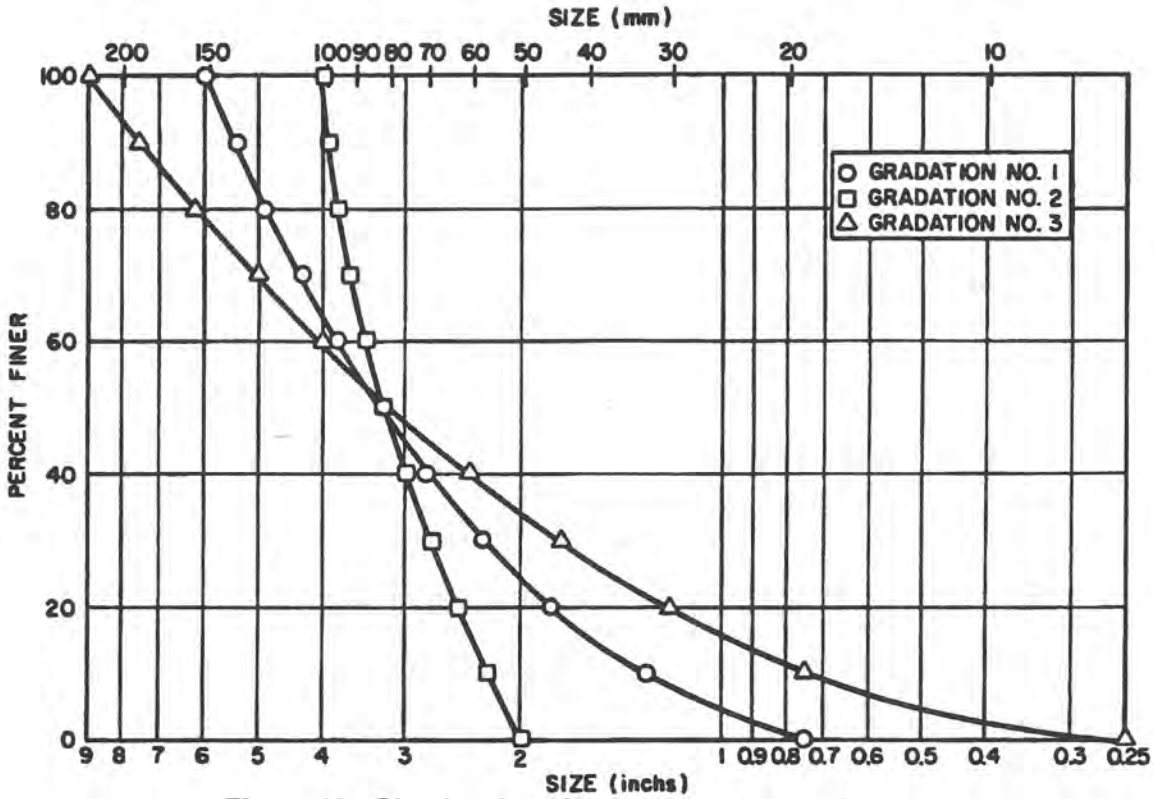


Figure 13. Size fractions for the three riprap mixtures.

Table 2. Gradation tabulations.

| Size Classification | Gradation #1 (inches) | Gradation #2 (inches) | Gradation #3 (inches) | Bedding (inches) |
|---|---|---|---|---|
| $D_{100}$ | 6 | 4.00 | 9 | 1.25 |
| $D_{90}$ | 5.4 | 3.95 | 7.5 | 0.72 |
| $D_{80}$ | 4.9 | 3.80 | 6.2 | 0.64 |
| $D_{70}$ | 4.3 | 3.65 | 5.0 | 0.50 |
| $D_{60}$ | 3.8 | 3.50 | 4.0 | 0.37 |
| $D_{50}$ | 3.3 | 3.25 | 3.2 | 0.25 |
| $D_{40}$ | 2.8 | 3.00 | 2.4 | 0.170 |
| $D_{30}$ | 2.3 | 2.75 | 1.75 | 0.105 |
| $D_{20}$ | 1.8 | 2.50 | 1.2 | 0.064 |
| $D_{10}$ | 1.3 | 2.25 | 0.75 | 0.037 |
| $D_0$ | 0.75 | 2.00 | 0.25 | 0.020 |

## Procedures

The experimental procedures include the collection of two divisions of data. The first data set includes the hydraulic properties, depth of flow, discharge, velocity and other physical conditions of the experiment. The second data set includes the observations of the investigators, photographs, and video recordings.

### *Data*

Prior to each test the flume was adjusted to the prescribed slope. The slope was verified by survey to the nearest one-hundredth of a percent. The bedding material was mixed and then subjected to a sieve analysis test according to applicable ASTM sieving procedures. The riprap mixture was similarly sieve tested for determination of gradation. To insure consistency of gradations, a batch of each gradation sufficient for all tests was initially mixed. As needed, riprap was used from each batch. Prior to use, the remaining portion of each batch was remixed to alleviate segregation that may have occurred during stockpiling.

The discharge was measured by orifice, Venturi and Annubar as previously described. These differential pressure flow elements were attached to mercury manometers. Each flow element had been calibrated in the Colorado State University calibration facility and the reported calibration is precise to ±0.25 percent.

Flow velocity and depth were each measured by two different methods. The discharge was established to the point where surface flow was just beginning, i.e. all flow was interstitial flow. Interstitial flow was determined to exist when roughly half of the surface rocks in the riprap blanket were submerged. This discharge was designated interstitial discharge, $Q_I$. The surface flow, $Q_s$, is defined as

$$Q_s = Q_T - Q_I \tag{35}$$

where $Q_T$ is the total discharge. At a flow of $Q_I$ the four piezometers were bled. These interstitial levels are the basis for zero surface flow depth. The depth of surface flow at each of those four points was subsequently defined as the piezometer reading minus this interstitial reading, the piezometric level at discharge $Q_I$. The average of the four surface flow depths was the first method of measuring the depth of flow. The average velocity, $V_s$ was calculated as

$$V_s = \frac{Q_s}{wh_s} \tag{36}$$

where $h_s$ is the average surface flow depth given by

$$h_s = \frac{\sum h_j - \sum h_i}{n} \tag{37}$$

and $h_j$ is the "n" number of piezometer readings at time or sequence "j" and $h_i$ is the initial "n" piezometer readings at the interstitial discharge, and $w$ is the width of the flume.

The flow velocity and depth were also measured at selected points with a magnetic current meter on a graduated rod. Generally, a point velocity and depth were measured after each increase in discharge, directly above piezometer h3. Additional point velocities and flow depths were measured when possible in zones of supercritical flow or zones of local erosion.

Photographs were taken many times during each test. Video in the VHS format was also recorded during several of the tests. Photographic and video data focused on the area around piezometer h3 as well as the general views of the flume, and the overtopping flow.

The placement of the rock specimen R2 prior to each test was verified by physical measurement and by photograph. A photograph was taken of the rock specimen in place from directly above the rock. After the test another photograph was taken of the rock to determine its displacement during the test.

The DAS collected two channels, x and z directions, of data from R2 after each increase in discharge. The two channels were digitized for six seconds at a rate of 166.667 samples per second. The data was then written to the hard disk of the personal computer. After recording the data, another six seconds of data was digitized and written again to the hard disk. This redundancy of measurement was intended to insure a faultless data transmission and provided a check on the repeatability of the data.

Observations were recorded during and after each test. The observations included two to three sentences each describing the amount, if any, of riprap movement, a qualitative estimate of the degree of air entrainment based upon the whiteness of the flow, the size of rocks moving, flow conditions in local zones of rapidly varied flow and general observations. At the end of each test, final observations were written and recorded and previous observations were reviewed and affirmed or modified by the observer. Then a post-test conference was held by the test participants where all observations were discussed and recorded in their final form. After processing, the photographs were interpreted and additional observations were made in the light of those already finalized.

The eroded material was retained in the tail box. After each test the material in the tail box was weighed and classified according to size by sieve analysis. Material from the sixth test was also weighed stone by stone to determine the weight and size distribution of the eroded material.

### *Order of the Experiment*

Each experiment began with the establishment of interstitial discharge. The Data Acquisition System was initialized and manometers and piezometers were bled. Initial readings from the DAS were recorded, initial piezometer readings were recorded and photographs were taken of the flow. Incrementally over roughly one hour, the discharge was increased until the

riprap failed or pump capacity was reached. In all, ten of the thirteen tests ran to failure of the riprap. After each increase of the discharge all data were again recorded. Depending on flume slope and riprap gradation, each test consisted of ten to twenty increments of discharge.

Care was taken, when increasing the discharge, not to change the flow too quickly. Generally each discharge increment was targeted to be five percent of the estimated failure discharge. Failure discharge was estimated by the Abt equation (44). As the riprap approached failure, the data collection procedures were modified. The frequency and amount of data recorded lessened as the elapsed time between increments of increased discharge was lessened to minimize time effects on the failure process. There were fewer point velocity and depth measurements, and piezometer levels other than h3 and PL were omitted. Photographs were taken throughout the test, though less frequently as the test progressed.

## *Testing Program*

The testing program included thirteen individual tests. A combination of four slopes and three gradations were tested. The test numbers were assigned as shown in Table 3. Data from these thirteen tests is tabulated in the Appendix, Hydraulic Data.

*Table 3. Test matrix.*

| | Test Number | | |
|---|---|---|---|
| | *Gradation #1* | *Gradation #2* | *Gradation #3* |
| *Slope, %* | $C_u = 2.92$ | $C_u = 1.56$ | $C_u = 5.33$ |
| 5 | 1,2 | 3 | 4* |
| 10 | 7* | 6* | 5* |
| 15 | 8* | 10* | 9* |
| 20 | 13* | 12* | 11* |

*Note: * indicates failure of the riprap.*

Test number 1 was a trial test wherein procedures were developed, the DAS was debugged, and the procedures for the remaining tests were refined. After each test the entire flume

was cleared and new bedding material and riprap were dump placed and leveled with a minimum of compaction. The gradations used are shown and tabulated in Figure 13 and Table 2, respectively.

### *Hydraulic Data*

The hydraulic data is tabulated in the Appendix, Hydraulic Data. The raw hydraulic data consisting of the piezometer readings, discharge readings and point velocity and depth readings, were recorded on data forms, and entered into a spreadsheet. The hydraulic radius, $R$, the average velocity, $V$, the average surface depth, $d$, the average slope of the water surface, $S$, and the Darcy coefficient of friction, $f$, were calculated in the spreadsheet. The shear stress, $\tau$, is given in the following expression.

$$\tau = \gamma RS \tag{38}$$

The Shields parameter, $T_c$, is given by this expression.

$$T_c = \frac{\tau}{\gamma(S_s - 1)D_{50}} \tag{39}$$

The Boundary Reynolds number, $\mathrm{Re}_*$, is calculated as

$$\mathrm{Re}_* = \frac{u_* D_{50}}{\nu} \tag{40}$$

where $\nu$ is the kinematic viscosity, $S_s$ is the specific gravity of the riprap. The shear velocity, $u_*$, is calculated as

$$u_* = \sqrt{gRS} \tag{41}$$

where $g$ is the acceleration of gravity, 32.16 ft/s$^2$ (9.81 m/s$^2$).

# CHAPTER 4

## CHARACTERIZATION OF A RIPRAP MIXTURE

The flow properties of the boundary layer and the mechanics of a single typical particle were presented in Chapter 2. The characteristic dimension of the particle was presented as $k$. The relationship of $k$ to an actual dimension of a typical rock and to the riprap mixture must be determined. According to the second hypothesis, a single factor is not sufficient to describe a riprap mixture. The previous sections on Shields parameter addressed the premises of the second hypothesis. Chapter 4 provides an empirical method for characterizing a mixture of riprap, thus supporting the hypothesis.

The Strickler expression relates $k_s$ and $n$, the Manning roughness coefficient.

$$n = 0.034 k_s^{1/6} \tag{42}$$

The Manning roughness coefficient, $n$, does not describe the roughness of a single particle. The Manning $n$ describes the roughness of the wetted perimeter, $P$, a factor of the hydraulic radius, $R$, in normal uniform flow. Equation 21 shows how the hydraulic radius is related to the roughness over a surface area of a control volume. Einstein [5] presents a thorough treatise on the "Hydraulic or Radius Profile". The particles that populate the area of the wetted perimeter over the length of the control volume are the particles that make up the riprap mixture. Therefore, since the Strickler equation directly relates a factor that describes the roughness of an area with a factor with the dimension of length, the characteristic dimension in the Shields parameter should not be construed as the diameter of a single particle. Rather, $k$ describes the roughness of an area as does the Manning $n$. In fact, there is no way to describe a riprap mixture with a single factor. One

approach for describing a riprap mixture is to adjust a representative size with various factors that represent the entire mixture. This chapter presents one method of achieving this end.

Results of the experiments described in Chapter 3, combined with the data from Abt [1], show that stability of riprap is proportional to the uniformity of the mixture. There are other factors have an influence upon stability not treated in this investigation. Examples of other factors include proper sizing of the bedding layer, and the behavior of the mixture as part of an overall structural unit is also a factor. Riprap consists of an interlocked matrix of rocks that forms a structural unit whose stability is greater than its individual members. The extent of interlocking is a function of mixture uniformity and rock shape.

## Factors Influencing the Stability of Riprap

There are many factors that influence the stability of riprap. Some of the factors are size, or weight, shape of the rock, the riprap layer thickness, the presence and makeup of the filters or bedding, and uniformity of the riprap mixture. The focus of this investigation is uniformity of the riprap mixture.

### *Background*

Riprap design procedures such as Safety Factors [22], COE [30], USBR [28], Stephenson [21], and others are reviewed by Abt [1]. Each procedure recommends a unique riprap gradation. Gradation is expressed as a uniformity coefficient that is normally a quotient of various size fractions of the riprap mixture. The size fractions are determined by sieve analysis.

The coefficient of uniformity, $C_u$, is defined as the size that sixty percent of riprap mixture by weight is finer, $D_{60}$, divided by the size that ten percent by weight, $D_{10}$, is finer.

$$C_u = \frac{D_{60}}{D_{10}} \tag{43}$$

The recommended values of $C_u$ for some of the design procedures are listed in Table 4. The designer is left to guess at the response to a gradation other than that specified by the design procedure. None of the design procedures offer a prescription for adjusting the median rock size based upon uniformity criteria. The question is, how does a gradation with $C_u$ greater or less than specified influence the stability of the riprap layer?

*Table 4. Institutional values of $C_u$.*

| *Design Procedure* | *SF* | *COE* | *USBR* | *FHWA* | *CDH* | *Abt et. al.* |
|---|---|---|---|---|---|---|
| $C_u$ | 2.50 | 1.75 | 2.55 | 2.70 | 1.10 | 2.15 |

SF- Safety Factors [22]; COE- Corps of Engineers [30]; USBR- US Bureau of Reclamation [28]; FHWA- Federal Highway Administration; CDH.- California Dept. of Highways [27]; Abt et. al.- Nuclear Regulatory Commission [1].

The results of three studies supports the second hypothesis, and yields an expression that describes the effects of varying the riprap mixture on stability. The first two studies are described by Abt [1] (1987-Phase I, 1988-Phase II). This investigation is the third study. In the studies by Abt, flumes of eight and twelve feet in width and embankment slopes of one percent to twenty percent were covered with one, two, four, five and six inch median diameter, angular riprap. Abt maintained a constant median diameter of either two or four inches while varying the gradation from 1.72 to 4.00. The minimum value of $C_u$ in this investigation was 1.56 and the maximum value of $C_u$ was 5.33 while the median diameter was fixed at roughly 3.2 inches.

The unit discharge at failure, $q_f$, for all three series of experiments ranged from 1.00 $ft^3/s/ft$ to 4.12 $ft^3/s/ft$. Abt correlated the unit failure discharge with the embankment slope, $S$, and the median diameter, $D_{50}$, for 18 tests. The result of the correlation is an expression for sizing riprap on embankments, the Abt equation.

$$D_{50} = 0.436 q_f^{0.56} S^{0.43} \tag{44}$$

Abt included all tests with a coefficient of uniformity between 1.72 and 2.30 in the correlation. The normal value of $C_u$ was defined as 2.15.

## The Coefficient of Stability

Fifteen tests from the three studies had coefficients of uniformity that deviated significantly from 2.15, and are summarized in Table 5. Equation 44 may be rearranged to solve for the unit failure discharge given the slope and median diameter

$$q_f^\circ = \left(D_{50}/5.23S^{0.43}\right)^{1.79} \tag{45}$$

where $q_f^\circ$ is the normal unit failure discharge of a riprap mixture with $C_u = 2.15$. The unit failure discharge of each of the fifteen mixtures divided by the corresponding normal unit failure discharge is defined as the coefficient of stability, $C_s$.

$$C_s = \frac{q_f}{q_f^\circ} \tag{46}$$

For example, a $C_s$ of 1.50 indicates a fifty percent increase in the failure discharge due to a change in uniformity. Table 5 includes the coefficient of stability from each test. The data from the two Abt studies is in italics. Figure 14 presents the coefficient of stability, $C_s$ versus the coefficient of uniformity, $C_u$. The maximum increase in stability occurs at the minimum values of uniformity. The stability continues to decrease for values of $C_u$ greater than 3.0. The greatest increase, forty-five percent, occurs at a $C_u$ of 1.56. The greatest decrease is thirty-four percent at $C_u = 4.00$.

The average decrease in stability for values of $C_u$ greater than 3.0 approaches twenty percent. The increase or decrease in stability is less than ten percent for values of $C_u$ between 1.8 and 3.0. Abt [1] fit a line to the five data points of the tests performed in the Phase I and Phase II studies shown in Figure 14 and referenced as the "1988" line. The additional ten tests performed in 1988 by Wittler [26] are also shown in Figure 14. A new "1990" curve has been fit to all fifteen points. The expression for this curve is

$$C_s = 0.75 + \left(\log C_u^6\right)^{-2}, \; R^2=0.79 \tag{47}$$

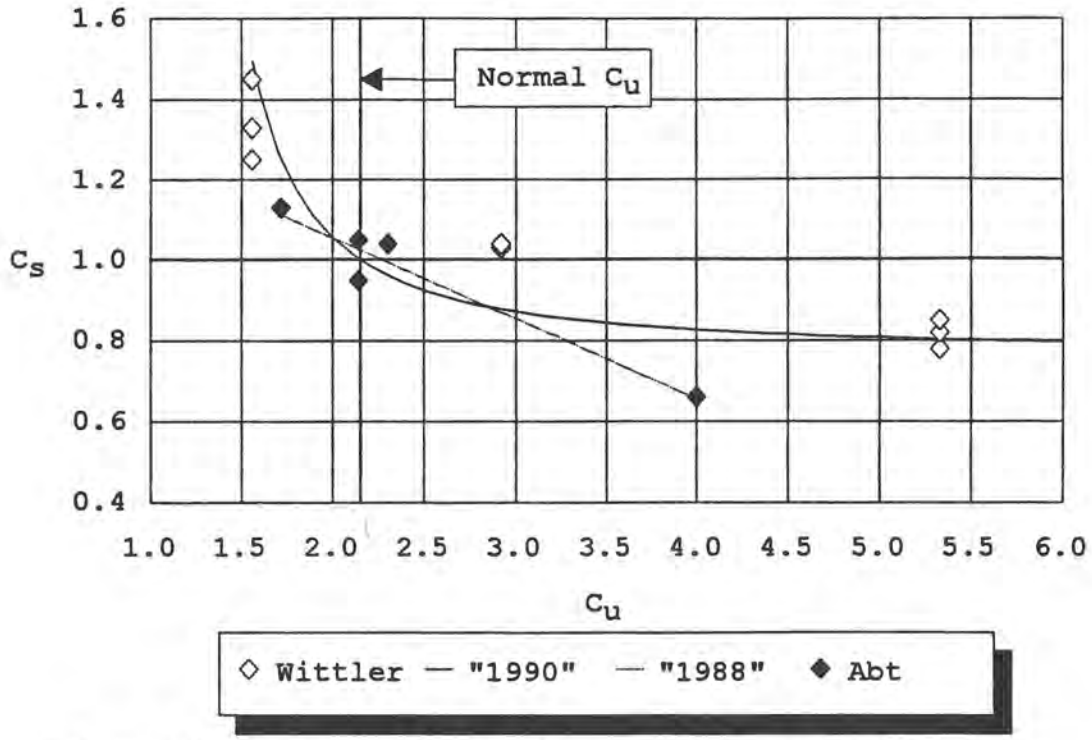


*Figure 14. Coefficient of Stability, $C_s$, versus Coefficient of Uniformity, $C_u$.*

*Table 5. Combined data for uniformity analysis.*

| | $D_{50}$ inches | $S$ ft/ft | $C_u$ $D_{60}/D_{10}$ | $q_f$ ft³/s/ft | $q_f^*$ ft³/s/ft | $C_s$ $q_f/q_f^*$ |
|---|---|---|---|---|---|---|
| Abt | 2 | 0.10 | 2.14 | 1.00 | 1.05 | 0.95 |
| | 2 | 0.10 | 2.14 | 1.11 | 1.05 | 1.05 |
| | 4 | 0.10 | 2.30 | 3.79 | 3.63 | 1.04 |
| | 4 | 0.10 | 4.00 | 2.41 | 3.63 | 0.66 |
| | 4 | 0.10 | 1.72 | 4.12 | 3.63 | 1.13 |
| Wittler | 3.3 | 0.15 | 1.56 | 2.67 | 1.84 | 1.45 |
| | 3.3 | 0.10 | 1.56 | 3.13 | 2.51 | 1.25 |
| | 3.3 | 0.20 | 1.56 | 1.96 | 1.47 | 1.33 |
| | 3.3 | 0.10 | 2.92 | 2.68 | 2.57 | 1.04 |
| | 3.3 | 0.20 | 2.92 | 1.58 | 1.51 | 1.04 |
| | 3.3 | 0.15 | 2.92 | 1.95 | 1.89 | 1.03 |
| | 3.2 | 0.05 | 5.33 | 3.24 | 4.15 | 0.78 |
| | 3.2 | 0.10 | 5.33 | 2.07 | 2.44 | 0.85 |
| | 3.2 | 0.15 | 5.33 | 1.46 | 1.79 | 0.82 |
| | 3.2 | 0.20 | 5.33 | 1.11 | 1.43 | 0.78 |

The observations discussed herein are derived from the two studies by Abt and this investigation. After witnessing more than 80 tests of riprap in overtopping flow, it is clear that

uniformity has a significant influence upon the stability of riprap. Observation of the tests performed in the three studies has identified several stages that the riprap layer transitions through prior to failure.

Data from the experiments show that immediately upon inception of surface flow the signal from the load beam and rock specimen R2 achieved the maximum value and did not change throughout the remainder of every test. Observations in later tests revealed that as the riprap was loaded by the flow, the entire mixture creeped down the slope, translating R2. When the translation exceeded the maximum range of motion of the load beam, the signal plateaued. This was not the purpose of the specimen and instrumentation. Nevertheless the observations provide information about an important behavior of the riprap matrix as it loads.

Failure is defined as rock movement that results in exposure of the underlying materials. The uniformity of the mixture magnifies some of these stages and minimizes others. As the riprap is inundated, voids fill with water and interstitial flow begins. Initial settling of the smallest particles occurs at this stage. As surface flow begins, the entire riprap layer settles and assumes the load imposed by the shear stress. The shallow surface flow breaking over the individual rocks causes fluctuating pressures that vibrate and settle the riprap layer. As the shear stress increases with increasing flow, the riprap layer continues to settle and some surface rocks are swept downstream by the moving water. Most of these rocks lodge a short distance downstream.

At roughly thirty-three percent of the failure discharge, settlement and initial movement decreases. Occasionally a single rock is dislodged and transported downstream. The load carrying capacity of the riprap layer is now fully developed. Observations indicate that the riprap layer has become a structural unit. The shear stress of the flowing fluid is transferred through the layer to the soil layers beneath. There is no direct correlation, but by this stage significant creep of the

layer down the slope has probably occurred. The creeping phenomenon is described in the load beam data section of Chapter 3.

The riprap layer is static until the flow reaches roughly seventy five percent of the failure discharge. An observable increase in the whiteness of the flow, indicating increasing aeration, is probably caused by surface rocks tipping up into the flow. Abt [1] describes this as the movement stage. There is some localized dislodging of the surface rocks and sometimes channels will form. Failure is initiated, in the majority of cases, by movement of several key stones. Rocks that support a local matrix of rocks are called keystones. When a keystone moves, the local matrix is destabilized and a number of surface rocks supported by the keystone move, resulting in a mass movement of the surrounding surface rocks.

Failure of the entire riprap layer occurs when the flow is concentrated in the spaces vacated by the surface rocks. The concentrated flow erodes through the lower layers of rock. Another type of failure, typical of poorly graded mixtures, is characterized by a large area of the surface rocks becoming mobile and piling up a short distance downstream. As in the case of well graded riprap, flow is concentrated in a weak area and failure follows.

The fluid shear stress is transferred to the surface rocks and subsequently through the riprap layer by the individual rocks. The gradation of the mixture influences the efficiency of the shear stress transfer. Well graded riprap transfers the load through large, medium and small particles. Because of the large number of particles in well graded riprap, there are numerous transfer points. The smaller particles fill the voids between the larger particles. The load paths do not intersect the centers of the majority of the particles. Instead, the larger particles tend to transfer the load to the smaller particles tangentially, and actually sliding on the smaller particles. The shear within the layer results in bearing stress on the small particles great enough to induce sliding between neighboring particles with instability resulting.

Poorly graded riprap has fewer transfer points than well graded riprap. The bearing stress in poorly graded riprap is uniform throughout the layer because the particles are similar in size. Loads are transferred through the centers of the particles rather than tangentially. Since the bearing stress is transferred more efficiently by poorly graded riprap, the overall stability of poorly graded riprap is greater than well graded riprap.

Different failure mechanisms for poorly graded and well graded riprap have been observed. Poorly graded riprap withstands substantially larger flows, all other factors being equal, than well graded riprap, as shown in Figure 14. The failure of poorly graded riprap is more sudden than well graded riprap. Well graded riprap tends to fill in voids in the post movement stage with small particles washed from upslope. The term for the void filling process is healing. Several instances of large rocks being swept away only to have their spaces filled immediately by many smaller rocks from just upstream have been observed. After the movement stage, there is very little incidental movement in poorly graded riprap. The failure of poorly graded riprap begins with numerous surface rocks moving very suddenly. Within moments the entire riprap layer becomes mobile. Little healing was observed in the poorly graded riprap tests. The suddenness of failure and the healing process both moderate in medium graded riprap mixtures.

The aftermath of a keystone failure is a deep, longitudinal scour in the embankment. The flow, concentrated in a narrow reach of the embankment, scours through the riprap layer into the material below. In many instances the longitudinal scour forms at an angle from the fall line of the slope. As the scour deepens, a greater percentage of the flow is captured and the unit discharge in the scour trench increases rapidly. The increase in unit discharge hastens the scour process. The shape of the scoured area is similar to a narrow "u" that opens downstream. The banks of the "u" are steep, often approaching ninety degrees, or vertical. The aftermath of a mobile bed failure is different than the keystone failure. Large areas of the riprap layer are removed during a mobile

bed failure. Mobile bed failures are characteristic of uniformly graded riprap and thus withstand substantially greater flows at failure. The particle transport capacity of the increased flow causes a large initial and sustained transport of the riprap layer.

Similar failure stages for riprap on side slopes with differing gradations have been identified by Ahmed [2] . Ahmed studied filter and gradation effects on side slope riprap stability. His observations included the movement of particles at relatively low flow rates to secondary and more stable positions. He also noted the vibration of the particles. Ahmed describes the threshold stage as the point when one particle is moved exposing some shielded particles. The failure stage followed the threshold stage and was characterized by a number of surface rocks moving and endangering the side slope stability. The conclusions of Ahmed for side slopes match the conclusions reached for embankment slopes. Ahmed identified an eight percent decrease in failure discharge for the well graded riprap ($C_u$~ 2.2) as opposed to the poorly graded riprap ($C_u$~ 1.10).

## Riprap Mixture Descriptor

If the characteristic dimension $k$ in Shields parameter is not sufficient to describe an entire mixture, then a more sufficient set of dimensions is necessary. As previously presented, Abt correlated slope and unit discharge with the median rock size fraction, $D_{50}$.

$$D_{50} = 5.23 S^{0.43} q_f^{0.56} \tag{48}$$

This chapter shows that $D_{50}$ alone is not sufficient to describe an entire mixture. The coefficient of uniformity provides two additional dimensions, $D_{60}$ and $D_{10}$. The coefficient of stability, $C_s$, adds these two dimensions to $D_{50}$ in the Abt equation.

$$C_s = 0.75 + \left(\log C_u^6\right)^{-2} \tag{49}$$

Equation 50 expresses $D_{50}$ given the discharge, slope and uniformity of the material.

$$D_{50} = 0.436S^{0.43}\left[\frac{q_f}{0.75+\left(\log C_u^6\right)^{-2}}\right]^{0.56} \tag{50}$$

Given the slope, median rock size and the uniformity of the material, the discharge is directly calculated by equation 51.

$$q_f = \left[0.75+\left(\log C_u^6\right)^{-2}\right]\left[\frac{D_{50}}{0.436S^{0.43}}\right]^{1.79} \tag{51}$$

## Conclusions

The stability of riprap protection on embankments and side slopes is significantly influenced by the gradation of the riprap mixture. In general, poorly graded riprap demonstrates increased stability while well graded riprap is less stable than normal gradations for overtopping flows. Well graded riprap fails over a period of time as voids are filled with eroded material from upstream. The filling process is called healing. Failure of poorly graded riprap occurs suddenly with little healing. The designer should consider the ramifications of gradation specifications both in design and quality control during construction.

The coefficient of stability, $C_s$, adds two size fractions to the median size fraction to describe the riprap mixture. It is clear, based upon the data in Figure 14, that stability is a function of uniformity. Since the bearing stress is transferred more efficiently by poorly graded riprap, the overall stability of poorly graded riprap is greater than well graded riprap. This finding supports the hypothesis that a single size fraction does not adequately describe the entire mixture. Though empirical, the coefficient of stability is calibrated for a slope of up to twenty percent, and a unit discharge of up to five cubic feet per second per foot.

# CHAPTER 5

## FORMULA FOR RIPRAP AT INCIPIENT MOTION

This chapter presents the derivation of a generalized form of the Abt equation. The generalization includes a correction factor and the coefficient of stability developed in the preceding chapter. In addition, a factor that adjusts the hydraulic radius for aeration effects is developed.

Design of riprap requires a method based upon fundamental flow principles, a method that considers the factors that influence stability, and a method that is relatively simple to execute. According to the third hypothesis, such a method is derivable starting with the Manning and Strickler equations. Then, using the critical shear stress specified by the Shields parameter, an analytical riprap design method results. The analytical method requires calibration with data from prototype scale experiments to adjust for variable riprap mixtures and account for the unknown or undetermined factors. The result is a reliable riprap design method.

The section on Shields parameter leads to the conclusion that shear stress, mass density of water and rock material, and a characteristic dimension are the pertinent factors relating to incipient motion. The assumptions necessary to arrive at Shields parameter obviate the precise usefulness of the parameter. However, knowing the pertinent factors, and relying on the constant value of Shields parameter in the extended region of Boundary Reynolds number provides a boundary condition in the derivation of a generalized analytical riprap design equation. The generalized formula begins with the established relationships such of Shields, Manning, shear

stress, and Strickler. After combining these equations, the resulting formula is calibrated with prototype size flume test data. The calibrated formula is highly applicable and reliable for design.

Flow on steep slopes becomes highly aerated. Chapter 4 postulated on the impact of an air-water mixture on the Shields parameter. To the designer, a discussion of aeration is academic as it presupposes a knowledge of the mean air concentration. In reality, air concentration is a major unknown factor. Air concentration has a profound impact on the riprap design process in that neglecting the factor results in oversized riprap. Wittler [25] demonstrated a two-fold increase in the estimate of the median rock size using the Stability Factors [22] method of riprap design when aeration is neglected. Therefore, a factor that describes the influence of aeration is necessary for economical design of riprap. A derivation of an aeration adjustment factor and a comparison to data from Gaston [7] will be presented.

## Formulation of the Abt Equation

Abt [1] empirically derived an equation for riprap on slopes less than 20% and for riprap less than 6 inches nominal median diameter. The multivariate regression variables came from the parameters of the full scale experiments conducted for the study by Abt. An analytical method of deriving an equation very similar to the Abt equation will be presented.

### *Manning Equation*

The Manning equation describes the relationship between discharge, slope, hydraulic radius, and roughness for normal flow. Normal flow has the characteristic of constant properties in the direction of flow. In order to apply the Manning equation to flow over riprap, the flow must be in a normal flow regime. Observations of flow in all experiments show that in the region where initiation of failure was observed, the flow was in a normal flow regime.

The discharge form of the Manning equation is

$$Q = \frac{1486}{n} A R^{2/3} S^{1/2} \tag{52}$$

where $Q$ is the discharge, $A$ is the cross-sectional area of the flow, and $n$ is the Manning roughness coefficient. If the channel is rectangular then the area, $A$, is given by the following expression.

$$A = wd \tag{53}$$

where $w$ is the width and $d$ is the depth of flow. Dividing the Manning equation by the width leaves the discharge expressed as a unit discharge, $q$.

$$q = Q/w \tag{54}$$

$$q = \frac{1.486}{n} dR^{2/3} S^{1/2} \tag{55}$$

The Manning equation establishes the relation between discharge, slope, and hydraulic radius. The Manning roughness coefficient is an inconvenient form for expressing the roughness of riprap. It is more convenient to define riprap by one or more of the fractional sizes of the riprap mixture.

### *Strickler Equation*

Henderson [11] provides an excellent explanation of the Strickler equation.

> *"If we replace $k_s$ with $d$, which will be used in a later chapter to indicate stone or gravel size on the channel bed, we can transpose Eq. (4-21) as follows:*
>
> $$f = \frac{8g}{C^2} = 0.113\left(\frac{d}{R}\right)^{1/3}$$
>
> *whence*
>
> $$C = \sqrt{\frac{8g}{0.113}}\left(\frac{R}{d}\right)^{1/6}$$
>
> $$= \frac{1.49R^{1/6}}{0.031d^{1/6}}$$
>
> *which is identical with the Manning formula, provided that*
>
> $$n = 0.031d^{1/6} \qquad (4\text{-}22)$$
>
> *where $d$ is measured in feet. Now in 1923 Strickler had independently produced an empirical equation relating $n$ and $d$:*
>
> $$n = 0.034d^{1/6} \qquad (4\text{-}23)$$
>
> *which is very close to Eq. (4-22). The correspondence appears even closer when it is pointed out that Strickler's work was based on gravel-bed streams in which $d$ was the median size of the bed material. However, the effective value of $d$ from the resistance viewpoint is that of the larger size (two or three times the median) with which the bed tends to become armored. Hence to make a direct comparison between Eqs. (4-22) and (4-23) the coefficient of Eq. (4-22)*

*should be reduced by a factor of the sixth root of a number between two and three-i.e., by between 10 and 20 percent. The effect is to make the agreement between the two equations even closer than it appears at first."*

The Strickler equation relates the Manning roughness coefficient to the median fraction of the material that forms the wetted perimeter. Combining the Manning and Strickler equation replaces the Manning roughness coefficient with the median rock size. In design, either the discharge or the median rock size will be unknown, if the geometry is given. If the hydrology is known, that is the discharge, then a designer wishes to know what size rock is required to withstand overtopping in that discharge. If a given riprap gradation is available from the quarry, the designer wishes to know how much flow the riprap can withstand before failing.

In the combined Manning and Strickler formula, only the hydraulic radius is free from constraint. However, a major factor in calculating the shear stress, the major motivating factor acting on the riprap, is the hydraulic radius. The Shields parameter indicates the critical shear stress of a particular size particle, relating the shear stress in a dimensionless form. If the value of the Shields parameter is constant, then the hydraulic radius can likewise be constrained, and the designer is free to employ the known information to design a riprap application.

### *Abt Equation: Empirical Derivation*

The US Nuclear Regulatory Commission sponsored a two phase study of riprap armoring for low level radioactive mill tailing impoundments. Abt et. al. [1] report on the experiments and conclusions. The variables of the experiments include median rock size, uniformity, layer thickness, slope, and the unit discharge at failure. The results shown in Table 6 are a subset of the data reported by Abt. The listed experiments have the same coefficient of uniformity, with two exceptions. They have the same ratio of layer thickness to median rock size, and all utilize angular granitic rock. The 80 tests occurred in three separate facilities over a course of 4 years. The results are plotted in Figure 15. Abt reports an $R^2$ of 0.98 for the equation of the correlation of the

data in Figure 15, equation 44. The slope in the equation is decimal, the unit discharge is $ft^3/s/ft$, and $D_{50}$ is in feet. The benefit of an empirical equation is that in addition to the factors of the correlation, all other factors are implicit in the formulation. The third hypothesis depends upon this premise, since an objective is to identify the macro-effect of the unspecified factors.

*Table 6. Data from Abt, Phase I and Phase II.*

| | *Test #* | *$D_{50}$ (in.)* | *$D_{50}$ (ft)* | *Thickness (in.)* | *S* | *$q_f$ ($ft^3$/s/ft)* |
|---|---|---|---|---|---|---|
| Phase I | 1 | 2.20 | 0.18 | 6.00 | 0.20 | 0.28 |
| | 1A | 2.20 | 0.18 | 6.00 | 0.20 | 0.29 |
| | 2 | 2.20 | 0.18 | 6.00 | 0.20 | 0.33 |
| | 7 | 4.10 | 0.34 | 12.00 | 0.20 | 1.82 |
| | 10A | 5.10 | 0.43 | 12.00 | 0.20 | 3.56 |
| | 15 | 6.20 | 0.52 | 12.00 | 0.20 | 4.43 |
| | 18 | 2.20 | 0.18 | 6.00 | 0.20 | 0.50 |
| | 20 | 1.02 | 0.09 | 3.00 | 0.01 | 1.50 |
| | 25 | 1.02 | 0.09 | 3.00 | 0.10 | 0.36 |
| | 26 | 1.02 | 0.09 | 3.00 | 0.10 | 0.34 |
| | 27 | 1.02 | 0.09 | 3.00 | 0.10 | 0.31 |
| | 28 | 1.02 | 0.09 | 3.00 | 0.10 | 0.42 |
| | 29 | 2.20 | 0.18 | 6.00 | 0.10 | 1.13 |
| | 30 | 2.20 | 0.18 | 6.00 | 0.10 | 1.25 |
| | 31 | 2.20 | 0.18 | 6.00 | 0.10 | 1.25 |
| | 32 | 2.20 | 0.18 | 6.00 | 0.08 | 1.81 |
| Phase II | 31 | 2.00 | 0.17 | 6.00 | 0.10 | 1.00 |
| | 32 | 2.00 | 0.17 | 6.00 | 0.10 | 1.11 |
| | 44 | 4.00 | 0.33 | 12.00 | 0.10 | 3.79 |

## *Abt Equation: Analytical Derivation*

The derivation of the Abt equation begins with the Manning equation. Assuming a wide channel, rearrange for the hydraulic radius and reduce the flow to unit discharge. Next, substitute the Strickler equation for the Manning roughness coefficient. Incipient motion is indicated by the Shields parameter. The hydraulic radius from the Manning and Strickler equations substitutes into the hydraulic radius in the shear stress factor in the Shields parameter. Finally, rearrange terms solving for $D_{50}$. The following equations demonstrate these steps.

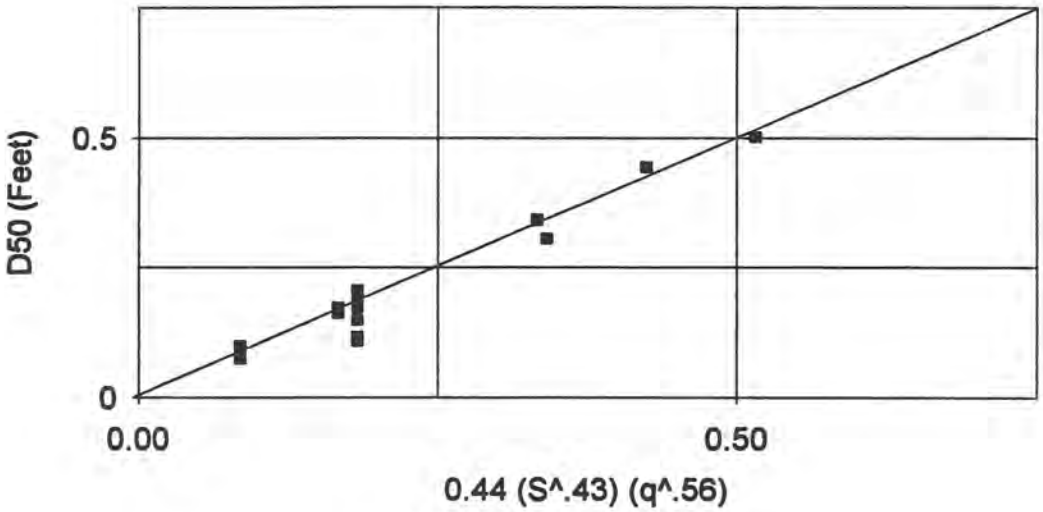


*Figure 15. Abt's data.*

Begin with the Manning equation in the discharge form.

$$Q = \frac{1.486}{n} A R^{2/3} S^{1/2} \tag{52}$$

Assume normal flow in a rectangular channel and reduce the discharge to unit discharge.

$$q = Q/w = \frac{1.486}{n} d R^{2/3} S^{1/2} \tag{56}$$

In a wide channel, the depth, $d$, is equivalent to $R$. Therefore

$$q = \frac{1.486}{n} R^{5/3} S^{1/2} \tag{57}$$

Solve for $R$

$$R = \left[\frac{qn}{1.486 S^{1/2}}\right]^{3/5} \tag{58}$$

The Shields Parameter in its simplest form includes a shear stress factor. Shear stress in this exercise is equal to $\gamma RS$, and $S$ is the slope, not $\sin\alpha$. Also assume that the flow regime is in a region of Boundary Reynolds number greater than $10^4$, and that Shields parameter is constant.

$$\tau_* = \frac{\tau}{\gamma(S_s - 1)k_s} = 0.047 \tag{59}$$

$$\tau = \gamma RS \tag{60}$$

$$\tau_* = \frac{RS}{(S_s - 1)k_s} = 0.047 \tag{61}$$

When the unit weight, γ, divides to unity, analytically the expression ignores the effects of aeration.

Next substitute hydraulic radius, $R$, from Manning into the Shields parameter.

$$\frac{\left[\frac{qn}{1.486S^{1/2}}\right]^{3/5} S}{(S_s - 1)k_s} = 0.047 \tag{62}$$

Solving for $n$ gives the following expression.

$$n = \frac{1.486S^{1/2}}{q}\left[\frac{0.047(S_s - 1)k_s}{S}\right]^{5/3} \tag{63}$$

Substitute the Strickler expression for $n$.

$$0.034k_s^{1/6} = \frac{1.486S^{1/2}}{q}\left[\frac{0.047(S_s - 1)k_s}{S}\right]^{5/3} \tag{64}$$

Solve for $k_s$, that according to Henderson [11], Strickler intended to be the median grain size diameter, or $D_{50}$.

$$D_{50} = 1.725q^{0.667}S^{0.778} \tag{65}$$

The Abt equation was previously shown to be

$$D_{50} = 0.436q_f^{0.56}S^{0.43} \tag{44}$$

Note that both equations have the same form, the product of a constant, the discharge raised to an exponent and the slope raised to an exponent. This strongly supports the third hypothesis by showing that derivation of an analytical equation is possible and that it parallels an empirical equation based upon reliable prototype scale data.

### *Comparison of Empirical and Analytical Abt Equations*

The Abt equation and equation 65, the Manning-Shields-Strickler equation (MSS), compare favorably. Both consist of a unit discharge and slope raised to respective powers. The constants differ by an order of magnitude, and the ratio of exponents varies from 0.85 to 1.3.

$$D_{50} = 0.436 q_f^{0.56} S^{0.43} \tag{44}$$

$$D_{50} = 1.725 q^{0.667} S^{0.778} \tag{65}$$

Ideally each equation should predict the same median rock size. The factor, $C_f$, that differentiates the two equations is determined by taking the ratio of the two equations.

$$C_f = \frac{D_{50_{Abt}}}{D_{50_{MSS}}} = \frac{0.436 q^{0.56} S^{0.43}}{1.725 q^{0.667} S^{0.778}} \tag{66}$$

$$C_f = 0.25 q^{-0.11} S^{-0.35} \tag{67}$$

The expression derived from the Manning, Shields, and Strickler equations, is 0.94 to 2.84 times greater than the Abt equation over the range $2\% < S < 20\%$ and 0.5 $ft^3/s/ft < q <$ 10 $ft^3/s/ft$. The difference is due to the aeration effect that is intrinsic in the Abt equation, and absent from the Manning-Shields-Strickler equation. The correction factor, $C_f$, applied to the MSS equation, results in predictions of median rock size identical to the Abt equation.

$$0.436 q^{0.56} S^{0.43} = C_f \left[ 1.725 q^{0.667} S^{0.778} \right] \tag{68}$$

Then, applying the coefficient of stability, $C_s$ to the MSS equation, a generalized form of the Abt riprap design equation results.

$$D_{50} = 1.725 C_f S^{0.778} \left[ \frac{q_f}{C_s} \right]^{0.667} \tag{69}$$

where

$$C_s = 0.75 + \left( \log C_u^6 \right)^{-2} \tag{47}$$

There is a factor, an aeration factor, $A_c$, that applied to the hydraulic radius term in the Manning equation, and following the same derivation, produces the Abt equation. The aeration factor, $A_c$, is given by

$$A_c = 0354q^{-0.096}S^{-0.313} \tag{70}$$

In Chapter 2 several examples were shown that demonstrated the effect of aeration upon the hydraulic radius and unit weight. Equation 61 shows how the unit weight effect divides to unity. Therefore, proper application the aeration factor, $A_c$, is to the hydraulic radius in the Manning equation, or in the hydraulic radius factor in the shear stress equation.

$$R_* = A_c R$$
$$R_* = 0354q^{-0.096}S^{-0.313}\left[\frac{qn}{1.486S^{1/2}}\right]^{3/5} \tag{71}$$

### *Discussion of the Aeration Factor, $A_c$*

One interpretation of the aeration factor, $A_c$, is as an estimate of the mean air concentration. The aeration examples in Chapter 2 are based upon the assumption that aeration directly deflates the unit weight of water, and over estimates the measured value of the hydraulic radius. Practically, the factor $A_c$ deflates the estimate of shear stress and indirectly the median particle size associated with the Manning-Shields-Strickler equation.

Figure 16 presents a comparison of $A_c$ and preliminary results from Gaston [7]. Gaston used an air concentration probe to physically measure the air concentration profile in flow on a 2:1 slope over stepped blocks. The calculated mean air concentrations from the measured concentration profiles make up the data shown in Figure 16 along with the factor $A_c$. The trends of the curves are similar, with the greatest deviation at the low range of unit discharge. The deviation could be caused by limitations in the air concentration probe data from Gaston. In low unit discharge flows, the depth is small compared to the diameter of the probe, prohibiting the probe

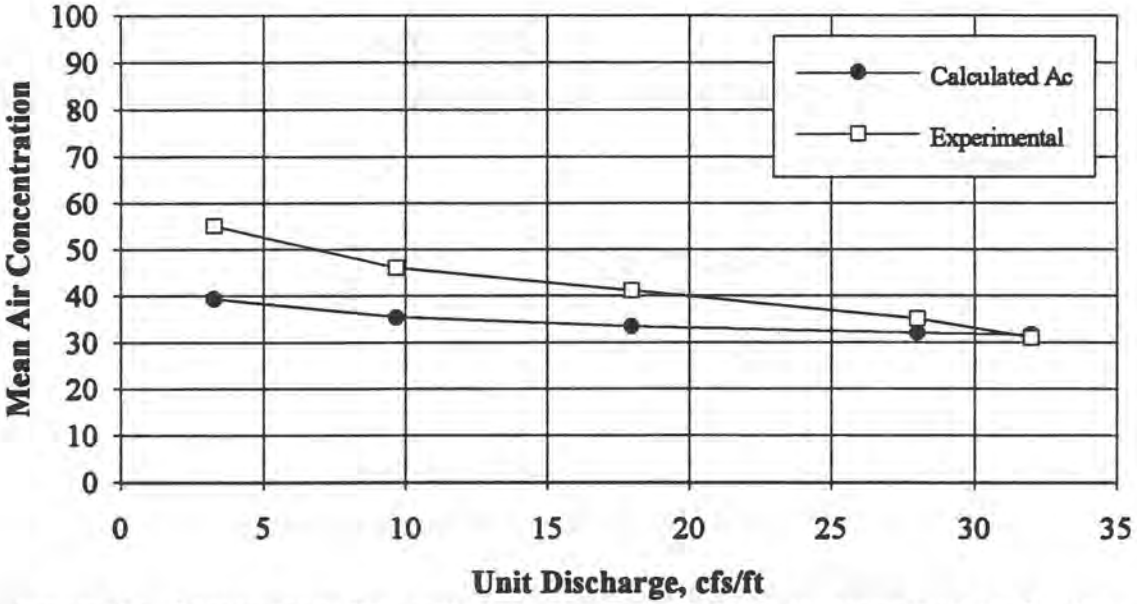


*Figure 16. Comparison of $A_c$ with data from 2:1 CSU overtopping study by Gaston.*

from measuring a significant portions of the flow near the boundaries. Nevertheless, based upon this comparison, the hypothesis of aeration effects appears to be well founded.

## *Example Application of Air Correction Factor*

This example utilizes the Stability Factors [22] riprap design method to demonstrate the magnitude of the correction due to aeration, and also the applicability of the aeration correction coefficient, $A_c$, to other design methods.

### *Given Values*

Three calculations are presented. The given values are either actual values from tests by Abt [1] or are standard values. Example of test values are the slope, coefficient of uniformity, depth/hydraulic radius, and angle of repose. A standard value for the safety factor is 1.1.

| *Factor* | *Value* |
|---|---|
| Unit Discharge | 5 $ft^3/s/ft$ |
| Slope | 20% |
| $C_u$ | 2.15 |
| Depth/Hydraulic Radius | 0.5 ft |
| Safety Factor | 1.1 |
| Angle of Repose | 42° |

### *Abt Equation*

From the modified Abt equation, an estimate for the median diameter is found based upon the given values.

$$D_{50} = 0.436S^{0.43}\left(\frac{q}{C_s}\right)^{0.56} \tag{44}$$

$$D_{50} = 6.5"$$

### *Stability Factors*

Stevens and Simons [22] analyzed the forces and moments acting on riprap. By balancing the turning forces or moments with the righting forces or moments, they created a stability factor for riprap mixtures based upon a characteristic particle size that was a function of the riprap gradation. A stability factor of 1.0 defines incipient motion. Values less than 1.0 indicate instability and values greater than 1.0 indicate stability. By definition, Stevens correlates a stability factor of 1.0 to a Shields parameter of 0.047. This correlation was a convenient method of estimating the forces by water parallel to the bed.

$$D_m = \frac{21\tau}{(S_s - 1)\gamma\eta} \tag{72}$$

$$\eta = \cos\alpha\left[\frac{1}{SF} - \frac{\tan\alpha}{\tan\phi}\right] \tag{73}$$

From these equations, an estimate for the median diameter is found based upon the given values.

$$D_m = 22.7"$$
$$D_{50} = \frac{D_m}{2} \tag{74}$$
$$D_{50} = 1135"$$

The estimate of Stability Factors exceeds the Abt estimate by a factor of roughly 2. Apply correction to the shear stress component of equation 72.

$$R_e = 037442q^{-0.096}S^{-0313}R \tag{75}$$

Recalculating the estimate by the Stability Factors method yields these values for the median riprap size.

$$D_m = 12"$$
$$D_{50} = \frac{D_m}{2}$$
$$D_{50} = 6.0"$$

After applying the correction, the two predictions are practically equivalent.

## Conclusions

The third hypothesis states that an expression based upon fundamental flow equations can be developed. Implicit in the expression are factors not explicitly treated, such as aeration and variation in the riprap mixture. The section on Shields parameter leads to the conclusion that shear stress, mass density of water and rock material, and a characteristic dimension, are the pertinent factors relating to incipient motion. The factors $A_c$ and $C_s$ are based upon prototype scale data from multiple studies. The factors show that riprap stability is a function of aeration, uniformity of the riprap mixture, the unit discharge, and slope.

Using the Manning, Strickler, and Shields equations, an equation (MSS) for the median size fraction of riprap as a function of unit discharge and slope was derived.

$$D_{50} = 1.725q^{0.667}S^{0.778} \tag{65}$$

The MSS equation and the Abt equation, equation 44, both are expressions for the median rock size, $D_{50}$, as a function of the slope, $S$, and unit discharge, $q$. The difference between the two equations, expressed by the factor $C_f$, is due to the implicit effect of aeration. Applying the correction factor, $C_f$, to the MSS equation yields the Abt equation.

The final step in generalizing the Abt equation is the addition of the stability coefficient, $C_s$. The following equation is the generalized form of the Abt equation.

$$D_{50} = 1.725 C_f S^{0.778} \left[ \frac{q_f}{C_s} \right]^{0.667} \tag{69}$$

$$C_f = 0.25 q^{-0.11} S^{-0.35} \tag{67}$$

As stated previously, the difference between the Abt and MSS equations is due to the aeration effect that is implicit in the Abt equation, and absent from the Manning-Shields-Strickler equation. The aeration effect is described by the aeration correction coefficient, $A_c$, given by

$$A_c = 0.354 q^{-0.096} S^{-0.313} \tag{70}$$

The aeration factor is applied to the hydraulic radius factor in the calculation of the shear stress. The factor $A_c$ has the effect of reducing the calculated shear stress due to aeration.

# CHAPTER 6

## CONCLUSIONS, FUTURE RESEARCH, AND EXAMPLES

### Conclusions

This investigation poses three hypothesis. The first hypothesis concerns the behavior of the Shields parameter in turbulent, overtopping flow. Investigation of the background and derivation of the Shields parameter indicates that the Shields parameter is constant when $Re_* > 10^4$. The apparent and reported increase in the Shields parameter is the result of false assumptions regarding the measurement of flow properties for the calculation of the parameter.

The second hypothesis concerns the influence of the uniformity upon the stability of a riprap mixture. The stability of riprap protection on embankments and side slopes is significantly influenced by the gradation of the riprap mixture. In general, poorly graded riprap demonstrates increased stability while well graded riprap is less stable than normal gradations for overtopping flows. Well graded riprap fails over a period of time as voids are filled with eroded material from upstream. The filling process is called healing. Failure of poorly graded riprap occurs very suddenly with very little healing. The designer should consider the ramifications of gradation specifications both in design and quality control during construction.

The second hypothesis states that a single factor is not sufficient to describe a riprap mixture. Based upon this investigation a mixture is now described with three sizes, $D_{10}$, $D_{50}$, and $D_{60}$. Though empirical, the adjustment factor, $C_s$, is calibrated for slopes less than twenty percent and unit discharges less than five cubic feet per second per foot. The expression of $C_s$ is given by:

$$C_s = 0.75 + \left(\log C_u^6\right)^{-2} \tag{47}$$

Since the bearing stress is transferred more efficiently by poorly graded riprap, the overall stability of poorly graded riprap is greater than well graded riprap.

The third hypothesis concerns the formulation of an analytical expression for riprap design, and the inclusion of all factors that influence the stability of riprap in overtopping flow. The section on Shields parameter leads to the conclusion that shear stress, mass density of water and rock material, and a characteristic dimension, are the pertinent factors relating to incipient motion. Using the Manning, Strickler, and Shields equations, an equation for the median size fraction of riprap as a function of unit discharge and slope was derived. This equation is the generalized form of the Abt equation.

$$D_{50} = 1.725 C_f S^{0.778} \left[\frac{q_f}{C_s}\right]^{0.667} \tag{69}$$

$$C_f = 0.25 q^{-0.11} S^{-0.35} \tag{67}$$

The difference between the Abt and MSS equations is due to the aeration effect that is intrinsic in the Abt equation, and absent from the Manning-Shields-Strickler equation. The aeration effect is described by the aeration correction coefficient, $A_c$, given by

$$A_c = 0.354 q^{-0.096} S^{-0.313} \tag{70}$$

The aeration coefficient is applied to the hydraulic radius factor in the calculation of the shear stress. The factor $A_c$ has the effect of reducing the calculated shear stress due to aeration.

## Future Research

- Gessler asserted a probability function for the Shields diagram. The family of probability curves is a function of the standard deviation, $\sigma$. The greater the value of $\sigma$, the greater the spacing between the probability curves. This implies that for a broad spectrum of turbulent

fluctuations, the probability of failure increases gradually for significant increases in applied shear stress. A narrow spectrum of turbulent fluctuations implies that the probability of failure increases rapidly for small increases in applied shear stress. Future research should focus on the exact behavior of $\sigma$ as a function of mixture uniformity.

- This investigation depends upon the first hypothesis, that the Shields parameter is constant and has a value of 0.047. Olivier [13] used a similar approach, but without the assumption that the local velocity is proportional to the shear velocity. He used approximations for the lift, drag, and other hydrodynamic forces. Measuring these forces directly would provide an opportunity to check the assumptions that Olivier made.
- The factor $(\cos\alpha \tan\psi - \sin\alpha)$ indicates the behavior of the Shields parameter on various slopes, $\alpha$, and for various angle of repose, $\psi$. This factor should be integrated into the generalized form of the Abt equation.
- Experiments at prototype scale on slopes greater than twenty percent and with median riprap sizes greater than six inches are necessary to extend the functional range of the generalized Abt equation, and to test the functionality of the aeration coefficient, $A_c$.
- Direct measurements of air concentration should be made with advanced technology air-concentration probes. Further analysis of the aeration effect is warranted.

## Examples

This sections presents four examples, two forward and two reverse solutions to the MSS equation. Each pair of solutions is for a poorly graded mixture, $C_u$~1.75, and a well graded mixture, $C_u$~3.5.

### *Example 1. Poorly graded, Forward solution.*

$q$: 5 ft$^3$/s/ft

$S$: 0.20

$C_u$: 1.75

$$D_{50} = 1.725 C_f S^{0.778} \left[\frac{q_f}{C_s}\right]^{0.667} \quad (69)$$

$D_{50} = 5.75"$

*Example 2. Well graded, Forward solution.*

$q$: 5 $ft^3/s/ft$

$S$: 0.20

$C_u$: 3.5

$$D_{50} = 1.725 C_f S^{0.778} \left[\frac{q_f}{C_s}\right]^{0.667} \quad (69)$$

$D_{50} = 7.1"$

*Example 3. Poorly graded, Reverse solution.*

$C_u$: 1.75

$D_{50}$:6"

$S$: 0.20

$$q_f = 0.441 C_s \left[\frac{D_{50}}{C_f S^{0.778}}\right]^{1.5} \quad (76)$$

$q_f = 5.4\ ft^3/s/ft$

*Example 4. Well graded, Reverse solution.*

$C_u$: 3.5

$D_{50}$:6"

$S$: 0.20

$$q_f = 0.441 C_s \left[\frac{D_{50}}{C_f S^{0.778}}\right]^{1.5} \quad (76)$$

$q_f = 3.7\ ft^3/s/ft$

## REFERENCES


1. Abt, S.R., Wittler, R.J., Ruff, J.F., LaGrone, D.L., Khattak, M.S., Nelson, J.D., Hinkle, N.E., Lee, D.W., "Development of Riprap Design Criteria by Riprap Testing in Flumes: Phase II. Followup Investigations." U.S. Nuclear Regulatory Commission, NUREG/CR-4651, ORNL/TM-10100/V2, Vol. 2. September, 1988.

2. Ahmed, A.F., "Filter and Gradation Effects on Side Slope Riprap Stability." Design of Hydraulic Structures 89, M.L. Albertson, R.A. Kia Editors. Balkema, Rotterdam, Brookfield, 1989. pp. 243-248.

3. Benedict, R. P., Fundamentals of Temperature, Pressure, and Flow Measurements, 3rd Ed., Wiley and Sons, New York, NY, 1984, p. 340.

4. Chow, V.T., Open Channel Hydraulics, McGraw-Hill Book Co., New York, 1959. Sec. 5.4, n.1, p. 94.

5. Einstein, H.A., "The Hydraulic or Radius Profile." Translated by Inge C. Hollingsworth, Division of Foreign Activities, Foreign Activities Technical Services Office, US Bureau of Reclamation Translations, Denver, Colorado, October, 1991. Source: "Schweizerische Bauzeitung Vol. 103, No. 8, February 24, 1934. pp. 89-91."

6. Einstein, H.A., "The Bed-Load Function for Sediment Transportation in Open Channel Flows." Technical Bulletin No. 1026, United States Department of Agriculture, Washington, D.C., 1950. p. 31.

7. Gaston, M., "Air Entrainment and Energy Dissipation on a Stepped Block Spillway." Thesis in partial fulfillment of the requirements for the degree Master of Science, Dept. of Civil Engineering, Colorado State University, Fort Collins, Colorado. 1994.

8. Gessler, J., "Beginning and Ceasing of Sediment Motion." River Mechanics, Vol. I., Chapter 7. Edited & Published by H.W. Shen, P.O. Box 606, Fort Collins, CO 80521. 1971.

9. Gessler, J., "The Beginning of Bedload Movement of Mixtures Investigated as Natural Armoring in Channels." W.M. Keck Laboratory of Hydraulics and Water Resources, California Institute of Technology, Pasadena, California. 1965-67.

10. Gilbert, G., "Transport of Debris by Running Water." Prof. Paper 86, US Geological Survey, Washington. 1914.

11. Henderson, F.M., Open Channel Flow, MacMillan Publishing Co., NY, 1966. p. 98.

12. Meyer-Peter, E., and Müller, R., "Formulas for Bed-Load Transport," Report on Second Meeting of IAHR, Stockholm, Sweden, 1948, pp. 39-64.

13. Olivier, H., "Through and Overflow Rockfill Dams - New Design Techniques." Proc. ICE, March, 1967. pp. 433-471.

14. Rouse, H., "An Analysis of Sediment Transportation in the Light of Fluid Turbulence.", Soil Conservation Service Report No. SCS-TP-25, United States Department of Agriculture, Washington, D.C., 1939.

15. Schlicting, H., Boundary Layer Theory. Translated by Dr. J. Kestin, Sixth Ed., McGraw-Hill, New York. 1968. p. 17.

16. Shen, H.W. and Wang, S., "Analysis of Commonly Used Riprap Design Guides Based on Extended Shields Diagram." Second Bridge Engineering Conference, Vol. 2, Transportation Research Record 950, Transportation Research Board, National Research Council, Washington D.C. 1984. pp. 217-221

17. Shen, H.W. and Wang, S., "Incipient Sediment Motion and Riprap Design." Journal of Hydraulic Engineering, ASCE, Vol. 111, No. 3, March, 1985. pp. 520-538.

18. Sherard, J.L., Richard, J.W., Stanley, F.G., William, A.C., Earth and Rock Dams, John Wiley, 1963.

19. Shields, A., "Anwendung der Aehnlichkeitsmechanik und der Turbulenzforschung auf die Geschiebebewegung": Mitteilung der Preussischen Versuchsanstalt fuer Wasserbau und Schiffbau, Heft 26, Berlin.

20. Shields, A., "Applications of Similarity Principles and Turbulence Research to Bed-Load Movements." Translated from "Anwendung der Aehnlichkeitsmechanik und der turbulenzforschung auf die geschiebebewegung", by Ott, W.P., Van Uchelen, J.C., U.S. Dept. Of Agriculture, Soil Conservation Service, Cooperative Laboratory, California Institute of Technology, Pasadena, California.

21. Stephenson, D., "Rockfill in Hydraulic Engineering." Developments in Geotechnical Engineering, Vol. 27, Elsevier Scientific Publishing Co.. pp. 50-60. 1979.

22. Stevens, M.A. and Simons, D.B., "Stability Analysis for Coarse Granular Material on Slopes." River Mechanics, Vol. I., Chapter 17. Edited & Published by H.W. Shen, P.O. Box 606, Fort Collins, CO 80521. 1971.

23. Whittaker, J., Jäggi, M., "Blockschwellen", Translated from the German, "Block Ramps", Reports by the Research Institute for Water Engineering, Hydrology and Glaciology, No. 91 - Zurich, 1986, by Inge C. Hollingsworth, Division of Foreign Activities, Foreign Activities Technical Services Office, US Bureau of Reclamation Translations, Denver, Colorado, November, 1988.

24. Williamson, J., "The Laws of Flow in Rough Pipes." La Houille Blance, vol. 6, no. 5, (September-October 1951), p. 738.

25. Wittler, R.J. and Abt, S.R., "Riprap Design by Modified Safety Factor Method." Hydraulic Engineering, Proceedings of the 1988 National Conference, ASCE. Edited by S.R. Abt and J. Gessler, ASCE, New York, New York. pp. 143-148.

26. Wittler, R.J. and Abt, S.R., "The Influence of Uniformity on Riprap Stability." Hydraulic Engineering, Proceedings of the 1990 National Conference, ASCE. Edited by H.H. Chang and J.C. Hill, ASCE, New York, New York. pp. 251-256.

27. California Division of Highways, Department of Public Works, "Bank and Shore Protection in California Highway Practice." p. 423. 1970.

28. Monograph 25, "Hydraulic Design of Stilling Basins and Energy Dissipaters." US Bureau of Reclamation, Denver, Colorado. 1978.

29. Sedimentation Engineering, ASCE-Manual and Reports on Engineering Practice-No. 54. Edited by Vito A. Vanoni, prepared by the ASCE Task Committee for the Preparation of the Manual on Sedimentation of the Sedimentation Committee of the Hydraulics Division. ASCE, New York, New York. 1975. p. 97.

30. US Army Corps of Engineers, "Engineering and Design, Additional Guidance for Riprap Channel Protection." ETL-1110-2-120, Office of the Chief of Engineers, US Army Corps of Engineers. May, 1971.

# APPENDIX A

## HYDRAULIC DATA

## Experiments

There were thirteen experiments. A combination of four slopes and three gradations were tested. The test numbers were assigned as shown in Table 3. Test number 1 was a trial test wherein procedures were developed, the DAS was debugged, and the procedures for the remaining tests were refined.

*Table 3. Test matrix.*

| | Test Number | | |
|---|---|---|---|
| | *Gradation #1* | *Gradation #2* | *Gradation #3* |
| *Slope, %* | $C_u = 2.92$ | $C_u = 1.56$ | $C_u = 5.33$ |
| 5 | 1,2 | 3 | 4* |
| 10 | 7* | 6* | 5* |
| 15 | 8* | 10* | 9* |
| 20 | 13* | 12* | 11* |

*Note: * indicates failure of the riprap.*

The following tables are a tabulation of the hydraulic data from the thirteen experiments. Each table is identified by the test number in the header. The header also contains the slope and the gradation of the experiment.

The run numbers refer to each pair of data recordings by the DAS. After each pair the discharge was incrementally increased. The point velocities, measured by the magnetic current meter, are indicated by V3. These velocities were measured directly above piezometer h3, at a depth of either 0.6, 0.2, or 0.8 of the local depth of flow, d3. The average velocity, Vavg, is the unit discharge, q, divided by the piezometric depth, d3. The hydraulic radius, Ravg, is the area of the flow, d3 times the width, three feet, divided by the quantity of two times the depth plus the width. The average slope, Savg, is the mean of three local slopes determined between the four piezometers, that is between h1 & h2, h2 & h3, and h3 & h4. In the same way, the average value of the Darcy friction factor, favg, is the mean of the values between the four piezometers. A relative submergence, Davg/D84, is the ratio of the average depth, Davg, and D84 of the respective riprap mixtures. The shear stress, $\tau$, is the product of the unit weight of water, for these

experiments assumed to be 62.4 pcf, the average hydraulic radius and the average slope. The Shields parameter, Tc, and Boundary Reynolds number, Re*, were calculated according to equations 1 and 16 respectively. The Froude number, Fr, is the ratio of the average velocity, Vavg, and the square root of gravity times the local depth, d3.

TEST-1 SLOPE=5% ROCK#1 .75"-6"

| RUN# | q | h1 | h2 | h3 | hL | h4 | V3 | d3 | Vavg | Davg | Ravg | Savg | favg | Davg | τ | To | Re* | Fr | d1 | d2 | d3 | d4 |
|---|---|---|---|---|---|---|---|---|---|---|---|---|---|---|---|---|---|---|---|---|---|---|
| | cfs/ft | in. | in. | in. | in. | in. | fps | ft. | fps | ft. | ft. | ft/ft | | D84 | | | | | Ft | Ft | Ft | Ft |
| 0 | 0.00 | 52.5 | 49.2 | 45.2 | | 42.4 | | | 0.00 | -0.86 | -2.02 | 0.0561 | N.A. | -2.00 | -7.07 | -0.257 | N.A. | N.A. | | | | |
| 1-3 | 0.11 | 62.7 | 59.4 | 56.1 | | 52.4 | | 0.00 | 0.00 | 0.00 | 0.00 | 0.0572 | N.A. | 0.00 | 0.00 | 0.000 | 0 | N.A. | | | | |
| 4-6 | 0.11 | 62.7 | 59.4 | 56.1 | | 52.4 | | 0.00 | 0.00 | 0.00 | 0.00 | 0.0572 | N.A. | 0.00 | 0.00 | 0.000 | 0 | N.A. | | | | |
| 7-10 | 0.11 | 62.7 | 59.4 | 56.1 | | 52.4 | | 0.00 | 0.00 | 0.00 | 0.00 | 0.0572 | N.A. | 0.00 | 0.00 | 0.000 | 0 | N.A. | 0.00 | 0.00 | 0.00 | 0.00 |
| 11-12 | 0.12 | 62.8 | 59.5 | 56.2 | | 52.5 | | | 0.80 | 0.01 | 0.01 | 0.0572 | 0.19 | 0.02 | 0.03 | 0.001 | 3398 | 1.54 | 0.01 | 0.01 | 0.01 | 0.01 |
| 13-14 | 0.28 | 63.9 | 60.6 | 57.5 | | 54.2 | 1.70 | 0.20 | 1.44 | 0.12 | 0.11 | 0.0542 | 0.72 | 0.27 | 0.36 | 0.013 | 11899 | 0.75 | 0.10 | 0.10 | 0.12 | 0.15 |
| 15-16 | 0.34 | 64.1 | 60.8 | 57.7 | | 54.4 | 1.98 | 0.25 | 1.70 | 0.13 | 0.12 | 0.0539 | 0.59 | 0.31 | 0.41 | 0.015 | 12676 | 0.82 | 0.12 | 0.12 | 0.13 | 0.17 |
| 17-18 | 0.38 | 64.3 | 61.0 | 57.9 | | 54.6 | 2.36 | 0.28 | 1.80 | 0.15 | 0.14 | 0.0539 | 0.58 | 0.35 | 0.46 | 0.017 | 13377 | 0.82 | 0.13 | 0.13 | 0.15 | 0.18 |
| 19-20 | 0.66 | 64.8 | 61.5 | 58.4 | | 55.1 | 2.82 | 0.30 | 2.85 | 0.19 | 0.17 | 0.0536 | 0.29 | 0.44 | 0.57 | 0.021 | 14859 | 1.15 | 0.17 | 0.18 | 0.19 | 0.23 |
| 21-22 | 0.74 | 65.0 | 61.7 | 58.6 | | 55.3 | 3.15 | 0.30 | 2.99 | 0.21 | 0.18 | 0.0539 | 0.28 | 0.49 | 0.62 | 0.022 | 15493 | 1.16 | 0.19 | 0.19 | 0.21 | 0.24 |
| 23-24 | 0.86 | 65.3 | 62.0 | 58.8 | | 55.6 | 3.60 | 0.30 | 3.26 | 0.23 | 0.20 | 0.0542 | 0.26 | 0.54 | 0.67 | 0.025 | 16225 | 1.20 | 0.22 | 0.22 | 0.23 | 0.26 |
| 25-26 | 0.96 | 65.4 | 62.1 | 58.9 | | 55.7 | 3.30 | 0.33 | 3.52 | 0.24 | 0.21 | 0.0539 | 0.23 | 0.56 | 0.69 | 0.025 | 16465 | 1.27 | 0.23 | 0.23 | 0.23 | 0.28 |
| 27-28 | 1.04 | 65.7 | 62.5 | 59.2 | | 56.0 | 3.95 | 0.35 | 3.50 | 0.26 | 0.22 | 0.0536 | 0.25 | 0.62 | 0.75 | 0.027 | 17135 | 1.20 | 0.25 | 0.25 | 0.26 | 0.30 |
| 29-30 | 1.14 | 65.8 | 62.6 | 59.3 | | 56.1 | 4.15 | 0.37 | 3.73 | 0.28 | 0.23 | 0.0539 | 0.23 | 0.64 | 0.78 | 0.028 | 17463 | 1.25 | 0.26 | 0.27 | 0.27 | 0.31 |
| 31-40 | 1.13 | 65.8 | 62.6 | 59.3 | | 56.1 | 4.15 | 0.37 | 3.70 | 0.28 | 0.23 | 0.0539 | 0.24 | 0.64 | 0.78 | 0.028 | 17463 | 1.24 | 0.26 | 0.27 | 0.27 | 0.31 |

TEST-2 SLOPE=5% ROCK#1 .75"-6"

| RUN# | q | h1 | h2 | h3 | hL | h4 | V3 | d3 | Vavg | Davg | Ravg | Savg | favg | Davg | τ | To | Re* | Fr | d1 | d2 | d3 | d4 |
|---|---|---|---|---|---|---|---|---|---|---|---|---|---|---|---|---|---|---|---|---|---|---|
| | cfs/ft | in. | in. | in. | in. | in. | fps | ft. | fps | ft. | ft. | ft/ft | | D84 | | | | | Ft | Ft | Ft | Ft |
| 1-2 | 0.14 | 62.9 | 59.6 | 56.5 | 53.0 | 52.9 | | | 0.00 | 0.00 | 0.00 | 0.0556 | N.A. | 0.00 | 0.00 | 0.000 | 0 | N.A. | 0.00 | 0.00 | 0.00 | 0.00 |
| 3-4 | 0.35 | 64.0 | 60.8 | 57.7 | 53.8 | 54.4 | 1.70 | | 2.04 | 0.10 | 0.10 | 0.0533 | 0.32 | 0.24 | 0.32 | 0.012 | 11194 | 1.12 | 0.09 | 0.10 | 0.10 | 0.13 |
| 5-6 | 0.56 | 64.7 | 61.4 | 58.3 | 54.2 | 55.0 | 2.75 | 0.26 | 2.67 | 0.16 | 0.14 | 0.0539 | 0.28 | 0.36 | 0.48 | 0.017 | 13627 | 1.19 | 0.15 | 0.15 | 0.15 | 0.18 |
| 7-8 | 0.78 | 65.2 | 61.9 | 58.8 | 54.5 | 55.5 | 3.60 | 0.30 | 3.25 | 0.20 | 0.17 | 0.0539 | 0.23 | 0.46 | 0.59 | 0.021 | 15147 | 1.29 | 0.19 | 0.19 | 0.19 | 0.22 |
| 9-10 | 1.07 | 65.6 | 62.3 | 59.3 | 54.7 | 56.0 | 3.60 | 0.35 | 3.94 | 0.24 | 0.20 | 0.0533 | 0.18 | 0.55 | 0.68 | 0.025 | 16256 | 1.43 | 0.23 | 0.23 | 0.23 | 0.26 |
| 11-12 | 1.20 | 66.0 | 62.6 | 59.5 | 54.8 | 56.3 | 3.90 | 0.40 | 4.09 | 0.26 | 0.22 | 0.0536 | 0.18 | 0.60 | 0.74 | 0.027 | 16991 | 1.41 | 0.25 | 0.25 | 0.25 | 0.28 |
| 13-14 | 1.41 | 66.5 | 63.1 | 59.9 | 55.0 | 56.8 | 4.15 | 0.45 | 4.27 | 0.30 | 0.25 | 0.0536 | 0.19 | 0.69 | 0.83 | 0.030 | 18013 | 1.38 | 0.30 | 0.29 | 0.28 | 0.33 |
| 15-16 | 1.71 | 66.9 | 63.4 | 60.3 | 55.2 | 57.1 | 4.65 | 0.50 | 4.78 | 0.33 | 0.27 | 0.0544 | 0.17 | 0.77 | 0.92 | 0.033 | 18918 | 1.47 | 0.33 | 0.32 | 0.32 | 0.35 |
| 17-18 | 1.86 | 67.1 | 63.6 | 60.5 | 55.6 | 57.3 | 4.80 | 0.50 | 4.96 | 0.35 | 0.28 | 0.0544 | 0.16 | 0.81 | 0.95 | 0.035 | 19303 | 1.49 | 0.35 | 0.33 | 0.33 | 0.37 |
| 19-20 | 1.92 | 67.2 | 63.7 | 60.5 | 55.6 | 57.4 | 4.80 | | 5.07 | 0.35 | 0.29 | 0.0544 | 0.16 | 0.82 | 0.97 | 0.035 | 19444 | 1.50 | 0.36 | 0.34 | 0.33 | 0.38 |
| 21-22 | 2.00 | 67.3 | 63.8 | 60.6 | 55.6 | 57.5 | 5.30 | | 5.15 | 0.36 | 0.29 | 0.0544 | 0.15 | 0.84 | 0.99 | 0.036 | 19628 | 1.51 | 0.37 | 0.35 | 0.34 | 0.38 |
| 23-24 | 2.05 | 67.4 | 63.9 | 60.7 | 55.7 | 57.6 | 5.30 | | 5.17 | 0.37 | 0.30 | 0.0544 | 0.16 | 0.86 | 1.01 | 0.037 | 19809 | 1.50 | 0.38 | 0.36 | 0.35 | 0.39 |
| 25-26 | 2.11 | 67.5 | 64.0 | 60.7 | 55.6 | 57.7 | 5.00 | | 5.24 | 0.38 | 0.30 | 0.0544 | 0.15 | 0.87 | 1.02 | 0.037 | 19943 | 1.51 | 0.38 | 0.37 | 0.35 | 0.40 |
| 27-28 | 2.15 | 67.6 | 64.0 | 60.8 | 55.6 | 57.8 | 5.40 | | 5.30 | 0.38 | 0.30 | 0.0547 | 0.15 | 0.89 | 1.04 | 0.038 | 20105 | 1.51 | 0.39 | 0.37 | 0.36 | 0.40 |
| 29 | 0.00 | 52.6 | 49.4 | 45.9 | 51.7 | 43.0 | 0.00 | 0.00 | | | | | | | | | | | | | | |

TEST-3 SLOPE=5% ROCK#2 2"-4"

| RUN# | q | h1 | h2 | h3 | hL | h4 | V3 | d3 | Vavg | Davg | Ravg | Savg | favg | Davg | τ | To | Re* | Fr | d1 | d2 | d3 | d4 |
|---|---|---|---|---|---|---|---|---|---|---|---|---|---|---|---|---|---|---|---|---|---|---|
| | cfs/ft | in. | in. | in. | in. | in. | fps | ft. | fps | ft. | ft. | ft/ft | | D84 | | | | | Ft | Ft | Ft | Ft |
| 0 | 0.00 | 51.4 | 48.5 | 44.9 | 58.9 | 42.6 | | | 0.00 | 0.00 | 0.00 | 0.0489 | | 0.00 | 0.00 | 0.000 | 0 | N.A. | 0.00 | 0.00 | 0.00 | 0.00 |
| 1-2 | 0.14 | 62.0 | 58.9 | 55.9 | 53.5 | 52.5 | | | 0.00 | 0.00 | 0.00 | 0.0528 | N.A. | 0.00 | 0.00 | 0.000 | 0 | N.A. | 0.00 | 0.00 | 0.00 | 0.00 |
| 3-4 | 0.81 | 64.6 | 61.2 | 58.4 | 54.9 | 55.3 | 0.65 | 0.18 | 3.15 | 0.21 | 0.19 | 0.0517 | 0.25 | 0.66 | 0.60 | 0.023 | 15071 | 1.21 | 0.22 | 0.19 | 0.21 | 0.23 |
| 5-6 | 1.47 | 65.8 | 62.5 | 59.5 | 54.9 | 57.0 | 1.35 | 0.42 | 4.13 | 0.32 | 0.27 | 0.0489 | 0.20 | 1.00 | 0.81 | 0.032 | 17516 | 1.28 | 0.32 | 0.30 | 0.30 | 0.38 |
| 7-8 | 2.09 | 66.9 | 63.3 | 60.5 | 55.0 | 58.0 | 1.85 | 0.48 | 4.83 | 0.40 | 0.32 | 0.0494 | 0.17 | 1.25 | 0.98 | 0.038 | 19282 | 1.34 | 0.41 | 0.37 | 0.38 | 0.46 |
| 9-10 | 2.61 | 67.5 | 63.9 | 61.1 | 60.2 | 58.8 | 2.10 | 0.55 | 5.38 | 0.46 | 0.35 | 0.0483 | 0.15 | 1.42 | 1.06 | 0.041 | 20019 | 1.40 | 0.46 | 0.42 | 0.43 | 0.53 |
| 11-12 | 0.19 | 62.1 | 59.0 | 56.1 | 53.2 | 53.1 | | | 0.00 | 0.00 | 0.00 | 0.0500 | N.A. | 0.00 | 0.00 | 0.000 | 0 | N.A. | 0.00 | 0.00 | 0.00 | 0.00 |
| 13-14 | 0.84 | 64.4 | 61.2 | 58.4 | 54.6 | 55.8 | 2.51 | 0.33 | 3.32 | 0.20 | 0.17 | 0.0478 | 0.20 | 0.61 | 0.52 | 0.020 | 14047 | 1.31 | 0.19 | 0.18 | 0.19 | 0.23 |
| 15-16 | 1.48 | 65.6 | 62.4 | 59.5 | 55.2 | 57.1 | 2.80 | 0.45 | 4.35 | 0.30 | 0.25 | 0.0472 | 0.16 | 0.92 | 0.73 | 0.029 | 16650 | 1.41 | 0.29 | 0.28 | 0.28 | 0.33 |
| 17-18 | 2.09 | 66.4 | 63.1 | 60.3 | 55.7 | 57.8 | 3.01 | 0.49 | 5.31 | 0.36 | 0.29 | 0.0478 | 0.13 | 1.11 | 0.86 | 0.034 | 18088 | 1.56 | 0.36 | 0.34 | 0.35 | 0.39 |
| 19-20 | 2.64 | 67.2 | 63.8 | 60.9 | 56.1 | 58.6 | 3.82 | 0.52 | 5.85 | 0.42 | 0.33 | 0.0475 | 0.12 | 1.30 | 0.97 | 0.038 | 19164 | 1.59 | 0.42 | 0.40 | 0.40 | 0.46 |

TEST-4 SLOPE=5% ROCK#3 .25"-9"

| RUN# | q | h1 | h2 | h3 | hL | h4 | V3 | d3 | Vavg | Davg | Ravg | Savg | favg | Davg | τ | To | Re* | Fr | d1 | d2 | d3 | d4 |
|---|---|---|---|---|---|---|---|---|---|---|---|---|---|---|---|---|---|---|---|---|---|---|
| | cfs/ft | in. | in. | in. | in. | in. | fps | ft. | fps | ft. | ft. | ft/ft | | D84 | | | | | Ft | Ft | Ft | Ft |
| 1-2 | 0.07 | 61.7 | 58.6 | 56.3 | 51.7 | 52.9 | 0.00 | 0.00 | 0.00 | 0.00 | 0.00 | 0.0489 | N.A. | 0.00 | 0.00 | 0.000 | 0 | N.A. | 0.00 | 0.00 | 0.00 | 0.00 |
| 3-4 | 0.43 | 63.7 | 60.4 | 58.0 | 52.9 | 54.6 | 2.45 | 0.28 | 2.37 | 0.15 | 0.14 | 0.0506 | 0.32 | 0.27 | 0.44 | 0.015 | 12643 | 1.07 | 0.17 | 0.15 | 0.14 | 0.15 |
| 5-6 | 1.01 | 65.0 | 61.8 | 59.4 | 53.7 | 55.9 | 3.35 | 0.31 | 3.58 | 0.26 | 0.22 | 0.0506 | 0.23 | 0.46 | 0.70 | 0.025 | 16082 | 1.23 | 0.28 | 0.26 | 0.25 | 0.25 |
| 7-8 | 1.46 | 65.8 | 62.4 | 59.9 | 54.1 | 56.6 | 4.20 | 0.38 | 4.35 | 0.32 | 0.26 | 0.0508 | 0.18 | 0.56 | 0.83 | 0.029 | 17469 | 1.36 | 0.34 | 0.32 | 0.30 | 0.31 |
| 9-10 | 2.03 | 66.4 | 63.3 | 60.6 | 54.7 | 57.2 | 4.60 | 0.45 | 5.23 | 0.38 | 0.30 | 0.0508 | 0.14 | 0.66 | 0.95 | 0.034 | 18687 | 1.50 | 0.39 | 0.39 | 0.36 | 0.36 |
| 11-12 | 2.41 | 66.8 | 63.7 | 61.1 | 55.0 | 57.4 | 4.90 | 0.48 | 5.73 | 0.41 | 0.32 | 0.0522 | 0.13 | 0.72 | 1.04 | 0.037 | 19571 | 1.58 | 0.43 | 0.43 | 0.40 | 0.38 |
| 13-14 | 2.67 | 67.2 | 64.1 | 61.3 | 55.1 | 57.4 | 5.30 | 0.52 | 6.06 | 0.43 | 0.33 | 0.0542 | 0.13 | 0.76 | 1.13 | 0.040 | 20325 | 1.63 | 0.46 | 0.46 | 0.42 | 0.38 |
| 15-16 | 2.99 | 67.5 | 64.7 | 61.4 | 55.2 | 57.5 | 5.60 | 0.58 | 6.47 | 0.45 | 0.35 | 0.0553 | 0.12 | 0.80 | 1.20 | 0.042 | 20950 | 1.70 | 0.48 | 0.51 | 0.43 | 0.39 |
| 17-18 | 3.24 | 67.8 | 65.0 | 60.9 | 54.7 | 58.2 | 6.50 | 0.70 | 6.76 | 0.47 | 0.36 | 0.0533 | 0.11 | 0.83 | 1.19 | 0.042 | 20884 | 1.74 | 0.51 | 0.53 | 0.38 | 0.45 |

TEST-5 SLOPE=10% ROCK#3 .25"-9"

| RUN# | q | h1 | h2 | h3 | hL | h4 | V3 | d3 | Vavg | Davg | Ravg | Savg | favg | Davg | τ | To | Re* | Fr | d1 | d2 | d3 | d4 |
|---|---|---|---|---|---|---|---|---|---|---|---|---|---|---|---|---|---|---|---|---|---|---|
| | cfs/ft | in. | in. | in. | in. | in. | fps | ft. | fps | ft. | ft. | ft/ft | | D84 | | | | | Ft | Ft | Ft | Ft |
| 1-2 | 0.11 | 72.8 | 67.1 | 60.5 | 58.7 | 55.0 | | | 0.00 | 0.00 | 0.00 | 0.0989 | N.A. | 0.00 | 0.00 | 0.000 | 0 | 0.00 | 0.00 | 0.00 | 0.00 | 0.00 |
| 3-4 | 0.37 | 74.0 | 68.3 | 61.6 | 59.3 | 56.1 | 1.70 | 0.20 | 2.68 | 0.10 | 0.09 | 0.0994 | 0.32 | 0.17 | 0.56 | 0.020 | 14322 | 1.52 | 0.10 | 0.10 | 0.09 | 0.09 |
| 5-6 | 0.89 | 74.9 | 69.4 | 62.7 | 59.8 | 57.3 | 2.10 | 0.22 | 4.19 | 0.19 | 0.17 | 0.0978 | 0.24 | 0.33 | 1.01 | 0.036 | 19221 | 1.71 | 0.18 | 0.19 | 0.18 | 0.19 |
| 7-8 | 1.23 | 75.2 | 69.8 | 62.9 | 59.8 | 57.7 | 3.30 | 0.32 | 5.24 | 0.21 | 0.19 | 0.0972 | 0.17 | 0.38 | 1.13 | 0.040 | 20356 | 2.00 | 0.20 | 0.23 | 0.20 | 0.23 |
| 9-10 | 1.46 | 75.5 | 70.0 | 62.9 | 60.0 | 57.7 | 4.10 | 0.45 | 6.06 | 0.22 | 0.19 | 0.0989 | 0.13 | 0.39 | 1.20 | 0.042 | 20963 | 2.26 | 0.23 | 0.24 | 0.20 | 0.23 |
| 11-12 | 1.77 | 75.8 | 70.1 | 63.6 | 60.7 | 58.9 | 3.40 | 0.45 | 6.13 | 0.27 | 0.23 | 0.0939 | 0.15 | 0.48 | 1.34 | 0.047 | 22208 | 2.08 | 0.25 | 0.25 | 0.26 | 0.33 |
| 13-14 | 2.07 | 75.6 | 69.6 | 63.3 | 60.8 | 57.9 | 3.90 | 0.52 | 8.56 | 0.23 | 0.20 | 0.0986 | 0.07 | 0.40 | 1.22 | 0.043 | 21145 | 3.16 | 0.23 | 0.21 | 0.23 | 0.24 |
| 15-16 | 2.37 | 75.9 | 69.6 | 63.2 | 61.1 | 58.0 | 4.10 | 0.45 | 9.64 | 0.23 | 0.20 | 0.0994 | 0.06 | 0.41 | 1.26 | 0.044 | 21484 | 3.51 | 0.26 | 0.21 | 0.22 | 0.25 |
| | | | | | | | 5.20 | 0.55 | | | | | | | | | | | | | | |

TEST-6 SLOPE=10% ROCK#2 2"-4"

| RUN# | q | h1 | h2 | h3 | hL | h4 | V3 | d3 | Vavg | Davg | Ravg | Savg | favg | Davg | τ | To | Re* | Fr | d1 | d2 | d3 | d4 |
|---|---|---|---|---|---|---|---|---|---|---|---|---|---|---|---|---|---|---|---|---|---|---|
| | cfs/ft | in. | in. | in. | in. | in. | fps | ft. | fps | ft. | ft. | ft/ft | | D84 | | | | | Ft | Ft | Ft | Ft |
| 1-2 | 0.26 | 73.4 | 67.5 | 60.6 | 58.6 | 55.0 | | | 0.00 | 0.00 | 0.00 | 0.1019 | N.A. | 0.00 | 0.00 | 0.000 | 0 | 0.00 | 0.00 | 0.00 | 0.00 | 0.00 |
| 3-4 | 0.64 | 74.4 | 68.7 | 61.7 | 59.4 | 56.1 | 2.50 | 0.13 | 4.07 | 0.09 | 0.09 | 0.1017 | 0.14 | 0.28 | 0.55 | 0.021 | 14403 | 2.37 | 0.09 | 0.10 | 0.09 | 0.09 |
| 5-6 | 1.01 | 75.3 | 69.9 | 62.4 | 59.8 | 56.9 | 4.20 | 0.21 | 4.51 | 0.17 | 0.15 | 0.1025 | 0.19 | 0.51 | 0.95 | 0.037 | 19003 | 1.95 | 0.16 | 0.20 | 0.15 | 0.15 |
| 7-8 | 1.57 | 76.2 | 70.2 | 63.2 | 60.3 | 57.7 | 4.30 | 0.32 | 5.80 | 0.23 | 0.20 | 0.1028 | 0.15 | 0.70 | 1.26 | 0.049 | 21837 | 2.15 | 0.24 | 0.23 | 0.22 | 0.23 |
| 9-10 | 1.92 | 76.7 | 70.6 | 63.3 | 60.2 | 58.0 | 6.60 | 0.37 | 6.56 | 0.25 | 0.22 | 0.1039 | 0.13 | 0.78 | 1.40 | 0.055 | 23053 | 2.30 | 0.28 | 0.26 | 0.23 | 0.25 |
| 11-12 | 2.37 | 77.2 | 71.0 | 63.7 | 60.4 | 58.3 | 6.50 | 0.39 | 7.39 | 0.29 | 0.24 | 0.1053 | 0.12 | 0.89 | 1.58 | 0.061 | 24418 | 2.44 | 0.32 | 0.29 | 0.26 | 0.27 |
| 13-14 | 2.52 | 77.3 | 71.0 | 63.8 | 60.4 | 57.9 | 6.50 | 0.40 | 8.01 | 0.28 | 0.24 | 0.1078 | 0.10 | 0.88 | 1.60 | 0.062 | 24592 | 2.66 | 0.33 | 0.29 | 0.27 | 0.24 |
| 15-16 | 2.67 | 77.5 | 71.1 | 64.2 | 60.8 | 58.2 | 6.70 | 0.40 | 7.98 | 0.30 | 0.25 | 0.1072 | 0.11 | 0.94 | 1.68 | 0.066 | 25234 | 2.56 | 0.35 | 0.30 | 0.30 | 0.27 |
| 17-18 | 2.93 | 77.8 | 71.4 | 64.4 | 60.9 | 58.6 | 6.90 | 0.45 | 8.14 | 0.33 | 0.27 | 0.1067 | 0.11 | 1.02 | 1.79 | 0.070 | 26044 | 2.50 | 0.37 | 0.33 | 0.32 | 0.30 |
| 19-20 | 3.13 | | | | | | 6.50 | 0.46 | 8.87 | 0.33 | 0.27 | 0.1000 | 0.09 | 1.02 | 1.68 | 0.065 | 25224 | 2.73 | | | | |

TEST-7 SLOPE=10% ROCK#1 .75"-6"

| RUN# | q | h1 | h2 | h3 | hL | h4 | V3 | d3 | Vavg | Davg | Ravg | Savg | favg | Davg | τ | To | Re* | Fr | d1 | d2 | d3 | d4 |
|---|---|---|---|---|---|---|---|---|---|---|---|---|---|---|---|---|---|---|---|---|---|---|
| | cfs/ft | in. | in. | in. | in. | in. | fps | ft. | fps | ft. | ft. | ft/ft | | D84 | | | | | Ft | Ft | Ft | Ft |
| 0 | 0.14 | 72.9 | 66.5 | 61.5 | | 55.5 | 0.00 | 0.00 | 0.00 | 0.00 | 0.00 | 0.0967 | N.A. | 0.00 | 0.00 | 0.000 | 0 | 0.00 | 0.00 | 0.00 | 0.00 | 0.00 |
| 1-2 | 0.27 | 72.9 | 66.5 | 61.5 | 59.5 | 55.5 | 0.00 | 0.00 | 0.00 | 0.00 | 0.00 | 0.0967 | N.A. | 0.00 | 0.00 | 0.000 | 0 | 0.00 | 0.00 | 0.00 | 0.00 | 0.00 |
| 3-4 | 0.72 | 74.3 | 67.7 | 62.8 | 60.3 | 57.1 | 2.20 | 0.25 | 5.09 | 0.11 | 0.11 | 0.0956 | 0.10 | 0.27 | 0.63 | 0.023 | 15739 | 2.65 | 0.12 | 0.10 | 0.11 | 0.13 |
| 5-6 | 1.18 | 75.2 | 68.6 | 63.5 | 60.5 | 57.8 | 3.60 | 0.28 | 5.79 | 0.18 | 0.16 | 0.0964 | 0.12 | 0.42 | 0.97 | 0.035 | 19432 | 2.40 | 0.19 | 0.18 | 0.17 | 0.19 |
| 7-8 | 1.46 | 75.8 | 69.1 | 63.9 | 60.6 | 58.4 | 4.90 | 0.30 | 5.92 | 0.22 | 0.19 | 0.0969 | 0.14 | 0.52 | 1.17 | 0.043 | 21405 | 2.21 | 0.24 | 0.21 | 0.20 | 0.24 |
| 9-10 | 1.84 | 76.4 | 69.7 | 64.4 | 61.2 | 59.0 | 4.50 | 0.33 | 6.27 | 0.27 | 0.23 | 0.0967 | 0.15 | 0.63 | 1.39 | 0.050 | 23276 | 2.12 | 0.29 | 0.27 | 0.24 | 0.29 |
| 11-12 | 2.09 | 76.4 | 69.5 | 64.5 | 61.7 | 59.2 | 5.60 | 0.38 | 7.08 | 0.28 | 0.23 | 0.0956 | 0.11 | 0.64 | 1.39 | 0.050 | 23254 | 2.38 | 0.29 | 0.25 | 0.25 | 0.31 |
| 13-14 | 2.49 | 77.2 | 69.7 | 64.6 | *61.0 | 59.3 | 5.80 | 0.55 | 7.92 | 0.30 | 0.25 | 0.0994 | 0.10 | 0.69 | 1.54 | 0.056 | 24498 | 2.56 | 0.35 | 0.27 | 0.25 | 0.31 |
| 15-16 | 2.68 | 75.5 | 69.6 | 60.9 | *64.9 | 60.3 | 4.80 | 0.40 | 12.38 | 0.21 | 0.18 | 0.0844 | 0.03 | 0.48 | 0.95 | 0.035 | 19266 | 4.82 | 0.22 | 0.26 | -0.05 | 0.40 |

TEST-8 SLOPE=15% ROCK#1 .75"-6"

| RUN# | q | h1 | h2 | h3 | hL | h4 | V3 | d3 | Vavg | Davg | Ravg | Savg | favg | Davg | τ | To | Re* | Fr | d1 | d2 | d3 | d4 |
|---|---|---|---|---|---|---|---|---|---|---|---|---|---|---|---|---|---|---|---|---|---|---|
| | cfs/ft | in. | in. | in. | in. | in. | fps | ft. | fps | ft. | ft. | ft/ft | | D84 | | | | | Ft | Ft | Ft | Ft |
| 0 | 0.14 | 83.9 | 75.4 | 65.3 | | 56.8 | | | 0.00 | 0.00 | 0.00 | 0.1506 | N.A. | 0.00 | 0.00 | 0.000 | 0 | N.A. | 0.00 | 0.00 | 0.00 | 0.00 |
| 1-2 | 0.26 | 84.8 | 76.0 | 66.1 | 60.9 | 57.1 | | | 2.32 | 0.05 | 0.05 | 0.1536 | 0.38 | 0.12 | 0.49 | 0.018 | 13854 | 1.78 | 0.07 | 0.05 | 0.07 | 0.03 |
| 3-4 | 0.62 | 86.2 | 77.2 | 67.4 | 61.7 | 58.9 | 1.60 | 0.20 | 2.78 | 0.17 | 0.16 | 0.1517 | 0.79 | 0.40 | 1.47 | 0.053 | 23929 | 1.18 | 0.19 | 0.15 | 0.18 | 0.18 |
| 5-6 | 1.05 | 87.1 | 78.2 | 68.2 | 61.9 | 59.7 | 3.50 | 0.26 | 3.73 | 0.24 | 0.21 | 0.1522 | 0.59 | 0.57 | 2.00 | 0.073 | 27930 | 1.33 | 0.27 | 0.23 | 0.24 | 0.24 |
| 7-8 | 1.33 | 87.3 | 78.3 | 68.6 | 62.4 | 59.8 | 3.80 | 0.38 | 4.55 | 0.26 | 0.22 | 0.1528 | 0.43 | 0.61 | 2.13 | 0.077 | 28829 | 1.56 | 0.28 | 0.24 | 0.28 | 0.25 |
| 9-10 | 1.49 | 87.4 | 78.5 | 68.6 | 62.3 | 59.8 | 4.20 | 0.40 | 5.09 | 0.27 | 0.23 | 0.1531 | 0.34 | 0.62 | 2.16 | 0.078 | 29001 | 1.74 | 0.29 | 0.25 | 0.27 | 0.25 |
| 11-12 | 1.68 | 87.5 | 78.7 | 68.8 | 62.1 | 59.8 | 4.80 | 0.35 | 5.55 | 0.28 | 0.23 | 0.1536 | 0.30 | 0.65 | 2.25 | 0.082 | 29625 | 1.85 | 0.30 | 0.28 | 0.29 | 0.25 |
| 13-14 | 1.75 | 87.7 | 78.8 | 68.9 | 61.9 | 60.0 | 4.10 | 0.35 | 5.57 | 0.29 | 0.24 | 0.1536 | 0.31 | 0.67 | 2.33 | 0.085 | 30132 | 1.82 | 0.31 | 0.28 | 0.30 | 0.27 |
| 15-16 | 1.86 | 87.4 | 78.7 | 69.0 | 62.2 | 59.8 | 3.00 | 0.20 | 6.13 | 0.28 | 0.24 | 0.1531 | 0.25 | 0.65 | 2.25 | 0.082 | 29664 | 2.04 | 0.29 | 0.28 | 0.31 | 0.25 |
| 17-18 | 1.95 | 87.3 | 78.8 | 69.4 | 62.6 | 59.5 | 2.70 | 0.30 | 6.41 | 0.28 | 0.24 | 0.1544 | 0.23 | 0.66 | 2.29 | 0.083 | 29892 | 2.13 | 0.28 | 0.28 | 0.34 | 0.23 |

TEST-9 SLOPE=15% ROCK#3 .25"-9"

| RUN# | q | h1 | h2 | h3 | hL | h4 | V3 | d3 | Vavg | Davg | Ravg | Savg | favg | Davg | τ | To | Re* | Fr | d1 | d2 | d3 | d4 |
|---|---|---|---|---|---|---|---|---|---|---|---|---|---|---|---|---|---|---|---|---|---|---|
| | cfs/ft | in. | in. | in. | in. | in. | fps | ft. | fps | ft. | ft. | ft/ft | | D84 | | | | | Ft | Ft | Ft | Ft |
| 1-2 | 0.10 | 83.4 | 75.5 | 65.8 | 61.6 | 56.3 | | | 0.00 | 0.00 | 0.00 | 0.1506 | N.A. | 0.00 | 0.00 | 0.000 | 0 | N.A. | 0.00 | 0.00 | 0.00 | 0.00 |
| 3-4 | 0.31 | 85.1 | 76.6 | 66.6 | 62.2 | 57.0 | | | 2.27 | 0.09 | 0.08 | 0.1561 | 0.66 | 0.16 | 0.82 | 0.029 | 17383 | 1.34 | 0.14 | 0.09 | 0.07 | 0.06 |
| 5-6 | 0.52 | 85.7 | 77.1 | 67.1 | 62.3 | 57.0 | 2.50 | 0.20 | 3.36 | 0.12 | 0.11 | 0.1594 | 0.41 | 0.22 | 1.13 | 0.040 | 20366 | 1.69 | 0.19 | 0.13 | 0.11 | 0.06 |
| 7-8 | 0.68 | 85.8 | 77.3 | 67.4 | 62.6 | 57.3 | 3.70 | 0.26 | 4.07 | 0.14 | 0.13 | 0.1583 | 0.32 | 0.25 | 1.28 | 0.045 | 21663 | 1.91 | 0.20 | 0.15 | 0.13 | 0.08 |
| 9-10 | 0.83 | 85.9 | 77.3 | 67.8 | 62.6 | 57.3 | 3.70 | 0.28 | 4.82 | 0.15 | 0.14 | 0.1586 | 0.24 | 0.26 | 1.35 | 0.048 | 22254 | 2.19 | 0.20 | 0.15 | 0.16 | 0.08 |
| 11-12 | 1.00 | 86.8 | 77.4 | 68.2 | 62.8 | 57.6 | 3.10 | 0.28 | 4.81 | 0.19 | 0.17 | 0.1622 | 0.30 | 0.33 | 1.68 | 0.059 | 24820 | 1.96 | 0.28 | 0.15 | 0.20 | 0.11 |
| 13-14 | 1.16 | 87.1 | 76.9 | 68.6 | 63.4 | 57.5 | 4.40 | 0.30 | 5.65 | 0.19 | 0.17 | 0.1644 | 0.22 | 0.33 | 1.71 | 0.060 | 25051 | 2.30 | 0.30 | 0.12 | 0.23 | 0.10 |
| 15-16 | 1.32 | 87.2 | 77.3 | 68.6 | 63.4 | 57.5 | 5.10 | 0.35 | 6.18 | 0.20 | 0.17 | 0.1650 | 0.19 | 0.35 | 1.79 | 0.063 | 25642 | 2.45 | 0.31 | 0.15 | 0.23 | 0.10 |
| 17-18 | 1.46 | 86.4 | | 68.2 | 62.7 | | | | 6.01 | 0.23 | 0.20 | 0.1517 | 0.21 | 0.40 | 1.85 | 0.065 | 26067 | 2.23 | 0.25 | | 0.20 | |

TEST-10 SLOPE=15% ROCK#2 2"-4"

| RUN# | q | h1 | h2 | h3 | hL | h4 | V3 | d3 | Vavg | Davg | Ravg | Savg | favg | Davg | τ | To | Re* | Fr | d1 | d2 | d3 | d4 |
|---|---|---|---|---|---|---|---|---|---|---|---|---|---|---|---|---|---|---|---|---|---|---|
| | cfs/ft | in. | in. | in. | in. | in. | fps | ft. | fps | ft. | ft. | ft/ft | | D84 | | | | | Ft | Ft | Ft | Ft |
| 1-2 | 0.24 | 84.0 | 74.9 | 65.7 | 61.5 | 56.7 | | | 0.00 | 0.00 | 0.00 | 0.1517 | N.A. | 0.00 | 0.00 | 0.000 | 0 | N.A. | 0.00 | 0.00 | 0.00 | 0.00 |
| 3-4 | 0.58 | 85.5 | 76.5 | 67.0 | 62.5 | 58.2 | 3.08 | 0.18 | 2.79 | 0.12 | 0.11 | 0.1517 | 0.57 | 0.38 | 1.08 | 0.042 | 20173 | 1.40 | 0.13 | 0.13 | 0.11 | 0.13 |
| 5-6 | 0.84 | 86.1 | 77.1 | 67.5 | 62.7 | 58.8 | 4.08 | 0.25 | 3.53 | 0.17 | 0.15 | 0.1517 | 0.48 | 0.53 | 1.45 | 0.057 | 23439 | 1.51 | 0.18 | 0.18 | 0.15 | 0.18 |
| 7-8 | 1.07 | 86.6 | 77.4 | 67.9 | 62.9 | 59.2 | 4.54 | 0.28 | 4.07 | 0.20 | 0.18 | 0.1525 | 0.43 | 0.63 | 1.71 | 0.067 | 25442 | 1.59 | 0.22 | 0.21 | 0.19 | 0.20 |
| 9-10 | 1.31 | 87.1 | 78.0 | 68.7 | 63.1 | 59.6 | 5.32 | 0.25 | 4.24 | 0.25 | 0.22 | 0.1528 | 0.47 | 0.78 | 2.06 | 0.080 | 27955 | 1.49 | 0.26 | 0.26 | 0.25 | 0.24 |
| 11-12 | 1.69 | 86.9 | 78.2 | 69.3 | 63.1 | 60.0 | 5.46 | 0.32 | 5.29 | 0.27 | 0.23 | 0.1494 | 0.32 | 0.85 | 2.16 | 0.084 | 28595 | 1.78 | 0.24 | 0.28 | 0.30 | 0.28 |
| 13-14 | 1.84 | 86.7 | 78.3 | 70.1 | 64.0 | 60.2 | 6.39 | 0.35 | 5.53 | 0.29 | 0.24 | 0.1472 | 0.30 | 0.90 | 2.24 | 0.087 | 29096 | 1.81 | 0.23 | 0.28 | 0.37 | 0.29 |
| 15-16 | 2.02 | 87.0 | 78.3 | 70.4 | 64.2 | 59.8 | 6.11 | 0.40 | 6.04 | 0.30 | 0.25 | 0.1511 | 0.26 | 0.92 | 2.33 | 0.091 | 29697 | 1.96 | 0.25 | 0.28 | 0.39 | 0.26 |
| 17-18 | 2.21 | 87.3 | 78.4 | 70.5 | 64.3 | 59.6 | 5.07 | 0.45 | 6.56 | 0.30 | 0.25 | 0.1539 | 0.23 | 0.93 | 2.41 | 0.094 | 30188 | 2.11 | 0.28 | 0.29 | 0.40 | 0.24 |
| 19-20 | 2.34 | 87.5 | 78.5 | 70.6 | 64.6 | 59.7 | 6.68 | 0.48 | 6.70 | 0.31 | 0.26 | 0.1544 | 0.23 | 0.97 | 2.50 | 0.097 | 30757 | 2.11 | 0.29 | 0.30 | 0.41 | 0.25 |
| 21-22 | 2.42 | 87.7 | 78.6 | 70.2 | 64.2 | 59.2 | 7.38 | 0.40 | 7.26 | 0.30 | 0.25 | 0.1583 | 0.19 | 0.93 | 2.48 | 0.096 | 30621 | 2.33 | 0.31 | 0.31 | 0.38 | 0.21 |

TEST-11 SLOPE=20% ROCK#3 .25"-9"

| RUN# | q | h1 | h2 | h3 | hL | h4 | V3 | d3 | Vavg | Davg | Ravg | Savg | favg | Davg | τ | To | Re* | Fr | d1 | d2 | d3 | d4 |
|---|---|---|---|---|---|---|---|---|---|---|---|---|---|---|---|---|---|---|---|---|---|---|
| | cfs/ft | in. | in. | in. | in. | in. | fps | ft. | fps | ft. | ft. | ft/ft | | D84 | | | | | Ft | Ft | Ft | Ft |
| 1-2 | 0.29 | 95.3 | 83.3 | 70.2 | 69.5 | 59.6 | | | 0.00 | 0.00 | 0.00 | 0.1983 | N.A. | 0.00 | 0.00 | 0.000 | 0 | N.A. | 0.00 | 0.00 | 0.00 | 0.00 |
| 3-4 | 0.46 | 95.6 | 83.7 | 70.5 | 69.6 | 60.1 | 2.53 | 0.15 | 5.44 | 0.03 | 0.03 | 0.1972 | 0.05 | 0.06 | 0.38 | 0.013 | 11758 | 5.42 | 0.02 | 0.03 | 0.02 | 0.04 |
| 5-6 | 0.60 | 95.9 | 84.1 | 70.8 | 69.9 | 60.4 | 3.33 | 0.18 | 5.35 | 0.06 | 0.06 | 0.1972 | 0.10 | 0.10 | 0.68 | 0.024 | 15786 | 3.94 | 0.05 | 0.07 | 0.05 | 0.07 |
| 7-8 | 0.70 | 96.0 | 84.2 | 71.0 | 70.1 | 60.5 | 4.18 | 0.20 | 5.92 | 0.07 | 0.07 | 0.1972 | 0.10 | 0.12 | 0.81 | 0.029 | 17230 | 3.98 | 0.06 | 0.08 | 0.07 | 0.07 |
| 9-10 | 0.81 | 96.4 | 84.3 | 71.2 | 70.0 | 60.7 | 4.67 | 0.25 | 6.05 | 0.09 | 0.08 | 0.1983 | 0.11 | 0.15 | 1.01 | 0.036 | 19268 | 3.63 | 0.09 | 0.08 | 0.08 | 0.09 |
| 11-12 | 0.90 | 96.5 | 84.3 | 71.3 | 70.1 | 60.8 | 4.92 | 0.28 | 6.58 | 0.09 | 0.09 | 0.1983 | 0.10 | 0.16 | 1.08 | 0.038 | 19913 | 3.81 | 0.10 | 0.08 | 0.09 | 0.10 |
| 13-14 | 0.94 | 96.5 | 84.4 | 71.3 | 70.3 | 60.8 | 3.82 | 0.25 | 6.82 | 0.10 | 0.09 | 0.1983 | 0.10 | 0.17 | 1.11 | 0.039 | 20226 | 3.88 | 0.10 | 0.09 | 0.09 | 0.10 |
| 15-16 | 1.04 | 96.5 | 84.4 | 71.4 | 70.3 | 60.9 | 5.22 | 0.25 | 7.58 | 0.10 | 0.09 | 0.1981 | 0.08 | 0.17 | 1.15 | 0.041 | 20518 | 4.25 | 0.10 | 0.09 | 0.10 | 0.10 |
| 17-18 | 1.11 | 95.8 | 84.6 | 71.7 | 70.2 | 61.1 | 4.11 | 0.25 | 8.23 | 0.10 | 0.09 | 0.1928 | 0.07 | 0.18 | 1.13 | 0.040 | 20343 | 4.59 | 0.04 | 0.11 | 0.13 | 0.13 |
| 19-20 | 1.20 | 95.8 | 85.0 | 71.7 | 70.0 | 61.1 | 2.23 | 0.25 | 8.40 | 0.11 | 0.10 | 0.1928 | 0.07 | 0.19 | 1.22 | 0.043 | 21119 | 4.50 | 0.04 | 0.14 | 0.13 | 0.13 |
| 21-22 | 1.27 | 95.9 | 85.0 | 71.7 | 70.0 | 61.2 | 3.68 | 0.20 | 8.85 | 0.11 | 0.10 | 0.1925 | 0.07 | 0.19 | 1.24 | 0.044 | 21291 | 4.69 | 0.05 | 0.14 | 0.13 | 0.13 |
| 23-24 | 1.31 | 95.9 | 85.1 | 71.8 | 70.0 | 61.2 | 3.27 | 0.15 | 8.93 | 0.11 | 0.11 | 0.1928 | 0.07 | 0.20 | 1.28 | 0.045 | 21677 | 4.65 | 0.05 | 0.15 | 0.13 | 0.13 |
| 25-26 | 1.40 | 96.0 | 85.5 | 71.8 | 70.1 | 61.5 | 2.19 | 0.20 | 8.39 | 0.13 | 0.12 | 0.1919 | 0.09 | 0.23 | 1.46 | 0.051 | 23115 | 4.07 | 0.06 | 0.18 | 0.13 | 0.15 |
| 27-28 | 1.50 | 96.1 | 85.8 | 71.8 | 70.0 | 61.5 | 3.88 | 0.30 | 8.54 | 0.14 | 0.13 | 0.1922 | 0.09 | 0.25 | 1.55 | 0.055 | 23869 | 4.00 | 0.07 | 0.21 | 0.13 | 0.16 |
| 29-30 | 1.56 | 96.1 | 85.8 | 72.4 | 69.6 | 62.2 | 7.43 | 0.50 | 7.57 | 0.17 | 0.15 | 0.1886 | 0.13 | 0.30 | 1.78 | 0.063 | 25524 | 3.26 | 0.07 | 0.21 | 0.18 | 0.21 |
| 31-32 | 1.64 | 96.2 | 85.9 | 72.6 | 70.1 | 62.2 | 7.46 | 0.55 | 7.70 | 0.18 | 0.16 | 0.1886 | 0.13 | 0.31 | 1.84 | 0.065 | 26016 | 3.24 | 0.07 | 0.22 | 0.20 | 0.22 |
| 33-34 | 1.72 | 96.3 | 86.0 | 72.8 | 70.0 | 62.1 | 3.68 | 0.45 | 7.91 | 0.18 | 0.16 | 0.1903 | 0.13 | 0.32 | 1.92 | 0.068 | 26544 | 3.27 | 0.08 | 0.23 | 0.21 | 0.20 |
| 35-36 | 1.76 | 96.3 | 86.1 | 72.5 | 69.9 | 61.0 | 2.05 | 0.40 | 9.56 | 0.15 | 0.14 | 0.1964 | 0.08 | 0.27 | 1.71 | 0.060 | 25073 | 4.29 | 0.08 | 0.23 | 0.19 | 0.11 |
| 37-38 | 1.86 | 96.3 | 86.3 | 72.5 | 69.6 | 61.0 | 2.24 | 0.40 | 9.77 | 0.16 | 0.14 | 0.1961 | 0.08 | 0.28 | 1.77 | 0.063 | 25510 | 4.30 | 0.08 | 0.25 | 0.19 | 0.12 |
| 39-40 | 2.00 | 97.3 | 86.4 | 73.5 | 69.9 | 61.4 | 3.82 | 0.45 | 8.13 | 0.21 | 0.18 | 0.1994 | 0.14 | 0.37 | 2.30 | 0.081 | 29030 | 3.12 | 0.17 | 0.25 | 0.27 | 0.15 |

TEST-12 SLOPE=20% ROCK#2 2"-4"

| RUN# | q | h1 | h2 | h3 | hL | h4 | V3 | d3 | Vavg | Davg | Ravg | Savg | favg | Davg | τ | To | Re* | Fr | d1 | d2 | d3 | d4 |
|---|---|---|---|---|---|---|---|---|---|---|---|---|---|---|---|---|---|---|---|---|---|---|
| | ofs/ft | in. | in. | in. | in. | in. | fps | ft. | fps | ft. | ft. | ft/ft | | D84 | | | | | Ft | Ft | Ft | Ft |
| 0 | 0.25 | 94.4 | 82.0 | 70.5 | | 57.7 | | | 0.00 | 0.00 | 0.00 | 0.2039 | N.A. | 0.00 | 0.00 | 0.000 | 0 | N.A. | 0.00 | 0.00 | 0.00 | 0.00 |
| 1-2 | 0.30 | 94.9 | 82.5 | 71.0 | 68.1 | 58.0 | | | 1.37 | 0.04 | 0.04 | 0.2050 | 1.00 | 0.11 | 0.46 | 0.018 | 13128 | 1.27 | 0.04 | 0.04 | 0.04 | 0.02 |
| 3-4 | 0.54 | 96.4 | 83.6 | 72.0 | 68.7 | 59.4 | 2.87 | 0.10 | 2.13 | 0.14 | 0.13 | 0.2056 | 1.50 | 0.43 | 1.64 | 0.064 | 24899 | 1.00 | 0.16 | 0.13 | 0.13 | 0.14 |
| 5-6 | 0.83 | 97.1 | 84.4 | 72.7 | 69.2 | 60.1 | 4.33 | 0.15 | 2.87 | 0.20 | 0.18 | 0.2056 | 1.14 | 0.63 | 2.28 | 0.089 | 29405 | 1.13 | 0.22 | 0.20 | 0.18 | 0.20 |
| 7-8 | 1.12 | 97.7 | 84.9 | 73.4 | 69.4 | 61.0 | 5.40 | 0.25 | 3.40 | 0.26 | 0.22 | 0.2039 | 1.00 | 0.79 | 2.78 | 0.108 | 32465 | 1.18 | 0.28 | 0.24 | 0.24 | 0.28 |
| 9-10 | 1.34 | 97.8 | 85.3 | 73.7 | 69.7 | 61.3 | 5.69 | 0.30 | 3.93 | 0.28 | 0.24 | 0.2025 | 0.80 | 0.87 | 2.97 | 0.116 | 33551 | 1.31 | 0.28 | 0.28 | 0.26 | 0.30 |
| 11-12 | 1.45 | 97.9 | 85.6 | 73.1 | 69.2 | 61.7 | 6.85 | 0.30 | 4.22 | 0.29 | 0.24 | 0.2011 | 0.70 | 0.89 | 3.01 | 0.117 | 33749 | 1.39 | 0.29 | 0.30 | 0.22 | 0.33 |
| 13-14 | 1.60 | 98.1 | 85.8 | 73.4 | 69.5 | 61.6 | 6.05 | 0.35 | 4.57 | 0.30 | 0.25 | 0.2031 | 0.62 | 0.92 | 3.13 | 0.122 | 34425 | 1.48 | 0.31 | 0.31 | 0.24 | 0.32 |
| 15-16 | 1.65 | 98.0 | 85.6 | 73.0 | 68.9 | 61.8 | 7.95 | 0.30 | 4.87 | 0.29 | 0.24 | 0.2011 | 0.53 | 0.89 | 3.03 | 0.118 | 33852 | 1.60 | 0.30 | 0.30 | 0.21 | 0.34 |
| 17-18 | 1.74 | 98.0 | 85.8 | 72.7 | 68.0 | 62.0 | 7.15 | 0.35 | 5.19 | 0.29 | 0.24 | 0.2000 | 0.46 | 0.89 | 3.01 | 0.117 | 33759 | 1.71 | 0.30 | 0.31 | 0.18 | 0.36 |
| 19-20 | 1.88 | 97.1 | 82.8 | 72.5 | 68.6 | 64.5 | 9.23 | 0.25 | 6.36 | 0.26 | 0.22 | 0.1811 | 0.25 | 0.79 | 2.47 | 0.096 | 30598 | 2.21 | 0.22 | 0.07 | 0.17 | 0.57 |

TEST-13 SLOPE=20% ROCK#1 .75"-6"

| RUN# | q | h1 | h2 | h3 | hL | h4 | V3 | d3 | Vavg | Davg | Ravg | Savg | favg | Davg | τ | To | Re* | Fr | d1 | d2 | d3 | d4 |
|---|---|---|---|---|---|---|---|---|---|---|---|---|---|---|---|---|---|---|---|---|---|---|
| | cfs/ft | in. | in. | in. | in. | in. | fps | ft. | fps | ft. | ft. | ft/ft | | D84 | | | | | Ft | Ft | Ft | Ft |
| 0 | 0.20 | 94.6 | 82.7 | 71.3 | 63.5 | 58.6 | | | 0.00 | 0.00 | 0.00 | 0.2000 | N.A. | 0.00 | 0.00 | 0.000 | 0 | N.A. | 0.00 | 0.00 | 0.00 | 0.00 |
| 1-2 | 0.32 | 95.8 | 83.7 | 72.1 | 67.9 | 59.5 | | | 1.52 | 0.08 | 0.08 | 0.2017 | 1.74 | 0.19 | 0.97 | 0.035 | 19455 | 0.94 | 0.10 | 0.08 | 0.07 | 0.07 |
| 3-4 | 0.52 | 96.4 | 84.2 | 72.6 | 68.4 | 60.0 | 3.12 | 0.15 | 2.51 | 0.13 | 0.12 | 0.2022 | 0.96 | 0.29 | 1.47 | 0.053 | 23928 | 1.25 | 0.15 | 0.13 | 0.11 | 0.12 |
| 5-6 | 0.73 | 96.9 | 84.7 | 73.2 | 68.8 | 60.4 | 1.85 | 0.17 | 3.18 | 0.17 | 0.15 | 0.2028 | 0.77 | 0.39 | 1.90 | 0.069 | 27216 | 1.37 | 0.19 | 0.17 | 0.16 | 0.15 |
| 7-8 | 0.87 | 97.3 | 85.0 | 73.4 | 69.0 | 60.7 | 3.85 | 0.20 | 3.53 | 0.19 | 0.17 | 0.2033 | 0.71 | 0.44 | 2.15 | 0.078 | 28939 | 1.43 | 0.22 | 0.19 | 0.18 | 0.17 |
| 9-10 | 1.02 | 97.6 | 85.2 | 73.7 | 69.0 | 60.9 | 2.45 | 0.25 | 3.89 | 0.21 | 0.19 | 0.2036 | 0.64 | 0.49 | 2.35 | 0.086 | 30314 | 1.49 | 0.25 | 0.21 | 0.20 | 0.19 |
| 11-12 | 1.11 | 97.8 | 85.5 | 73.8 | 68.5 | 61.2 | 2.80 | 0.27 | 3.94 | 0.23 | 0.20 | 0.2033 | 0.68 | 0.54 | 2.54 | 0.092 | 31497 | 1.44 | 0.27 | 0.23 | 0.21 | 0.22 |
| 13-14 | 1.22 | 97.9 | 85.5 | 73.7 | 68.5 | 61.4 | 2.55 | 0.32 | 4.32 | 0.24 | 0.20 | 0.2028 | 0.57 | 0.55 | 2.57 | 0.094 | 31698 | 1.57 | 0.28 | 0.23 | 0.20 | 0.23 |
| 15-16 | 1.31 | 98.2 | 85.6 | 73.9 | 68.6 | 61.6 | 5.75 | 0.38 | 4.43 | 0.25 | 0.21 | 0.2033 | 0.57 | 0.58 | 2.72 | 0.099 | 32573 | 1.56 | 0.30 | 0.24 | 0.22 | 0.25 |
| 17-18 | 1.39 | 98.1 | 85.7 | 73.4 | 68.5 | 61.8 | 5.40 | 0.36 | 4.85 | 0.24 | 0.21 | 0.2017 | 0.47 | 0.57 | 2.65 | 0.096 | 32148 | 1.73 | 0.29 | 0.25 | 0.18 | 0.27 |
| 19-20 | 1.48 | 98.2 | 86.7 | 73.4 | 68.5 | 61.9 | | | 4.71 | 0.27 | 0.23 | 0.2017 | 0.54 | 0.63 | 2.90 | 0.105 | 33620 | 1.59 | 0.30 | 0.33 | 0.18 | 0.28 |
| 21-22 | 1.53 | 98.1 | 85.8 | 72.9 | 68.4 | 61.8 | 6.45 | 0.60 | 5.56 | 0.24 | 0.21 | 0.2017 | 0.35 | 0.56 | 2.59 | 0.094 | 31792 | 2.01 | 0.29 | 0.26 | 0.14 | 0.27 |
| 23-24 | 1.58 | 98.3 | 85.8 | 72.9 | 68.4 | 61.9 | | | 5.71 | 0.24 | 0.21 | 0.2022 | 0.33 | 0.56 | 2.63 | 0.096 | 32014 | 2.05 | 0.30 | 0.26 | 0.13 | 0.27 |